INSTITUTE FOR FUSION STUDIES

DOE/ET-53088-506 IFSR #506

Magnetohydrodynamic Studies of Ideal and Resistive Tearing Modes with Equilibrium Shear Flow

X-L. CHEN
Institute for Fusion Studies
The University of Texas at Austin
Austin, Texas 78712

June 1991

THE UNIVERSITY OF TEXAS

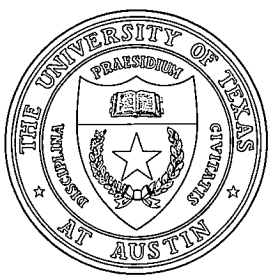

AUSTIN

MAGNETOHYDRODYNAMIC STUDIES OF IDEAL AND RESISTIVE TEARING MODES WITH EQUILIBRIUM SHEAR FLOW

APPROVED BY

SUPERVISORY COMMITTEE:

Philip J. Morrison

Richard S. Steinolfson

Richard D. Hazeltine

Wendell Horton

[illegible]

Copyright
by
Xiao-Liang Chen
1991

MAGNETOHYDRODYNAMIC STUDIES OF IDEAL AND RESISTIVE TEARING MODES WITH EQUILIBRIUM SHEAR FLOW

by

XIAO-LIANG CHEN, B.S.

DISSERTATION

Presented to the Faculty of the Graduate School of

The University of Texas at Austin

in Partial Fulfillment

of the Requirements

for the Degree of

DOCTOR OF PHILOSOPHY

THE UNIVERSITY OF TEXAS AT AUSTIN

August, 1991

TO

MY PARENTS AND MY WIFE

Acknowledgments

It is a great privilege to learn from and collaborate with Professor Philip J. Morrison. Without his many productive suggestions and constant encouragement, this dissertation would have been impossible. His guidance, patience, and knowledge are deeply appreciated.

I am very grateful to Professors R. Hazeltine, W. Horton, and T. Tajima. Through the years studying in Austin, they have always been very kind and generously offered their knowledge and advice.

I would like to thank Dr. R.S. Steinolfson for serving as my committee member, and also for many useful discussions.

I have also benefited from the association with my fellow students. Among those who stand out in mind are R. Acevedo, F. Y. Gang, C. Kueny, H. Lin, L. Ofman, S. N. Su, X. Xu, and H. Ye.

I want to acknowledge financial support from the Institute for Fusion Studies. Also I want to thank the staff members who provided various conveniences during my stay in Austin.

Finally, I wish especially to thank my wife Wu Zheng, my parents, and my parents in law, for their love and support through the difficult times.

Xiao-Liang Chen

The University of Texas at Austin

August, 1991

MAGNETOHYDRODYNAMIC STUDIES OF IDEAL
AND RESISTIVE TEARING MODES WITH
EQUILIBRIUM SHEAR FLOW

Publication No. _____

Xiao-Liang Chen, Ph.D.
The University of Texas at Austin, 1991

Supervisor: Philip J. Morrison

In this dissertation, two magnetohydrodynamic (MHD) instabilities are studied. A simple sufficient condition is given for the linear ideal instability of plane parallel equilibria with antisymmetric shear flow and symmetric or antisymmetric magnetic field. Application of this condition demonstrates the destablizing effect of the magnetic field on shear flow driven Kelvin-Helmholz instabilities. For the resistive tearing instability the effect of equilibrium shear flow is systematically studied, using the boundary layer approach. Both the constant-ψ tearing mode and the nonconstant-ψ tearing mode are analyzed in the presence of flow. It is found that the shear flow has a significant influence on both the external ideal region and the internal resistive region. In the external ideal region, the shear flow can dramatically change the value of the matching

quantity Δ'. In the internal resistive region, the tearing mode scalings are sensitive to the flow shear at the magnetic null plane. When the flow shear is larger than the magnetic field shear at the magnetic null plane, both tearing modes are stabilized. Also, the transition to ideal instability has been traced. Furthermore, the influence of small viscosity on the constant ψ tearing mode in the presence of shear flow is considered. It is found that the influence of viscosity depends upon the parameter $\frac{V_0'(0)}{B_0'(0)}$, where $V_0'(0)$ and $B_0'(0)$ denote the flow shear and magnetic field shear at the magnetic null plane, respectively. Viscosity basically tends to suppress the tearing mode. Finally, the nonlinear interaction of two near marginal tearing modes in the presence of shear flow is studied. To find the time asymptotic states, the resistive MHD equations are reduced to four amplitude equations, using center manifold reduction. These amplitude equations are subject to the constraint of translational symmetry of the physical problem. Bifurcation analysis is employed to find various possible time asymptotic states.

Table of Contents

Acknowledgments v

Table of Contents viii

List of Figures xi

1. Introduction 1

1.1 Overview 1

1.2 Model Equations 5

1.3 Organization of this Dissertation 7

2. Ideal Instability of Shear Flow with a Magnetic Field 10

2.1 Introduction 10

2.1.1 Review of Shear Flow Driven Kelvin-Helmhotz Instability 12

2.1.2 Previous Related Works 14

2.2 A Sufficient Condition for Instability 16

2.3 Applications of the Sufficient Condition 22

2.3.1 Plane Couette Flow 22

2.3.2 Hyperbolic Tangent Shear Flow 23

2.4 Summary and Conclusions 24

2.5 Appendix - Nyquist Method 24

3. Resistive Tearing Instability with Equilibrium Shear Flow 26

3.1 Introduction 26

3.2 Basic Equations 34

3.3 External Ideal Region 36

3.4 Internal Resistive Region 38

3.4.1 Slow growth; $\left|\frac{\gamma}{kB_0'(0)\epsilon}\right| \ll 1$. 39

3.4.2 Fast growth; $\left|\frac{\gamma}{kB_0'(0)\epsilon}\right| \sim 1$ 50

3.5 Transition to Ideal Instability 53

3.6 Summary 60

3.7 Appendix A - Δ' Value in the Presence of Equilibrium Flow . . 63

3.8 Appendix B - Nonconstant-ψ Tearing Mode with $\left|kB_0'S_R^{-1/3}\Delta'\right| \gg 1$ 68

4. Effect of Viscosity on Resistive Tearing Mode with Equilibrium Shear Flow 75

4.1 Introduction 75

4.2 Basic Equations 76

4.3 Internal Singular Layer 77

4.3.1 Very small shear flow 78

4.3.2 Comparable shear flow 84

4.4 Summary and Discussion 87

4.5 Appendix – Solution of General Second Order Singular Layer Equation 88

5. Nonlinear Interactions of Resistive Tearing Modes in the Presence of Equilibrium Shear Flow 90

5.1 Introduction 90

5.2 Model and Linear Problem 94
5.3 Center Manifold Reduction 96
5.4 Solutions of the Reduced Equations 101
5.4.1 Pure mode solution ($r_1 = 0, r_2 \neq 0$) 105
5.4.2 Mixed mode solution ($r_1 r_2 \neq 0$) 106
5.5 Discussion and Summary 110
5.6 Appendix - Calculation of Coefficients 112

BIBLIOGRAPHY 117

Vita

3. Resistive Tearing Instability with Equilibrium Shear Flow **26**

3.1 Introduction 26

3.2 Basic Equations 34

3.3 External Ideal Region 36

3.4 Internal Resistive Region 38

3.4.1 Slow growth; $\left|\frac{\gamma}{kB_0'(0)\epsilon}\right| \ll 1$ 39

3.4.2 Fast growth; $\left|\frac{\gamma}{kB_0'(0)\epsilon}\right| \sim 1$ 50

3.5 Transition to Ideal Instability 53

3.6 Summary 60

3.7 Appendix A - Δ' Value in the Presence of Equilibrium Flow . . 63

3.8 Appendix B - Nonconstant-ψ Tearing Mode with $\left|kB_0'S_R^{-1/3}\Delta'\right| \gg 1$ 68

4. Effect of Viscosity on Resistive Tearing Mode with Equilibrium Shear Flow **75**

4.1 Introduction 75

4.2 Basic Equations 76

4.3 Internal Singular Layer 77

4.3.1 Very small shear flow 78

4.3.2 Comparable shear flow 84

4.4 Summary and Discussion 87

4.5 Appendix – Solution of General Second Order Singular Layer Equation 88

5. Nonlinear Interactions of Resistive Tearing Modes in the Presence of Equilibrium Shear Flow **90**

5.1 Introduction 90

5.1 Center manifold depiction 97

5.2 Contour plots of magnetic flux function. 104

Chapter 1

Introduction

1.1 Overview

Plasma is a kind of matter in which charged particles (ions and unbound electrons) are sufficiently numerous to influence the behavior appreciably (Van Kampen and Felderhof, 1967). Plasma is often referred to as the "fourth state of matter". Although our earth consists mainly of the other three states, solid, liquid and gas, this cannot be said about most of the stars and interstellar matter. It is often said that ninety-nine percent of the matter in the universe is in the plasma state (Chen, F. 1984). Both planetary atmosphere and the gas in the vicinity of stars are ionized due to radiation , while in the interior of stars the ionization is caused by enormously high temperature. The full scope of possible applications of plasmas on earth is still unknown, but one of the most important possibilities is the application of plasma physics in understanding thermonuclear fusion, which requires a very high temperature (of order 10^8 degrees), a temperature at which all matter is ionized. It is the stimulus of trying to achieve controlled thermonuclear fusion which started the rapid development of plasma physics.

Plasmas are very good conductors due to the freely moving charged particles. As a consequence strong electric currents can occur, and the interaction of the magnetic field in plasmas is important. On the other hand, freely moving charged particles gives rise to screening of electric fields, and

the effective length for the electric interaction is reduced to the Debye length $\lambda_D = \sqrt{T/4\pi ne^2}$. Thus on the scale $L \gg \lambda_D$, the plasmas can be considered as quasineutral and electric interactions are negligible. However, for rapid phenomena, electrostatic interaction is important and give rise to, e.g. high frequency oscillation of electrons at the so-called plasma frequency $\omega_{pe} = \sqrt{\frac{4\pi ne^2}{m_e}}$.

When $n\lambda_D^3 \gg 1$, where $n\lambda_D^3$ is the number of particles in a volume with linear dimension λ_d, the thermal energy exceeds the electrostatic interaction energy. This is generally taken as the working definition of a plasma. For high density plasmas, when $\frac{\hbar}{m_e V_{Te}} \geq 1/n^{1/3}$ is satisfied, i.e. the deBroglie length is larger than the average distance between nearest electrons, the electrons must be described by quantum mechanics. In such quantum degenerate plasmas, the Fermi energy E_F is greater than the thermal energy, i.e. $E_F \sim \hbar^2(3\pi^2 n)^{2/3}/2m_e > T$. Plasmas existing in nature can be characterized by a temperature vs. density diagram such as that shown in Fig(1.1) (from Galeev and Sudan, 1989). We can see that the majority of plasmas fall into the region of the ideal classical plasma, which is also the case of interest of this dissertation.

The charged particles in a plasma interact not only with external electromagnetic fields, but also the fields created by the plasma particles. In order to completely describe the particle created fields, it would be necessary to know the position and velocity of every particle at all times. This is an impossible task for a plasma with a huge number of particles (usually particle densities are $10^5 \sim 10^{12} cm^{-3}$). However in order to describe the collective nature of plasma phenomena, a suitable way to treat a collection of many charged particles in the self-consistent electromagnetic field is presented by

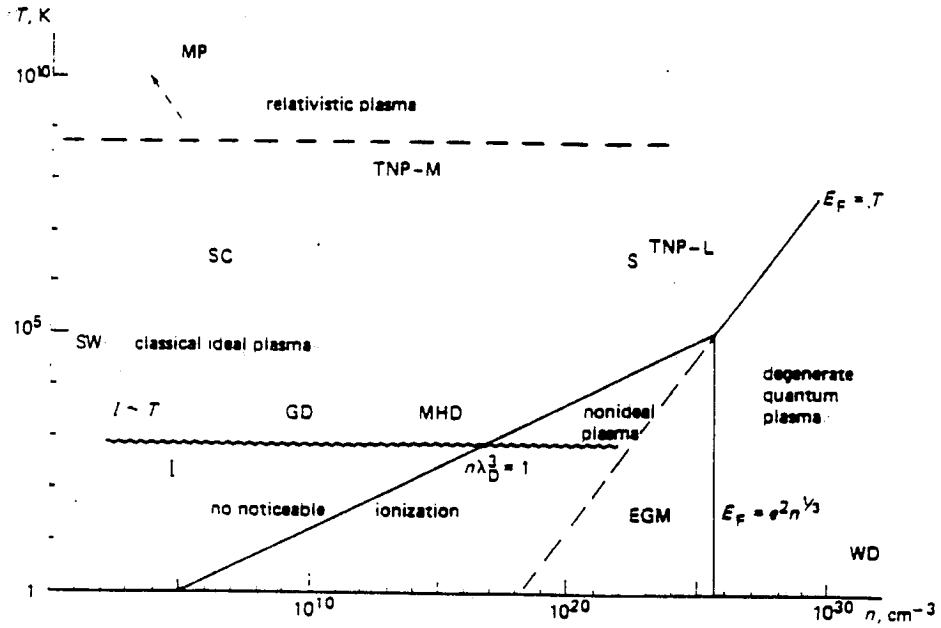

Figure 1.1: Classification of plasma types. WD: the degenerate electron gas in white dwarfs; GD: the gas discharge plasma; I: the ionospheric plasma; MHD: the plasma in magnetohydrodynamic generators; MP: the plasma in pulsar magnetosphere; S: the plasma in the center of the sun; SW: the solar wind plasma; SC: the solar coronal plasma; TNP-L: the plasma under the condition of laser thermonuclear fusion; TNP-M: the plasma in thermonuclear magnetic traps; EGM: the electron gas in metals.

a kinetic theory. Taking moments in velocity of this kinetic theory leads to continuum equations in three dimensional space and time, but these equations are not closed. In the collision dominated limit, with low frequency and long wave length asymptotic ordering, the moment equations are reduced to a set of single fluid magnetohydrodynamic (MHD) equations (see e.g. Freidberg, 1982)

$$\rho(\frac{\partial \vec{V}}{\partial t} + \vec{V} \cdot \nabla \vec{V}) = -\nabla P + \vec{j} \times \vec{B} + \rho \nu \nabla^2 \vec{V} \tag{1.1}$$

$$\frac{\partial \rho}{\partial t} + \nabla \cdot (\rho \vec{V}) = 0 \tag{1.2}$$

$$(\frac{\partial}{\partial t} + \vec{V} \cdot \nabla)(\frac{P}{\rho^\gamma}) = 0 \tag{1.3}$$

$$\frac{\partial \vec{B}}{\partial t} = -\nabla \times \vec{E} \tag{1.4}$$

$$\vec{E} + \vec{V} \times \vec{B} = \eta \vec{j} \tag{1.5}$$

$$\vec{j} = \frac{1}{4\pi} \nabla \times \vec{B} \tag{1.6}$$

$$\nabla \cdot \vec{B} = 0, \tag{1.7}$$

where ρ is the mass density, $\vec{V}$ the fluid velocity, $\vec{B}$ the magnetic field, $\vec{E}$ the electric field, P the scalar kinetic pressure, $\vec{j}$ the current density, η the resistivity, and ν the kinematic viscosity. Equation (1.3) is the equation of state for each separate fluid element following the motion. It is valid only when heat flow is negligible. Note $\frac{P}{\rho^\gamma}$ is related to the entropy per unit mass of a fluid element. For adiabatic process γ is 5/3, while for isothermal process γ is 1. The units used in the above equations are the CGS system with the speed light c set to unity.

Even though many assumptions are made in deriving the MHD equations, empirically it is found that many plasma phenomena observed in experiments can be explained by the MHD model, especially the macroscopic properties of equilibrium and stability. In this dissertation the single fluid MHD model is used to study two macroscopic instabilities: the Kelvin-Helmholz and the resistive tearing instabilities. Both instabilities are long wavelength modes.

1.2 Model Equations

For the sake of making the calculations easy and exhibiting just the essential physics for the problems to be considered, the following simplifications are made:

(i) We assume that the plasma is incompressible and that the mass density ρ is constant. Hence in dimensionless form Eqs.(1.1)-(1.7) become

$$\frac{\partial \vec{V}}{\partial t} + \vec{V} \cdot \nabla \vec{V} = -\nabla P + (\nabla \times \vec{B}) \times \vec{B} + S_V^{-1} \nabla^2 \vec{V}$$

$$\frac{\partial \vec{B}}{\partial t} = -S_R^{-1} \nabla \times (\nabla \times \vec{B}) + \nabla \times (\vec{V} \times \vec{B}) \tag{1.8}$$

$$\nabla \cdot \vec{V} = 0$$

$$\nabla \cdot \vec{B} = 0.$$

The following scalings have been used in deriving the above equations

$$\vec{r} \rightarrow a\vec{r},\ t \rightarrow \tau_A t,\ \vec{B} \rightarrow \tilde{B}\vec{B},\ \vec{V} \rightarrow \frac{a}{\tau_A}\vec{V},\ P \rightarrow \rho(\frac{a}{\tau_A})^2 P,$$

where a is a typical macroscopic length, such as the flow shear length or the width of a current sheet. $\tilde{B}$ is the measure of the magnetic field, τ_A is the

Alfvén time $\tau_A = \frac{\tilde{B}}{\sqrt{4\pi\rho}}$, $S_R = \frac{4\pi a^2}{\eta\tau_A}$ is the magnetic Reynolds number, and $S_V = \frac{a^2}{\nu\tau_A}$ is the Prandtl number.

(ii) Simple slab geometry is adopted throughout this dissertation. For the two instabilities considered, the essential physics is the same for different geometries. Further, assuming that the problem is independent of the z coordinate, the magnetic field and flow velocity can be represented by scalar stream functions: $\vec{B} = \hat{z} \times \nabla\tilde{\psi}(x,y) + B_z\hat{z}$, $\vec{V} = \hat{z} \times \nabla\tilde{\phi}(x,y)$, where B_z is a constant magnetic field in the z direction. Thus Eqs.(1.8) can be rewritten as

$$\frac{\partial\Omega}{\partial t} + \vec{V} \cdot \nabla\Omega = \vec{B} \cdot \nabla j + S_V^{-1}\nabla_\perp^2\Omega + \hat{z} \cdot \nabla \times \vec{F} \tag{1.9}$$

$$\frac{\partial\tilde{\psi}}{\partial t} + \vec{V} \cdot \nabla\tilde{\psi} = S_R^{-1}j - E_z, \tag{1.10}$$

where Ω and j are respectively the vorticity and the current in the z direction, i.e. $\Omega = \nabla_\perp^2\tilde{\phi} = (\frac{\partial^2}{\partial x^2} + \frac{\partial^2}{\partial y^2})\tilde{\phi}$ and $j = \nabla_\perp^2\tilde{\psi} = (\frac{\partial^2}{\partial x^2} + \frac{\partial^2}{\partial y^2})\tilde{\psi}$. $\vec{F}$ and E_z are the external force and the electrical field respectively, which are applied to compensate for the natural diffusion in the equilibrum state. For an equilibrium state as shown in Fig(1.2), the equilibrium magnetic field $B_0(y)$ and the equilibrium velocity field $V_0(y)$ are directed along the x axis. Let $\tilde{\psi} = \psi_0(y) + \psi(x,y,t)$, $\tilde{\phi} = \phi_0(y) + \phi(x,y,t)$, where $\psi_0'(y) = -B_0$, $\phi_0' = -V_0$, and the subscript 0 denote equilibrium. Thus Eqs.(1.9) and (1.10) become

$$\frac{\partial}{\partial t}\begin{pmatrix}\nabla_\perp^2\phi \\ \psi\end{pmatrix} = \mathbf{L}\begin{pmatrix}\phi \\ \psi\end{pmatrix} + N(\phi,\psi), \tag{1.11}$$

where

$$\mathbf{L} = \begin{pmatrix} S_V^{-1}\nabla_\perp^4 - V_0(y)\frac{\partial}{\partial x}\nabla_\perp^2 + V_0''(y)\frac{\partial}{\partial x} & B_0(y)\frac{\partial}{\partial x}\nabla_\perp^2 - B_0''(y)\frac{\partial}{\partial x} \\ B_0(y)\frac{\partial}{\partial x} & S_R^{-1}\nabla_\perp^2 - V_0\frac{\partial}{\partial x}\end{pmatrix},$$

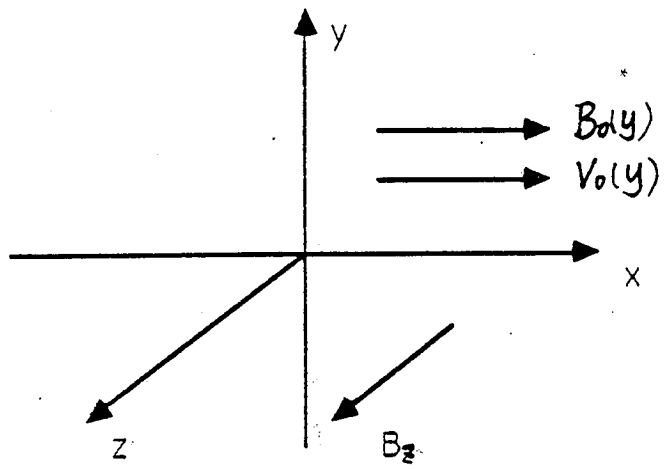

Figure 1.2: Slab geometry showing the equilibrium magnetic field $B_0(y)$ and the flow velocity $V_0(y)$ along the x direction.

and

$$N(\phi,\psi) = \hat{z}\cdot\begin{pmatrix}\nabla\psi\times\nabla j_1 - \nabla\phi\times\nabla\Omega_1\\ -\nabla\phi\times\nabla\psi\end{pmatrix}.$$

Here prime denotes differentiation with respect to y, $\Omega_1 = \nabla_\perp^2\phi$, $j_1 = \nabla_\perp^2\psi$. In later chapters, Eq.(1.11) will be our starting point.

1.3 Organization of this Dissertation

In Chaper 2, we consider the effect of the magnetic field on the Kelvin-Helmholtz instabilities. Kelvin-Helmholtz instability is driven by free energy contained in the shear flow. The presence of the magnetic field has a dual role for the stability of shear flow. It exerts a tension on the fluid which usually acts as a restoring force on a disturbance, but on the other hand, the magnetic field breaks the constraint of local conservation of vorticity and therefore makes the shear flow energy accessible. The actual influence of the magnetic field depends

on the specific profiles of both the magnetic field and flow. We have studied the special case where the flow profile is antisymmetric and magnetic field profile has parity; i.e. it is either symmetric or antisymmetric. A simple sufficient condition is given to demonstrate the destablizing effect of the magnetic field.

In Chapter 3, the influence of equilibrium shear flow on the resistive tearing instability is studied. The essential feature of resistive tearing instability is that resistivity allows a change of the magnetic field topology, and in special configurations with a place where one component of the magnetic field vanishes, there exists an instability with a time scale that is hybrid of the magnetohydrodynamic and resistive time scales. The presence of shear flow enhances the inertial terms. Systematic calculations show that shear flow is not only important in the resistive tearing layer, but is also important in the ideal region. Depending on the specific profiles, shear flow can either completely stabilize the tearing instability or destabilize it.

In addition to the influence of equilibrium shear flow, viscosity can also be included in the resistive tearing instability. This is the subject of Chap. 4. Since the tearing instability produces vorticity, and shear flow can enhance this production, the diffusive nature of viscosity should have a significant influence, one that depends on the equilibrium shear flow. It is found that generally viscosity tends to suppress the tearing mode.

Chapter 5 is devoted to the study of nonlinear interactions of two near marginal tearing modes with the presence of shear flow. To find the time asymptotic states of the nonlinear evolution, the MHD equations are reduced to amplitude equations for the two modes. The method of center manifold reduction is used. The amplitude equations are subject to the constraint of

translational symmetry. Bifurcation analysis is employed to unfold the new branches of time asymptotic states. Various type of solutions have been found, and their corresponding parameter ranges are discussed.

Chapter 2

Ideal Instability of Shear Flow with a Magnetic Field

2.1 Introduction

Shear flow is a very common phenomenon. It appears in such diverse areas as in astrophysical jets (Begelman and Blandford, 1984), the magnetosphere (Burch, 1983), and rotating plasmas. Recently, experiments (Groebner et al., 1989) in the DIII-D tokamak discovered that there is a substantial increase in the perpendicular component of the plasma flow velocity associated with the L (low) to H (high) confinement mode transition. Since shear flow contains a source of free energy, it can give rise to the Kelvin-Helmholtz (K-H) instability (Chandraseker, 1961, Drazin and Howard, 1966).

In order to focus on the shear flow driven K-H instability, we neglect dissipation in Eqs.(1.11). This is justified since usually the dissipation diffusion time scale is much longer than the K-H time scale. We assume that the flow is confined between rigid walls located at $y = l_1$ and $y = l_2$ and all the perturbed field components have the form $f(k, c, y) \exp ik(x - ct)$. The normal mode equations, ie. the linear part of Eqs.(1.11), for the transverse displacement $w = \phi/(V_0 - c)$ are

$$((V_0 - c)^2 - B_0^2)w')' - k^2((V_0 - c)^2 - B_0^2)w = 0 \ , \tag{2.1}$$

where $V_0(y)$ and $B_0(y)$ are the (dimensionless) equilibrium velocity and magnetic field, respectively (One can interpret $B_0(y)$ as the local Alfvén velocity).

Since the transverse displacement vanishes at the rigid walls, Eq. (2.1) has the boundary conditions $w(l_1) = w(l_2) = 0$. Equation (2.1) together with the boundary conditions gives the dispersion relation $c = c(k^2)$.

Note that for real c the eigenequation (2.1) is singular at places where $V_0(y) \pm B_0(y) = c$. The singularity admits solutions with discontinuous derivatives and continuous spectra in addition to well-behaved solutions with a discrete spectrum. All these solutions are necessary to form a complete set, capable of representing an arbitray initial perturbation. Some care must be taken in the normal mode method because of the continuous spectrum, whose eigenfunctions usually exhibit singular behavior at the singular points. However well behaved solutions can be obtained by integrating the continuous singular modes over the entire spectrum (Barston, 1964). In this way it is possible to obtain the asymptotic behavior of non-collective oscillating modes of continuous spectrum, which results in a (dissipationless) damping proportional to the inverse power of time. Also, the connection between the continuous spectrum for spatially non-uniform plasma and the initial value problem (collective mode) has be investigated (Drazin and Howard, 1966). It was found that the continuous spectrum manifests itself in unstable plasma by yielding non-exponentially growing modes (Kent, 1968), while for stable plasma, the continuous spectrum leads to the damping of propagating waves through phase mixing (Case, 1960, Sedlacek, 1971, Tataronis and Grossmann, 1973, Grossman and Tataronis, 1973, Ionson, 1978).

Though the continuous spectrum is also important, we consider here only the exponentially growing modes, and the normal mode equation (2.1) is used in the following discussions. When c is complex for a certain range

of wavenumbers k, the shear flow is unstable. Since Eq. (2.1) is regular for complex c, $c(k^2)$ in this case is an analytic function.

2.1.1 Review of Shear Flow Driven Kelvin-Helmhotz Instability

First we give a brief review of Kelvin-Helmhotz instability without the magnetic field. setting $B_0 = 0$, Eq.(2.1) becomes

$$((V_0 - c)^2 w')' - k^2((V_0 - c)^2)w = 0 \ . \tag{2.2}$$

Multiplying Eq.(2.2) by w^* (complex conjugate of w) and integrating yields

$$\int_{l_1}^{l_2} (V_0 - c)^2 (\left|w'\right|^2 + k^2 \left|w\right|^2) dy = 0,$$

The imaginary part of the above equation is

$$c_i \int_{l_1}^{l_2} (V_0 - c_r)(\left|w'\right|^2 + k^2 \left|w\right|^2) dy = 0,$$

which implies that c_r must lie between the maximum and minimum of $V_0(y)$. Howard (1961) has shown that the growth rate is bounded by $kc_i \leq \frac{1}{2} max \left|V_0'\right|$, however, recently Gu (1990) improved this result, and obtained $kc_i \leq \frac{k(max\left|V_0'\right|)}{\sqrt{4k^2+\pi}}$.

Rewriting Eq.(2.2) in terms of $\phi = w(V_0 - c)$, we have

$$\phi'' - k^2\phi - \frac{V_0''}{(V_0 - c)}\phi = 0, \tag{2.3}$$

with the boundary conditions $\phi(l_1) = \phi(l_2) = 0$. Again multiplying Eq.(2.3) by the complex conjugate of ϕ and integrating yields

$$\int_{l_1}^{l_2} (\left|\phi'\right|^2 + k^2 \left|\phi\right|^2) dy = -\int_{l_1}^{l_2} \frac{V_0''}{V_0 - c} \left|\phi\right|^2 dy. \tag{2.4}$$

The imaginary part of Eq.(2.4) gives

$$ic_i \int_{l_1}^{l_2} \frac{V_0''}{|V_0 - c|^2} |\phi|^2 \, dy = 0.$$

Obviously a necessary condition for K-H instability to occur ($c_i \neq 0$) is that V_0'' must changes sign somewhere in the domain l_1 and l_2. This is called the Rayleigh inflection point condition. Corresponding to the inflexion point $V_0''(y_s) = 0$ is an extremum of the flow vorticity $V_0'(y)$. The physical role of the inflection point condition is explained by the conservation of vorticity (Lin, 1945): in order to release the free energy contained in the shear flow there needs to be a vorticity-extremum, since only then does the restoring force against a perturbation vanishes. In 1950 Fjortoft derived a stronger necessary condition for instability. Combining the real and imaginary part of Eq.(2.4) yields

$$\int_{l_1}^{l_2} \frac{(V_0(y) - V_0(y_s))V_0''}{|V_0 - c|^2} |\phi|^2 \, dy = -\int_{l_1}^{l_2} (\left|\phi'\right|^2 + k^2 \left|\phi^2\right|^2) dy < 0.$$

Thus instability requires $(V_0(y) - V_0(y_s))V_0'' < 0$ somewhere in the domain (l_1, l_2). In the case where $V_0(y)$ is monotonic and V'' vanishes only once, the necessary condition becomes $(V_0(y) - V_0(y_s))V_0'' \leq 0$ throughout the flow with equality only at $y = y_s$. This means that instability requires the vorticity to have an extremum point.

The conditions discussed above are not sufficient to judge the instability of flows. Friedrichs (1942) has proven that when $K(y) \equiv -\frac{V_0''(y)}{V_0(y) - V_0(y_s)} > \pi^2/(l_2 - l_1)^2$, there exists a neutrally stable eigensolution with $c = V_0(y_s)$. Later on Lin (1955) derived a theorem which states that near a marginally stable wavelength k_c, the K-H mode becomes unstable when the wavenumber decreases. Using this theorem, Rosenbluth and Simon (1963) derived a necessary and sufficient condition for the stability of monotonic shear flow, by

looking at the mode k=0. When k=0, Eq.(22) together with the boundary conditions give

$$F(c) = \int_{l_1}^{l_2} \frac{dy}{(V_0 - c)^2} = 0 \ .$$

Then the Nyquist diagram method (see the Appendix) is used to derive a condition for unstable solutions, i.e. solutions with $c_i \neq 0$. It is found that for monotonic profiles with only one inflection point in the domain $l_1 < y < l_2$, the shear flow is stable iff

$$P \int_{l_1}^{l_2} \frac{dy}{(V_0 - c)^2} = \frac{1}{V_0'(c_s - V_0)} \Big|_{l_1}^{l_2} - \int_{l_1}^{l_2} \frac{V_0''}{V_0'^2 (V_0 - c_s) dy} > 0,$$

where $c_s = V_0(y_s)$, and y_s corresponds to the inflection point, i.e. $V_0''(y_s) = 0$. For profiles with more than one inflection point and with their vorticity gradient expressible as

$$V_0''(y) = -K(y)(V_0 - c_s),$$

where $K(y)$ is continuous, or piecewise continuous and non-negative, and c_s is some number, Howard (1964) has shown that the number of unstable modes cannot exceed the number of inflection points.

2.1.2 Previous Related Works

As noted above, the presence of the magnetic field plays a dual role for the instability of shear flow. The magnetic field exerts a tension on the fluid which usually acts as a restoring force on a disturbance. So it is easy to imagine that the flow is completely stabilized if the magnetic energy overpowers the kinetic energy everywhere (Kent,1968); i.e. $B_0^2 > V_0^2$ in the whole region, where B_0 can be thought of as the local Alfvén speed. This condition need only hold in some reference frame for stability to be established. It was also

shown by using the semicircle theorem (Chandra, 1973) that the flow is stable if $|B_0|_{\min} > (V_{\max} - V_{\min})/2$. Chiueh et al(1986) and Tajima et al (1990) have discussed the stabilizing effect of magnetic shear. On the other hand, sometimes the magnetic field can destabilize the shear flow, since it breaks the constraint of local conservations of vorticity and thus makes the shear flow free energy accessible. In this case the existence of an inflection point is not necessary for instability. Kent (1966) has shown that a stable symmetric flow can be driven unstable by a symmetric magnetic field if, on the boundary $B_0 = 0$ and $V'V'' - B'B'' > 0$, where prime denotes differentiation with respect to y. Stern (1963) has also discussed the destabilizing effect of a piecewise continuous magnetic field on plane Couette flow. The actual influence of the magnetic field depends on the specific profiles of both the flow and the magnetic field. Kent (1968) has shown that a constant magnetic field stabilize some, while destabilize other monotonic flow profiles.

In the next section, we present a sufficient condition for instability, by assuming that the flow is antisymmetric and that the magnetic field has parity; i.e. it is either symmetric or antisymmetric (Chen and Morrison, 1991). A technique (Morrison, 1979) which is based on the use of symmetries and the Nyquist method is used to obtain a simple formula. Though the symmetries we assume may limit application to some practical problems, results obtained from these special profiles provide insight into the physics and will be helpful in more realistic situations. In many circumstances, the shear flow can be approximated by antisymmetric profiles. An antisymmetric hyperbolic tangent profile has been used to model the edge flow in tokamaks (Chiueh et al, 1986).

2.2 A Sufficient Condition for Instability

Here we consider an extreme case with wavenumber $k = 0$. If there exists an eigenvalue where $\mathrm{Im}(c) \equiv c_i \neq 0$ for $k = 0$, then this is sufficient to say that the system is unstable. Strictly speaking, the growth rate kc_i is zero when $k = 0$, but analyticity of $c(k^2)$ ensures a finite growth rate near $k = 0$. This argument has previously been used by Rosenbluth and Simon (1960) and Kent(1968).

Setting $-l_1 = l_2 = l$ and $k = 0$ in Eq. (2.1), integrating, and applying the boundary conditions leads to

$$F(c) = \int_{-l}^{l} \frac{dy}{(V_0 - c)^2 - B_0^2} = 0 \ . \tag{2.5}$$

Without solving the above integral equation for the eigenvalue c, we can use the Nyquist diagram method in a manner similar to the Penrose criterion (Penrose, 1960, Krall et al, 1973) to determine whether or not there exist unstable modes (see Appendix). The number of roots of an analytic function like F in the upper half-plane ($\mathrm{Im}(c) > 0$) is given by the number of times a polar plot of F encircles the origin as c traces out the curve as shown in Fig. 2.1. Path 3-1 has a distance ϵ from the real axis so that the singularity on the real axis is avoided. Thus $F(c)$ is an analytic function. However, in order not to miss any possible unstable modes, we take the limit $\epsilon \to 0$.

Along the path 1-2-3, $c = \mathrm{Re}^{i\theta}$ and in the limit $R \to \infty$, $F(c) \sim 2le^{-2i\theta}/R^2$. The corresponding plot of F is shown in Fig. 2.2. Since we assume that the shear flow is antisymmetric and that the magnetic field is either symmetric or antisymmetric, we have along path 3-1 in Fig. 2.1.

$$F(c_r + i\epsilon) = F^*(-c_r + i\epsilon) \ ,$$

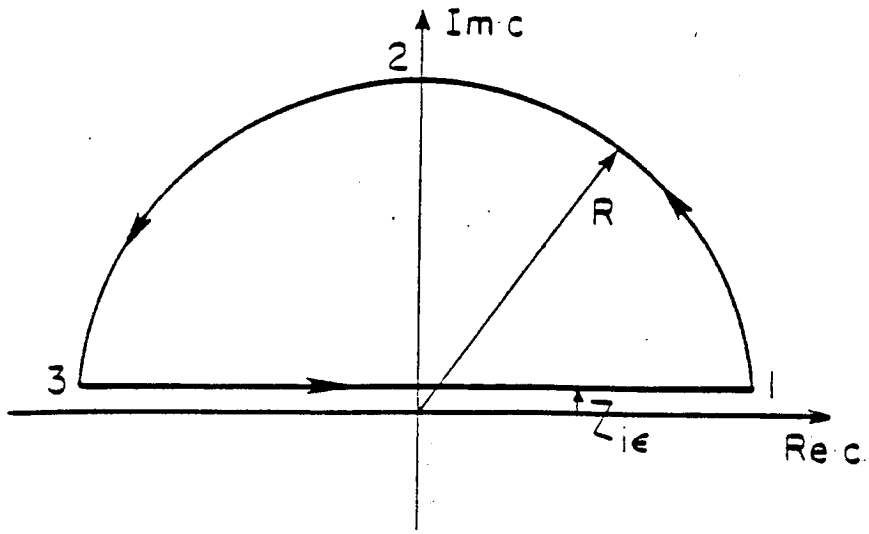

Figure 2.1: Nyquist diagram in the C-plane

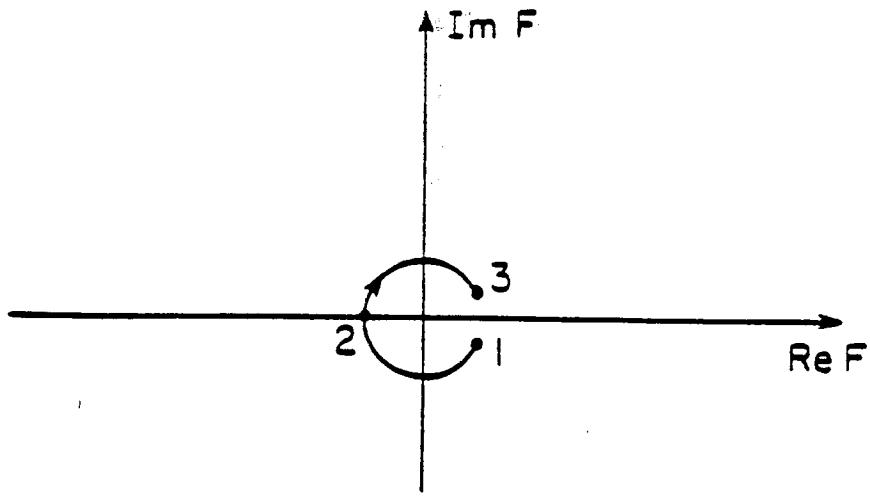

Figure 2.2: Nyquist diagram in F-plane

where "$*$" means complex conjugate. Thus we have the following conclusions:

(i) Im $F(0+i\epsilon)=0$,

(ii) If Im $F(c_r+\epsilon)=0$, $(c_r\neq 0)$, then
Im $F(-c_r+i\epsilon)=0$, and
Re $F(c_r+i\epsilon)=$ Re $F(-c_r+i\epsilon)$.

To determine the winding number (the number of times $F(c)$ encircles the origin), we can just count the points of crossing of the real axis. Denote crossing points by n; associated with such points are two quantities:

$$\sigma_n=\begin{cases} 1, & \text{crossing of real axis with up direction} \\ -1, & \text{crossing of real axis with down direction} \end{cases}$$

and

$$r_n=\begin{cases} 1, & \text{Re } F_n>0 \\ 0, & \text{Re } F_n=0 \\ -1, & \text{Re } F_n<0\ . \end{cases}$$

Since the Nyquist diagram must be closed as c traces the path of Fig. 2.1, this implies the following conclusions:

(i) The total number of crossing points is even and $\sum_n \sigma_n=0$;

(ii) For crossing points i and j with $r_i=r_j$ and $\sigma_i+\sigma_j=0$, there is cancellation and thus no contribution to the winding number.

As an example note that the Nyquist diagrams of Fig. 2.3 and Fig. 2.4 produce the same winding number (Here the double arrows designate two crossings). In both cases, the winding number is unity, and there exists one unstable mode. For the present problem, if Re $F(0+i\epsilon)>0$, then the total number of crossing points with positive and negative Re F are both odd numbers, and we

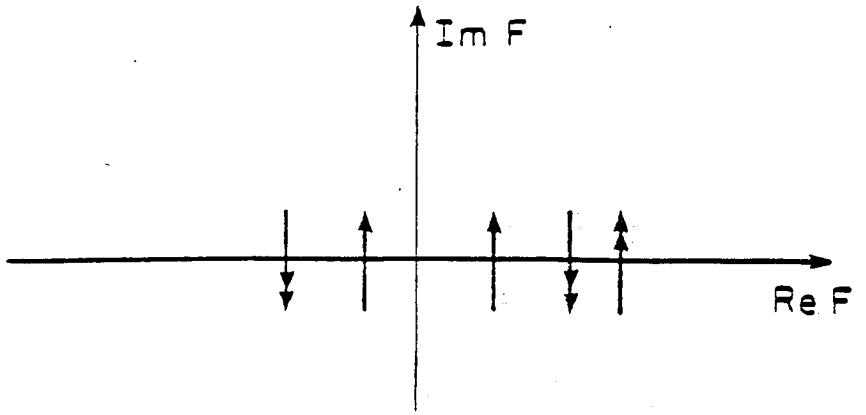

Figure 2.3: Nyquist diagram with 8 crossings. Double arrows indicate two crossings.

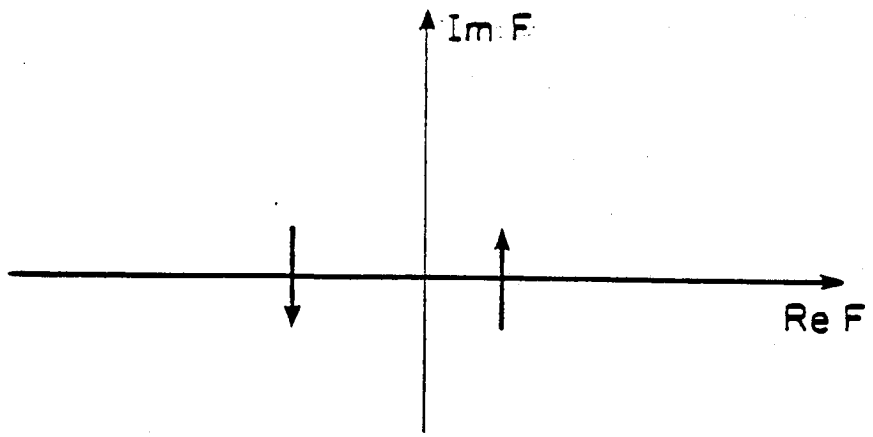

Figure 2.4: A Nyquist diagram equivalent to that of Fig.2.3.

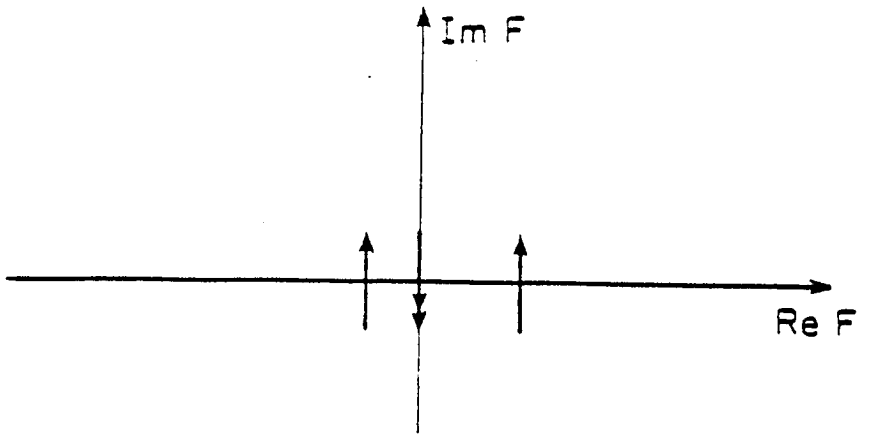

Figure 2.5: A Nyquist diagram having crossingspoints with Re F=0, and with the net crossings on both sides of the real axis pointing in the same direction.

always have net crossing on each side of the real axis of $F(c)$. Now we consider respectively two possible cases.

Case I: In this case we suppose there are no crossing points with Re $F = 0$. Thus the net crossing with Re $F > 0$ and Re $F < 0$ must point in opposite directions. Hence, the Nyquist diagram encircles the origin at least once, and there exsits at least one unstable mode.

Case II: In this case there exist crossing points with Re $F(\pm c_r + i\epsilon) = 0$, which implies that there exist marginal modes with $c = \pm c_r$. When this occurs we can prove that the Nyquist diagram always indicates a none zero winding number. In other words, it is impossible to have a Nyquist diagram with the net crossing for Re $F > 0$ and the net crossing for Re $F < 0$ pointing in the same direction. For the moment suppose this is the case. The Nyquist diagram will be as shown in Fig. 2.5 and there exists no unstable mode. Now

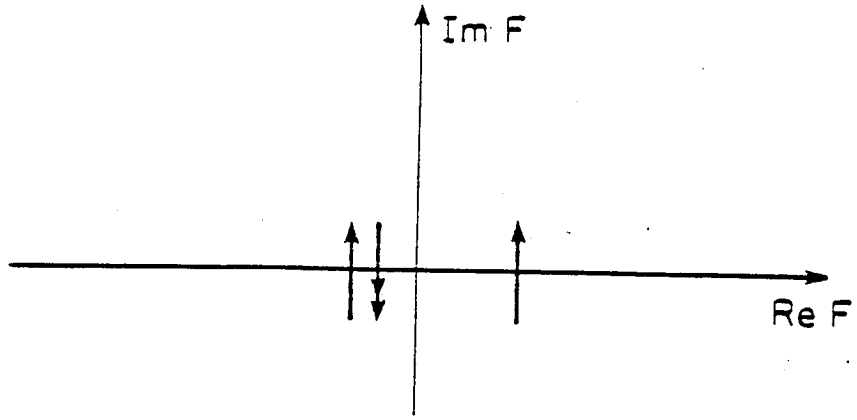

Figure 2.6: The Nyquist diagram of Fig.2.5 with finite but small values of ϵ, instead of $\epsilon = 0$.

we change the c contour a little bit, so that ϵ is very small but with finite value; instead of proceeding to the limit $\epsilon \to 0$. Since there exists no unstable mode, there are no crossing points with Re $F = 0$ along the new contour. Furthermore, we still have Re $F(0 + i\epsilon) > 0$, since ϵ is very small. Using the argument of Case I, there exists an unstable mode as the example shown in Fig. 2.6 indicates. This contradicts our original assumption and thus the proof is established.

From the above discussion, a sufficient condition for instability with antisymmetric shear flow and antisymmetric or symmetric magnetic fields is given by

$$F(0 + i\epsilon) = \int_{-l}^{l} \frac{dy}{(V - i\epsilon)^2 - A^2} > 0 \,, \tag{2.6}$$

where the limit $\epsilon \to 0$ from above is assumed. For the case of antisymmetric shear flow with only one inflection point, the inflection point should be at $y = 0$.

When $B_0 = 0$, our sufficient condition Eq. (2.6) reduces to that obtained by Rosenbluth and Simon (1963), and this condition becomes both sufficient and necessary for instability because of Lin's theorem (Lin, 1955).

2.3 Applications of the Sufficient Condition

In this section we apply the simple sufficient condition just derived to two examples which demonstrate the effect of the magnetic field on the stability of shear flow.

2.3.1 Plane Couette Flow

For a plane Couette flow profile $V(y) = by$, there is no vorticity extremum and thus this flow is K-H stable (Case, 1960). Stern (1963) has shown that the Couette flow can be destabilized by a piecewise continuous magnetic field. Here we add a symmetric magnetic field $B_0(y) = ay^2$ to the Couette flow equilibrium. The destabilizing effect of this symmetric magnetic field is easily demonstrated from our simple sufficient condition. Equation (2.6) gives

$$F(0+i\epsilon) = \frac{1}{V_0(l)b}\left(-2 + \frac{B_0(l)}{V_0(l)}\log\left|\frac{1+B_0(l)/V_0(l)}{1-B_0(l)/V_0(l)}\right|\right) . \qquad (2.7)$$

When the magnetic field at the boundaries is sufficiently strong; i.e. $B_0(l)/V_0(l) > f$, where $f \approx 0.834$ is the value at which $F(0+i\epsilon) = 0$, $F(0+i\epsilon) > 0$ and there is instability.

2.3.2 Hyperbolic Tangent Shear Flow

For the second example, we consider a hyperbolic tangent shear flow profile $V_0(y) = V_0 \tanh(y/d_1)$. In the case without magnetic field, Eq. (2.6) is both sufficient and necessary for instability; it indicates that the hyperbolic tangent shear flow is unstable if and only if $l/d_1 > 2.39$. Now we add magnetic shear, assuming $B_0(y) = B_0 y/d_2$. When the magnetic shear is strong enough so that $B_0/d_2 > V_0/d_1$, the shear flow will be stable since the magnetic energy overpowers the kinetic energy everywhere; i.e. $B_0(y)^2 > V_0(y)^2$ for all y. We want to know what happens if the magnetic shear is not this strong. For simplicity in evaluating the integral in Eq. (2.6), we approximate the hyperbolic tangent profile by a piecewise continuous one

$$V_0(y) = \begin{cases} V_0 & y > d_1 \\ V_0 y/d_1 & |y| < d_1 \\ -V_0 & y < -d_1 \end{cases} .$$

With these assumed forms of V_0 and B_0, Eq. (2.6) yields

$$F(0+i\epsilon) = 1/d_1 \left(\frac{1}{V'B'} \log \frac{(V'+B'l/d_1)(V'-B')}{(V'+B')\,|V'-B'l/d_1|} - \frac{2}{V'^2 - B'^2} \right) , \qquad (2.8)$$

where $V' = V_0/d_1$, $B' = B_0/d_2$, and $V' > B'$, $l > d_1$ are assumed. In order to stabilize the unstable shear flow, it is necessary to have $F(0+i\epsilon) < 0$. When $B' > \bar{B}'$, where $\bar{B}'$ satisfies $\sqrt{\frac{d_1}{l}} V' > \bar{B}' > \frac{d_1}{l} V'$, the necessary condition is satisfied. However it is interesting to notice that when $B' \sim \frac{d_1}{l} V'$; i.e. $B_0(l) \sim V_0(l)$, $F(0+i\epsilon)$ is always positive. A stable flow ($l/d_1 < 2.39$) can be driven unstable by the magnetic shear in this range. Thus magnetic shear does not always stabilize the K-H instability.

2.4 Summary and Conclusions

A simple sufficient condition was given for the linear ideal instability of plane parallel equilibria with antisymmetric shear flow and symmetric or antisymmetric magnetic field. We concluded from the application of this condition that the magnetic field in the midplane tends to stabilize the shear flow, while the magnetic field at the boundaries tends to destabilize the shear flow, especially when $B_0(l) \sim V_0(l)$. In the plane Coutte flow example $B_0(0)/V_0(0) = 0$, and this flow was destabilized by the magnetic field at the boundaries. In the hyperbolic tangent flow example, the magnetic shear destabilizes the flow when $B' \sim \frac{d_1}{l} V'$; i.e. $B_0(l) \sim V_0(l)$. However, a large magnetic shear stabilizes the flow. In this case, the stabilizing effect of the magnetic field in the midplane overpowers the destabilizing effect of the magnetic field at the boundaries.

2.5 Appendix - Nyquist Method

The Nyquist method is a way to determine wether or not an analytic function has roots (Krall and Trivelpiece, 1973, Penrose, 1960). We consider a general function of a complex variable $f(z)$ that is analytic within and on a contour Γ except for a finite number of poles within Γ. At a zero z_i, the function can be expanded in a Taylor series

$$f(z) = c_1(z - z_i)^{m_i} + c_2(z - z_i)^{m_i+1} + \cdots,$$

where $c_1 \neq 0, m_i$ is the order of zero z_i and $m_i \geq 1$. The ratio $\frac{f'(z)}{f(z)}$ near z_i becomes

$$\frac{f'(z)}{f(z)} = \frac{m_i}{z - z_i} + \cdots$$

Obviously $\frac{f'(z)}{f(z)}$ has a simple pole at z_i with residue m_i.

At a pole z_j, the function $f(z)$ can be expanded in a Laurant series

$$f(z) = \frac{d_1}{(z-z_j)^{l_j}} + \frac{d_2}{(z-z_j)^{l_j-1}} + \cdots,$$

where $d_1 \neq 0$ and $l_j \geq 1$. Near z_j the ratio $\frac{f'(z)}{f(z)}$ becomes

$$\frac{f'(z)}{f(z)} = -\frac{l_j}{z-z_i} + \cdots,$$

Therefore $\frac{f'(z)}{f(z)}$ has a simple pole at z_j with residue equal to $-l_j$.

Since there are no other singularities of $\frac{f'(z)}{f(z)}$, we obtain from Cauchy's theorem

$$\int_\Gamma \frac{f'(z)}{f(z)} dz = 2\pi i(\sum_i m_i - \sum_j l_j),$$

where $\sum_i m_i$ is the number of simple zeros and $\sum_j l_j$ is the number of simple poles of function $f(z)$. If function $f(z)$ is analytic throughout the region enclosed by Γ, then $\sum_j l_j = 0$. Alternatively We have

$$\int_\Gamma \frac{f'(z)}{f(z)} dz = ln f(z)|_\Gamma = arg\, f(z)|_\Gamma.$$

In the complex plane, $arg\, f(z)|_\Gamma$ is the change of phase angle of $f(z)$ or winding number around origin when z traces contour Γ. Thus roots of the analytic function $f(z)$ inside a close contour Γ can be detected through the winding number of $f(z)$. If the winding number is zero, then there exists no roots of f(z) inside the contour Γ.

Chapter 3

Resistive Tearing Instability with Equilibrium Shear Flow

3.1 Introduction

We have discussed the ideal instability of shear flow with magnetic field in the last chapter. If the plasma is dissipative, usually one would think that the growth rate will decrease since dissipation tries to diminish free energy sources. However this is not always true. The introduction of dissipation can eliminate constraints which prevent the plasma from relaxing to lower energy states, and new types of instabilities will appear. In this Chapter we will consider the instability due to resistivity: the resistive tearing mode.

In the ideal MHD model magnetic field is frozen into the plasma, and its topology cannot be changed (see e.g. Van Kampen and Felderhof, 1967, Bateman, 1978). Resistivity allows the magnetic field to be broken and to reconnect. The characteristic time scale for the resistive diffusion rate is S_R, the magnetic Renolds number defined in chapter 1. Generally, S_R is very large, ranging from 10^6 in magnetic confined fusion plasma to 10^{12} in solar corona plasma. Thus this natural resistive diffusion is a rather slow process. However for a special configuration such as that shown in Fig. 3.1, where the current is distributed so that the equilibrium magnetic field reverses direction, say at y=0, the reconnection can occur on a much faster time scale, a scale which is a hybrid of the resistive and Alfvén time scales. On this time scale the magnetic

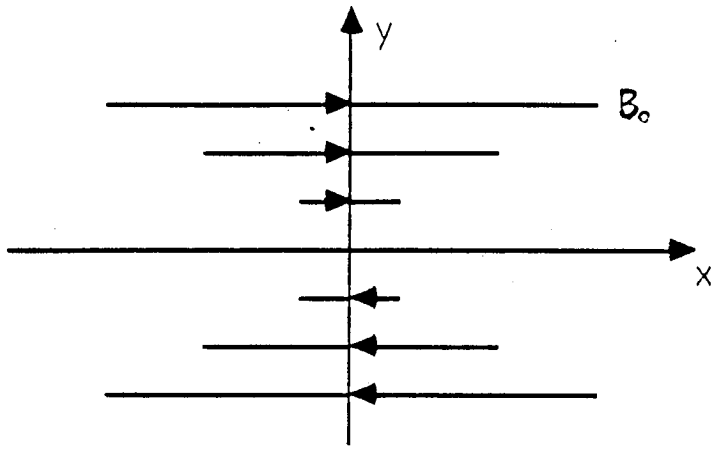

Figure 3.1: The basic tearing model

field will reconnect to form a magnetic island structure as shown in Fig. 3.2 .

Dungey (1958) first suggested that magnetic reconnection could explain the energy release in solar flares and other astrophysical phenomena. Later Furth, Killeen and Rosenbluth (1963, hereafter referred as FKR) developed a boundary layer theory of resistive tearing instability. They found that with a constant-ψ approximation in the resistive layer the growth rate scales as $S_R^{-3/5}$, and the width of resistive layer scales as $S_R^{-2/5}$. When the constant-ψ approximation is not satisfied, Coppi et al (1976) and Ara et al (1978) found another resistive tearing mode with a growth rate scaling as $S_R^{-1/3}$, and the width of the resistive layer scaling as $S_R^{-1/3}$. Numerical techniques have also been applied to the tearing problem (Killeen 1970, Steinolfson and Van Hoven, 1983), and both tearing mode scalings have been verified.

For the FKR tearing model to be applicable, it is required that $\nu \gg \omega \gg \omega_*$, where ν is the collision frequency, ω is the mode frequency, and ω_*

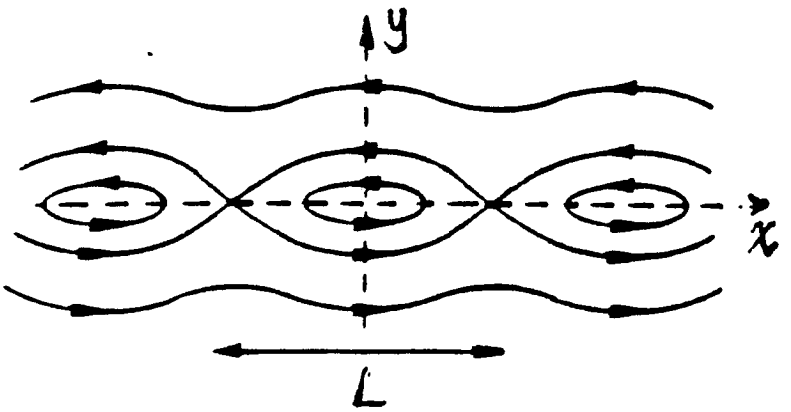

Figure 3.2: The magnetic island structure

is the diamagnetic frequency. When this condition is not satisfied, the drift tearing mode (see e.g. Hazeltine, 1977, Hazeltine and Meiss,1985) and the collisionless tearing mode (see e.g. Drake and Lee, 1977, Drake, 1978, Porcelli, 1991) have also been treated. However, here we consider only the resistive tearing mode.

The original FKR theory in slab geometry was extended to cylindrical geometry (Coppi et al, 1966, Furth et al, 1973), and toroidal geometry (Glasser et al, 1975, Glasser et al, 1977, Wesson, 1978), with the inclusion of important pressure and curvature effects. For the tearing modes of interest in this dissertation, instability requires that $\Delta' = \frac{1}{\psi_1}\frac{d\psi_1}{dy}\Big|_{0^-}^{0^+} > 0$, where Δ' is the logrithmatic jump of the magnetic flux function at the magnetic null plane. However, the stable modes can be forced unstable by perturbing the boundary surrounding an incompressible plasma (Hu, 1983, Hahm and Kulsrud, 1985, Shivamoggi, 1987). Also, the magnetic energy released during tearing instability has been

calculated for the constant ψ tearing mode by Adler et al (1980) and Bondeson and Sobel (1984). It is found that the magnetic energy released is proportional to Δ'. In the case without viscosity, 1/4 of the released magnetic energy goes into kinetic energy, and 3/4 into Joule heating.

In the above discussion, the current around the magnetic null plane is assumed to be regular, i.e. $B_0' \sim \vartheta(1)$. In order to explain the fast conversion of magnetic energy in the solar corona, a singular current sheet model with $B_0' \sim y^{-1/2}$ has been proposed (Chiueh and Zweibel, 1987). This current sheet was assumed to arise as a result of global magnetic stresses associated with ideal MHD instabilities in the corona. In this model the tearing growth rate scales as $S_R^{-1/5}$ and the width of the resistive layer scales as $S_R^{-2/5}$. Also the unstable band of wavenumbers is broader than in the regular current sheet. This model was later studied numerically (Liewer and Payne, 1989, 1990), and scalings that agree with the analytical results were obtained. In the above treatments, only one magnetic null plane was assumed to exist. If there exsist more than one magnetic null plane, they will influence with each other and make the tearing mode more complicated. Prichett, Lee and Drake (1980) studied the case of two magnetic null planes, termed double tearing. It is found that double tearing is very sensitive between the distance of the two tearing layers. When the distance is large, the system behaves like the constant-ψ tearing mode, however when they are very close, it behaves like the non-constant ψ tearing mode.

If in the equilibrium state as shown in Fig. 3.1, the external electric field E_z is not applied, then there exsits an equilibrium diffusion velocity $V_y = \frac{B_0''}{B_0'} S_R^{-1} \hat{y}$ across the equilibrium magnetic field. Even though this velocity is very

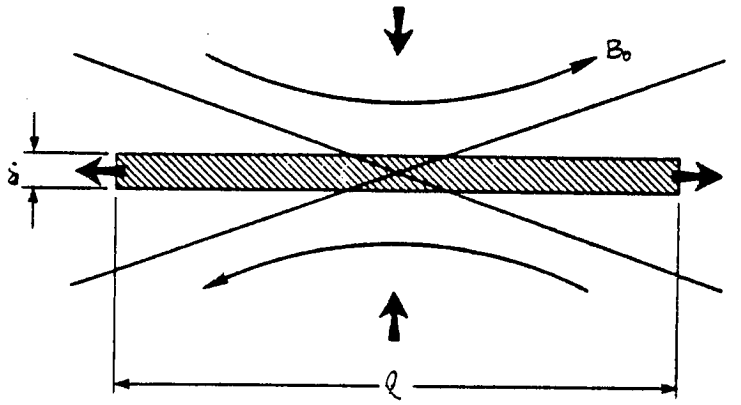

Figure 3.3: Steady state reconnection model

small, the time to cross the resistive layer (with width $S_R^{-2/5}$) is $\sim S_R^{3/5}$, which is comparable to the resistive tearing time (Dobrott et al, 1977). Hence the effect of this diffusion velocity is not negligible. It was found that the growth rate of the tearing modes are reduced, and the stability threshold is raised. Pollard and Taylor (1978) generalized the problem and considered arbitrary flow, but of the same order of magnitude. This generalized flow stabilizes the tearing modes if it is in the same direction as the diffusion velocity, while destabilizes the tearing modes if in the opposite direction.

Another class of problem assumes that the plasma is forced to flow in toward the magnetic null plane as shown in fig. 3.3. An x-point forms and magnetic field lines are reconnected in a resistive layer in the vicinity of the x-point. This is called steady state reconnection. There are many steady state reconnection models, but the major ones are the Sweet and Parker model and the Petschek model (Vasyliunas, 1975, Sonnerup, 1979, Hones, 1984, Priest,

1985, White, 1986). Using the idea that different models result from different inflow conditions, Priest and Forbes (1986) developed a theory for an entire family of incompressible models. Later on, Jardin and Priest (1988 a,b,) produced a family of incompressible models for the down stream region, which can be matched to the previous upstream solutions. These coupled solutions demonstrate how the overall configuration of the reconnection region responds to changes in the external boundary conditions. They also showed how the energy conversion in both the upstream and downstream regions depends on the particular form of the inflow (Jardine and Priest, 1988c).

Strauss (1988) considered the reconnection rate in the presence of tearing mode turbulence. Tearing mode turbulence in a three dimensional sheared magnetic fields can produce an anomalous electron viscosity (Diamond et al, 1984, Chiueh and Zweibel, 1986) and hyper-resistivity (Strauss, 1986), which yield a reconnection rate proportional to the ratio of the magnetic fluctuations to mean magnetic field.

Recently, in order to explain some new features observed in numerical simulations, Priest and Lee (1990) proposed a theory for fast steady-state magnetic reconnection. In this new model, the magnetic field lines in the inflow region are highly curved, instead of being almost straight, and a seperatrix jet of plasma is ejected from the central diffusion region along the magnetic seperatrix.

For the case where flow is parallel to the magnetic field, this problem is of interest in rotating plasmas and in astrophysics, for example, in coronal loops, the magnetopause boundary, in plasma streams in the solar wind, and in extragalactic jets. Below we describe works related to that described in

the remainder of this chapter (Chen and Morrison, 1990a). Assuming that the equilibrium flow and magnetic field have approximately the same spatial profile, Hofmann (1975) derived a dispersion relation in which the growth rate scales like $S_R^{-1/2}$. Paris and Sy (1983) found that the scaling remains unchanged when the flow is significantly below the Alfvén speed. Dobrowolny et al. (1983), by using the "frozen-in" equation for the internal solutions, have shown the possible existence of a number of scalings with and without viscosity. Bondeson and Persson (1986) used the constant-ψ approximation and Fourier transformed the internal equation in order to study the problem with and without viscosity. All of the above discussions pertain to the constant-ψ tearing mode. To our knowledge, no one has studied the effect of shear flow on the nonconstant-ψ tearing mode. Also, except for Hofmann (1975), the important effect of shear flow on the external ideal region has not been considered. Einaudi and Rubini (1986) have studied the problem numerically. They do not find instabilities when the flow shear is large, in contrast to the results of Paris and Sy (1983) and Bondeson and Persson (1986). Also Einaudi and Rubini (1986) and Wang et al (1988) observed a transition to ideal instability.

In remainder of this chapter, we adopt the boundary layer approach to study the resistive tearing mode in the presence of shear flow. Both the constant-ψ and nonconstant-ψ tearing modes are treated. By introducing an assumption similar to that of Dobrowolny et al , and carefully comparing the orders of the parameters involved, we arrive at general conclusions. In Table I we summarize the main conclusions that arise primarily from the affect of shear flow on the internal resistive region. Also, this table describes the transition to ideal instability. An additional main result of this chapter is the recognition

Table I.

	"constant-ψ" tearing mode	"nonconstant-ψ" tearing mode
$\left\|\frac{V_0'(0)}{B_0'(0)}\right\| \ll 1$	(a) The growth rate and scale length of the resistive region are respectively $\gamma \sim k^{2/5}\Delta'^{4/5}S^{-3/5}$, $\epsilon \sim (kS)^{-2/5}\Delta'^{1/5} \ll 1$ (b) The "constant-ψ" approximation is valid if $\epsilon\|\Delta'\| \ll 1$ (c) Small flow shear $V_0'(0)$ destabilizes the "constant-ψ" tearing mode	(a) The growth rate and scale length of the resistive region are respectively $\gamma \sim k^{2/3}S^{-1/3}$, $\epsilon \sim (kS)^{-1/3} \ll 1$ (b) In this limit, we have $\epsilon\|\Delta'\| \gg 1$, $1 - V_0'(0)^2/B_0'(0)^2 \neq 0$ (c) Small flow shear $V_0'(0)$ stabilizes the "nonconstant-ψ" tearing mode with sufficiently large Δ' (d) There exists a transition to ideal instability when Δ' becomes negative through $\Delta' = \infty$ (which is made possible by the flow on the external region)
$\left\|\frac{V_0''(0)}{B_0'(0)}\right\| \lesssim 1$	(a) The growth rate and scale length of the resistive region are respectively $\gamma \sim (k\|\Delta'\|)^{1/2}S^{-1/2}$, $\epsilon \sim (kS)^{-1/3} \ll 1$ (b) If $V_0'(0)V_0''(0) - B_0'(0)B_0''(0) \neq 0$, $\Delta' > 0$ instability criterion is removed (c) The "constant-ψ" approximation is valid if $\left\|\sqrt{(1 - V_0'(0)^2/B_0'(0)^2)\,\Delta'\epsilon}\right\| \ll 1$	
$\left\|\frac{V_0''(0)}{B_0'(0)}\right\| > 1$	stabilized	stabilized

that the presence of flow affects the analysis in the external ideal region. Flow can drastically change the value of Δ'. We are able to explain the numerical results obtained by Einaudi and Rubini, and Wang et al. In the present Chapter, viscosity is neglected, but this possibly important effect will be treated in chapt. 4.

In the next section, the basic equations are written down, and the notations are indicated. Section (3.3) is devoted to the shear flow affect on the external solutions. In Sec. (3.4), we discuss the internal solution in the limits of slow growth and fast growth, which correspond to the constant-ψ and nonconstant-ψ tearing modes, respectively. Also, we consider the limits of small flow shear and flow shear that is comparable to magnetic shear at the magnetic null plane. Comparisons are made with previous work. In Sec. (3.5), we discuss the transition to ideal instability. This is followed by a summary (3.6).

3.2 Basic Equations

The linearized equations, obtained by neglecting terms of second order, with the neglect of viscosity in Eq.(3.11), and assuming perturbations of the form $\sim e^{ikx+\gamma t}$, are

$$(\gamma + ikV_0)\left(\phi'' - k^2\phi\right) - ikV_0''\phi = ikB_0\left(\psi'' - k^2\psi\right) - ikB_0''\psi \qquad (3.1)$$

$$(\gamma + ikV_0)\psi - ikB_0\phi = S_R^{-1}\left(\psi'' - k^2\psi\right), \qquad (3.2)$$

where γ is the growth rate. The above equations are conventional, except we have scaled the growth rate γ by τ_H, the Alfvén time, rather than the resistive

diffusion time, and velocity by the Alfvén velocity, rather than the diffusion velocity.

Equations.(1) and (2) can be reduced to the form

$$S_R^{-1}\left[B_0^2(\gamma+ikV_0)\psi''''+\cdots\right]-B_0^2\left[k^2B_0^2+(\gamma+ikV_0)^2\right]+\cdots=0. \qquad (3.3)$$

The first part of Eq. (3) is introduced because of resistivity, and contains the highest derivative, the second part comes from the ideal equation. Since resistivity is very small ($S_R \ll 1$), it is only important in a thin layer around the ideal singularities. Thus one can separate the problem into two regions: the ideal exterior region which is governed by ideal equations; and the resistive interior layer around the singularity where resistivity is important. The solutions in the two regions are then matched asymptotically to give the growth rate (Wasow, 1948, 1953). This method was first developed in fluid dynamics, and is called the boundary layer approach.

Defining $u = \gamma/k + iV_0$ and $w = i\phi/u$, where w is the transverse displacement, Eqs. (1) and (2) become

$$\left(u^2w'\right)' - k^2u^2w = -\left[B_0\left(\psi''-k^2\psi\right)-B_0''\psi\right] \qquad (3.4)$$

$$u(\psi - B_0w) = (kS_R)^{-1}\left(\psi''-k^2\psi\right). \qquad (3.5)$$

In the case of ideal MHD ($S_R \to \infty$), and Eqs. (4) and (5) reduce to

$$\left[\left(u^2+B_0^2\right)w'\right]' - k^2\left(u^2+B_0^2\right)w = 0. \qquad (3.6)$$

Extending Eq. (6) into the complex y-plane, we note the presence of a singularity that occurs at a point where

$$u^2 + B_0^2 = \left(\frac{\gamma}{k} + iV_0\right)^2 + B_0^2 = 0. \tag{3.7}$$

If we assume a magnetic null plane occurs at $y = 0$; i.e., $B_0(0) = 0$, then by selecting an appropriate reference frame, we can always let the equilibrium velocity be zero at $y = 0$; i.e., $V_0(0) = 0$. In the case of very small growth rate γ, there exists a ideal MHD singularity near $y = 0$. For the tearing mode under discussion, this is the only singularity of interest. Below, we adopt the boundary layer approach and assume $B_0'(0) \neq 0$, and without loss of generality $B_0'(0) > 0$. Also, we assume $k \lesssim O(1)$, $V_0''(0)/B_0'(0) \lesssim O(1)$, and $B_0''(0)/B_0'(0) \lesssim O(1)$.

3.3 External Ideal Region

Away from the singularity discussed above, we can neglect resistivity ($S_R \to \infty$). This external ideal region is treated here with the assumption that the growth rate scales as follows:

$$\gamma \sim S_R^{-\sigma} \quad (0 < \sigma < 1).$$

Equations (4) and (5) reduce to

$$\psi - B_0 w = 0 \tag{3.8}$$

$$\left[\left(B_0^2 - V_0^2\right) w'\right]' - k^2 \left(B_0^2 - V_0^2\right) w = 0. \tag{3.9}$$

Now consider the behavior of Eqs. (8) and (9) as $y \to 0$. Taylor expanding the functions B_0 and V_0, keeping the leading term in Eq. (8) and keeping terms to $O(y^3)$ in Eq. (9) yields

$$\psi \sim B_0'(0) y w \tag{3.10}$$

$$\left\{\left[\left(B_0'(0)^2 - V_0'(0)^2\right)y^2 + \left(B_0'(0)B_0''(0) - V_0'(0)V_0''(0)\right)y^3\right]w'\right\}'$$

$$-k^2\left[\left(B_0'(0)^2 - V_0'(0)^2\right)y^2 + \left(B_0'(0)B_0''(0) - V_0'(0)V_0''(0)\right)y^3\right]w \sim 0. \quad (3.11)$$

The reason we retain the term $O(y^3)$ in Eq. (11) is to resolve the behavior for the case $B_0''^2(0) \sim V_0''^2(0)$.

Assuming $B_0'(0)^2 - V_0'(0)^2 \neq 0$, the solutions of Eqs. (10) and (11) behave as follows near $y = 0$

$$w \sim \frac{C_0}{y}\left(1 + \frac{B_0'(0)B_0''(0) - V_0'(0)V_0''(0)}{B_0'(0)^2 - V_0'(0)^2} y \ln|y|\right) + C_{1\pm} + \cdots$$

$$\psi \sim B_0'(0)C_0\left(1 + \frac{B_0'(0)B_0''(0) - V_0'(0)V_0''(0)}{B_0'(0)^2 - V_0'(0)^2} y \ln|y|\right) + B_0'(0)C_{1\pm}y + \cdots .$$

Formally, this solution is the same as the case without flow ($V_0'(0) = V_0''(0) = 0$), thus we can still define the matching quantity Δ'

$$\Delta' = \frac{1}{\psi}\frac{d\psi}{dy}\Big|_{0-}^{0+} = \frac{C_{1+} - C_{1-}}{C_0}.$$

When $C_0 \neq 0, \Delta'$ has finite value, and the leading order of ψ around the magnetic null plane is the constant $B_0'C_0$, this corresponds to the "constant ψ" tearing mode; however if $C_0 \to 0, \Delta' \to \infty$, and this corresponds to the nonconstant ψ tearing mode.

Note that Eqs. (8) and (9) have the same structure as those without shear flow, although they differ by the presence of the term with V_0^2. Thus the shear flow can have as much influence on Δ' as the magnetic field. This is not a surprise, since in this region the magnetic field is frozen into the flow. Hofmann (1975) has made some general comments on the shift of the wavenumber k_0

defined by $\Delta'(k_0) = 0$, caused by shear flow. In Appendix A we consider two examples that demonstrate the importance of shear flow when calculating Δ'.

To conclude this section, we obtain the constraint on the internal solutions that is imposed by the external solutions. To this end, we assume that the internal scale length is ϵ, where $\epsilon \ll 1$. In the border between the internal and external regions, we obtain from Eq. (10)

$$\psi \sim B_0'(0)\epsilon w \sim \frac{iB_0'(0)\epsilon}{\gamma/k + iV_0'(0)\epsilon}\phi \,. \tag{3.12}$$

Since the internal region is very thin, we can say that throughout, ψ, w, and ϕ scale as in relation (12). This is something similar to what Dobrowolny et al. (1983) called the "use of the frozen-in law for internal solutions." In the case of no shear flow, this reduces to

$$\psi \sim \frac{ikB_0'(0)\epsilon}{\gamma}\phi,$$

which is the assumption adopted in FKR (1963).

3.4 Internal Resistive Region

The internal resistive region is so thin that the derivatives of ψ and ϕ are very sensitive to the variation of ψ and ϕ in this region. This suggests the introduction of a stretched variable ζ, defined as

$$\zeta = \frac{y}{\epsilon},$$

where, as noted above, ϵ is the scale length of the internal region. Using Eqs. (1) and (2), the rescaled internal equations become

$$\left(\frac{\gamma}{kB_0'(0)\epsilon} + i\frac{V_0'(0)}{B_0'(0)}\zeta + \frac{1}{2}i\frac{V_0''(0)}{B_0'(0)}\epsilon\zeta^2\right)\frac{\partial^2\phi}{\partial\zeta^2} - i\epsilon\frac{V_0''(0)}{B_0'(0)}\phi =$$

$$\left(i\zeta + \frac{1}{2}i\frac{B_0''(0)}{B_0'(0)}\epsilon\zeta^2\right)\frac{\partial^2\psi}{\partial\zeta^2} - i\epsilon\frac{B_0''(0)}{B_0'(0)}\psi + O\left(\epsilon^2\right) \quad (3.13)$$

$$\left(\frac{\gamma}{kB_0'(0)\epsilon} + i\frac{V_0'(0)}{B_0'(0)}\zeta + \frac{1}{2}i\frac{V_0''(0)}{B_0'(0)}\epsilon\zeta^2\right)\psi - \left(i\zeta + \frac{1}{2}i\frac{B_0''(0)}{B_0'(0)}\epsilon\zeta^2\right)\phi =$$

$$\left(kB_0'(0)\epsilon^3 S\right)^{-1}\frac{\partial^2\psi}{\partial\zeta^2} + O\left(\epsilon^2\right). \quad (3.14)$$

Because of the difficulty in solving the above equations directly, we are going to discuss them in different parameter limits. There are two parameters of interest. The first is $\left|\frac{\gamma}{kB_0'(0)\epsilon}\right|$, which is the ratio of the local Alfvén time to the anticipated growth time, $1/\gamma$. Equivalently, this parameter is the ratio of the growth "phase velocity" to the Alfven velocity in the resistive region. The second parameter is $|V_0'(0)/B_0'(0)|$, which is the ratio of the flow shear to the magnetic field shear at the magnetic null plane. We consider two cases: case A has $|\gamma/kB_0'(0)\varepsilon| \ll 1$. Here the growth time is assumed to be long compared to the local Alfvén time scale. We refer to this as slow growth. Case B has $|\gamma/kB_0'(0)\varepsilon| \sim 1$ which we term fast growth. The case

$$\left|\frac{\gamma}{kB_0'(0)\epsilon}\right| \gg 1,$$

where the growth time scale is in the global Alfven regime, i.e.,

$$\left|\frac{\gamma}{kB_0'(0)\epsilon}\right| \sim 1$$

is not discussed here.

3.4.1 Slow growth; $\left|\frac{\gamma}{kB_0'(0)\epsilon}\right| \ll 1$.

As noted above, in this limit, the anticipated growth time scale is assumed to be much longer than the local Alfven time scale. We expect that

magnetic diffusion is going to be effective on this time scale. In the case of no flow, this limit corresponds to the classical "constant-ψ" tearing mode, which has a growth rate that scales as $S^{-3/5}$. Below we consider the problem in two different flow shear limits. In both cases, since the quantity that we want to match is $\psi \sim C_0 + C_\pm y = C_0 + C_\pm \epsilon\zeta$, order ϵ is the highest order to be matched.

Very small internal flow shear In this limit,

$$\left|\frac{V_0'(0)}{B_0'(0)}\right| \lesssim \left|\frac{\tilde{\gamma}}{kB_0'(0)\epsilon}\right|,$$

which implies

$$\left|\frac{kV_0'(0)\epsilon}{\tilde{\gamma}}\right| \lesssim 1,$$

i.e., the internal shear flow velocity is smaller than the growth "phase velocity."

We find it convenient to introduce a new variable φ defined by

$$\varphi = \left(\phi - \frac{V_0'(0)}{B_0'(0)}\psi\right) \Big/ \left(-i\frac{\gamma}{kB_0'(0)\epsilon}\right). \tag{3.15}$$

Using (12), the constraint imposed by the outer solution, implies $\varphi \sim \psi$. Now, let

$$\gamma = \tilde{\gamma}\hat{\gamma}, \tag{3.16}$$

where $\tilde{\gamma}$ is the measure of γ, and $\hat{\gamma}$ is a factor of $O(1)$. Equations (13) and (14) become:

$$\left(\frac{\tilde{\gamma}}{kB_0'(0)\epsilon}\right)^2 \hat{\gamma}\left(\hat{\gamma} + i\frac{kV_0'(0)\epsilon}{\tilde{\gamma}}\right)\frac{\partial^2\varphi}{\partial\zeta^2} = -\left[\zeta\left(1 - \frac{V_0'(0)^2}{B_0'(0)^2}\right) + i\frac{\tilde{\gamma}\hat{\gamma}}{kB_0'(0)\epsilon}\frac{V_0'(0)}{B_0'(0)}\right.$$

$$\left. + \epsilon\zeta^2\frac{B_0''(0)}{2B_0'(0)}\right]\frac{\partial^2\psi}{\partial\zeta^2} + \epsilon\frac{B_0''(0)}{B_0'(0)}\psi + O\left(\frac{\tilde{\gamma}}{kB_0'(0)\epsilon}\epsilon\right) \tag{3.17}$$

$$\left(\frac{\tilde{\gamma}}{kB_0'(0)\epsilon}\right)^2 \hat{\gamma}(\psi - \zeta\varphi) = \frac{\tilde{\gamma}}{(kB_0'(0))^2 \epsilon^4 S}\frac{\partial^2\psi}{\partial\zeta^2} + O\left(\frac{\tilde{\gamma}}{kB_0'(0)\epsilon}\epsilon\right). \tag{3.18}$$

Using $\left(\frac{\tilde{\gamma}}{kB_0'(0)\epsilon}\right)^2$ as a small parameter, we expand φ and ψ as follows:

$$\varphi = \sum_{n=0}^{\infty}\left(\frac{\tilde{\gamma}}{kB_0'(0)\epsilon}\right)^{2n}\varphi_n$$

$$\psi = \sum_{n=0}^{\infty}\left(\frac{\tilde{\gamma}}{kB_0'(0)\epsilon}\right)^{2n}\psi_n. \tag{3.19}$$

Consistency at leading order requires that

$$\frac{\tilde{\gamma}}{(kB_0'(0))^2 \epsilon^4 S_R} \sim O(1),$$

or

$$\left|\tilde{\gamma}\epsilon^2 S\right| \sim \left|\left(\frac{\tilde{r}}{kB_0'(0)\epsilon}\right)^2\right| \ll 1,$$

which implies the resistive skin diffusion time is much shorter than the anticipated growth time. For convenience, we set

$$\frac{\tilde{\gamma}}{(kB_0'(0))^2 \epsilon^4 S} = 4. \tag{3.20}$$

Thus $\tilde{\gamma}$ is the growth rate for the flow free tearing mode. Inserting Eq. (19) into Eqs. (17) and (18) yields to leading order

$$\frac{\partial^2\psi_0}{\partial\zeta^2} = 0; \tag{3.21}$$

hence, $\psi_0 = C_0 + C_1\zeta$. It is evident from Sec. (3.4) that matching to the external solutions can only be achieved if

$$\lim_{|\zeta|\to\infty}\psi_0 = \text{const.}$$

This implies $C_1 = 0$ and,

$$\psi_0 = C_0 = \text{const.} \tag{3.22}$$

This is the so-called "constant-ψ approximation."

In first order we obtain the equations

$$\hat{\gamma}\left(\hat{\gamma} + i\frac{kV_0'(0)\epsilon}{\tilde{\gamma}}\zeta\right)\frac{\partial^2\psi_0}{\partial\zeta^2} = -\zeta\frac{\partial^2\psi_1}{\partial\zeta^2} + \frac{\epsilon}{\left(\frac{\tilde{\gamma}}{kB_0'(0)\epsilon}\right)^2}\frac{B_0''(0)}{B_0'(0)}\psi_0 \tag{3.23}$$

$$\hat{\gamma}\left(\psi_0 - \zeta\varphi_0\right) = 4\frac{\partial^2\psi_1}{\partial\zeta^2}. \tag{3.24}$$

Let $\hat{\gamma}\varphi_0 = -h/4$, $\psi_0 = 1$, and define

$$\lambda = \frac{kV_0'(0)\epsilon}{\tilde{\gamma}} = \frac{V_0'(0)}{B_0'(0)}\frac{kB_0'(0)\epsilon}{\tilde{\gamma}} \gg \frac{V_0'(0)}{B_0'(0)}$$

$$\lambda_F = \frac{4\epsilon B_0''(0)/B_0'(0)}{\left(\frac{\tilde{\gamma}}{kB_0'(0)\epsilon}\right)^2} = \frac{1}{\tilde{\gamma}\epsilon S_R}\frac{B_0''(0)}{B_0'(0)}.$$

Using the above definition Eqs. (23) and (24) become

$$\left(\hat{\gamma} + i\lambda\zeta\right)\frac{\partial^2 h}{\partial\zeta^2} - \frac{1}{4}\zeta^2 h = \hat{\gamma}\zeta - \lambda_F \tag{3.25}$$

$$\frac{\partial^2\psi_1}{\partial\zeta^2} = \frac{1}{4}\left(\hat{\gamma} + \frac{1}{4}\zeta h\right). \tag{3.26}$$

These equations are equivalent to those obtained by Paris and Sy, which yield the following upon enforcing matching to the external solutions

$$\tilde{\gamma} = \left(\frac{\Gamma(1/4)}{2\pi\Gamma(3/4)}\right)^{4/5}\left(kB_0'(0)\Delta'^2\right)^{2/5}S_R^{-3/5},$$

$$\epsilon = \left(\frac{\Gamma(1/4)}{2^{7/2}\Gamma(3/4)\pi}\right)^{1/5}\left(kB_0'(0)\right)^{-2/5}\Delta'^{1/5}S_R^{-2/5},$$

$$\hat{\gamma} = 1 - \frac{2}{5}i\lambda\lambda_F + \lambda^2\left(\frac{\pi}{16} + \frac{7}{50}\lambda_F^2\right) + O\left(\lambda^3\right), \tag{3.27}$$

where $\Gamma(x)$ is the gamma function. In the case where the internal flow shear is very small, the internal analysis remains the same as that without flow, as a result the scaling is unchanged. From the results of Eqs. (27), Paris and Sy, and Bondeson and Persson conclude that small flow shear destabilizes the tearing mode. This conclusion does not necessariely follow since even though the flow shear at the magnetic null plane is small, the flow in the external region could be large, in which case there is a significant influence on the value of Δ', as discussed in Appendix A.

Now let us check our assumptions. For the expansion in Eqs. (19) to be valid, we require

$$\left|\frac{\gamma}{kB_0'(0)\epsilon}\right|^2 \sim (kS_R)^{-2/5}\,|\Delta'|^{6/5} \sim \epsilon\,|\Delta'| \ll 1. \tag{3.28}$$

For the boundary layer approach to be valid, we must have $\epsilon \ll 1$; i.e.,

$$(kS_R)^{-2/5}\,|\Delta'|^{1/5} \ll 1, \tag{3.29}$$

which implies the resistivity must be very small. When Δ' is very large, the above assumptions are not valid. When k is very small, we assume $\Delta' \sim 1/k$ and Eq. (28) yields

$$k \gg S_R^{-1/4}, \tag{3.30}$$

which is consistent with the limit obtained by FKR for the constant-ψ tearing mode in the case of no flow.

Comparable internal flow shear In this limit we suppose $|V_0'(0)/B_0'(0)| \sim O(1)$; i.e., the kinetic and magnetic energies are comparable in the internal region. This limit has been studied by Hofmann with the assumptions $V_0''(0) =$

0, $B_0''(0) = 0$, and $1 - V_0'(0)^2/B_0'(0)^2 > 0$. But here we remove these constraints. Equation (12) implies here $\psi \sim \phi$, and now in Eqs. (13) and (14) the natural expansion parameter is $\left(\frac{\gamma}{kB_0'(0)\epsilon}\right)$, instead of $\left(\frac{\gamma}{kB_0'(0)\epsilon}\right)^2$. Thus the equations analogous to Eqs. (19) are

$$\psi = \sum_{n=0}^{\infty} \left(\frac{\gamma}{kB_0'(0)\epsilon}\right)^n \psi_n$$

$$\phi = \sum_{n=0}^{\infty} \left(\frac{\gamma}{kB_0'(0)\epsilon}\right)^n \phi_n. \tag{3.31}$$

This is the same expansion as that adopted by Hofmann (1975). Similarly, we assume

$(kB_0'(0)\epsilon^3 S)^{-1} \sim O(1)$; i.e.,

$$\left|\gamma\epsilon^2 S_R\right| \sim \left|\frac{\gamma}{kB_0'(0)\epsilon}\right| \ll 1,$$

which implies the internal resistive skin time is much shorter than the anticipated growth time. For definiteness we choose $(kB_0'(0)\epsilon^3 S_R)^{-1} = 1$, which implies that the internal scale length

$$\epsilon = (kB_0'(0)S_R)^{-1/3}. \tag{3.32}$$

To leading order, the solutions that match to the external solutions, are

$$\frac{V_0'(0)}{B_0'(0)}\psi_0 = \phi_0 = \text{const.} \tag{3.33}$$

To first order Eqs. (13) and (14) yield

$$\frac{V_0'(0)}{B_0'(0)}\frac{\partial^2\phi_1}{\partial\zeta^2} = \frac{\partial^2\psi_1}{\partial\zeta^2} \tag{3.34}$$

$$\psi_0 + i\zeta\left(\frac{V_0'(0)}{B_0'(0)}\psi_1 - \phi_1\right) = \frac{\partial^2\psi_1}{\partial\zeta^2}. \tag{3.35}$$

Equation (34) implies $\phi_1 = \frac{B_0'(0)}{V_0'(0)}\psi_1$ (generality is not lost by dropping the two integration constants). We insert this into Eq. (35) and obtain

$$\psi_0 - i\zeta\frac{B_0'(0)}{V_0'(0)}\left(1 - \frac{V_0'(0)^2}{B_0'(0)^2}\right)\psi_1 = \frac{\partial^2\psi_1}{\partial\zeta^2}. \tag{3.36}$$

This is an inhomogeneous Airy equation, which has the following solution (Udell and Luke, 1962):

$$\psi_1 = e^{-i4m\pi/3}\lambda^2\pi\psi_0 Hi\left(-\lambda^{-1}\zeta e^{i2m\pi/3}\right), \tag{3.37}$$

where m is an integer,

$$\lambda = \left[i\frac{B_0'(0)}{V_0'(0)}\left(1 - \frac{V_0'(0)^2}{B_0'(0)^2}\right)\right]^{-1/3},$$

and $Hi(\zeta)$ is the inhomogeneous Airy function. It is algebraic for large $|\zeta|$ when $\left|\arg\left(e^{i2m\pi/3}\lambda^{-1}\zeta\right)\right| < 2\pi/3$. Choosing $m = 0$ if

$$\frac{B_0'(0)}{V_0'(0)}\left(1 - \frac{V_0'(0)^2}{B_0'(0)^2}\right) < 0,$$

and $m = -1$ if

$$\frac{B_0'(0)}{V_0'(0)}\left(1 - \frac{V_0'(0)^2}{B_0'(0)^2}\right) > 0,$$

yields a solution that is algebraic in a sector that includes the real axis. For large $|\zeta|$ the asymptotic behavior satisfies

$$\psi_1 \sim \frac{\lambda^3\psi_0}{\zeta}\left(1 + O\left(\frac{1}{\zeta^3}\right)\right), \tag{3.38}$$

which is valid in the sector $-7\pi/6 < \arg\zeta < \pi/6$, when

$$\frac{B_0'(0)}{V_0'(0)}\left(1 - \frac{V_0'(0)^2}{B_0'(0)^2}\right) < 0,$$

while if

$$\frac{B_0'(0)}{V_0'(0)}\left(1-\frac{V_0'(0)^2}{B_0'(0)}\right)>0,$$

it is valid in the sector $-\pi/6<\arg\zeta<7\pi/6$.

To second order, Eqs. (13) and (14) yield

$$\frac{V_0'(0)}{B_0'(0)}\frac{\partial^2\phi_2}{\partial\zeta^2}=\frac{\partial^2\psi_2}{\partial\zeta^2}+\frac{i\frac{V_0'(0)}{B_0'(0)}\frac{\partial^2\psi_1}{\partial\zeta^2}}{\zeta-i\frac{\gamma}{kV_0'(0)\epsilon}}-\frac{\epsilon}{\left(\frac{\gamma}{kB_0'(0)\epsilon}\right)^2}\frac{\frac{B_0''(0)}{B_0'(0)}\psi_0-\frac{V_0''(0)}{B_0'(0)}\phi_0}{\zeta-i\frac{\gamma}{kV_0'(0)\epsilon}} \tag{3.39}$$

$$\psi_1+i\frac{V_0'(0)}{B_0'(0)}\zeta\psi_2-i\zeta\phi_2+\frac{1}{2}i\frac{\epsilon}{\left(\frac{\gamma}{kB_0'(0)\epsilon}\right)^2}\left(\frac{V_0''(0)}{B_0'(0)}\psi_0-\frac{B_0''(0)}{B_0'(0)}\phi_0\right)=\frac{\partial^2\psi_2}{\partial\zeta^2}. \tag{3.40}$$

Note, we have kept the singularity at $\zeta=i\frac{\gamma}{kV_0'(0)\epsilon}$ in Eq. (39). Equation (39) yields upon insertion of Eq. (35), and integration

$$\frac{V_0'(0)}{B_0'(0)}\int_{-\infty}^{\infty}\frac{\partial^2\phi_2}{\partial\zeta^2}d\zeta=\int_{-\infty}^{\infty}\frac{\partial^2\psi_2}{\partial\zeta^2}d\zeta+i\int_{-\infty}^{\infty}\frac{\psi_0-\lambda^{-3}\psi_1\zeta}{\zeta-i\frac{\gamma}{kV_0'(0)\epsilon}}d\zeta$$

$$\frac{\epsilon}{\left(\frac{\gamma}{kB_0'(0)\epsilon}\right)^2}\int_{-\infty}^{\infty}\frac{d\zeta}{\zeta-i\frac{\gamma}{kV_0'(0)\epsilon}}\frac{B_0'(0)B_0''(0)-V_0'(0)V_0''(0)}{B_0'(0)^2}\psi_0. \tag{3.41}$$

Now consider each of the integrals of Eq. (41):

$$\int_{-\infty}^{\infty}\frac{\partial^2\psi_2}{\partial\zeta^2}d\zeta=\frac{\partial\psi_2}{\partial\zeta}\Big|_{-\infty}^{\infty}=\epsilon\Delta'\psi_0\Big/\left(\frac{\gamma}{kB_0'(0)\epsilon}\right)^2, \tag{3.42}$$

where Δ' is the matching quantity defined in Sec. (3.3). From Eq. (40) we obtain

$$\int_{-\infty}^{\infty}\frac{\partial^2\phi_2}{\partial\zeta^2}d\zeta=\int_{-\infty}^{\infty}\frac{V_0'(0)}{B_0'(0)}\frac{\partial^2\psi_2}{\partial\zeta^2}d\zeta$$

$$=\frac{V_0'(0)}{B_0'(0)}(\epsilon\Delta'\psi_0)\Big/\left(\frac{\gamma}{kB_0'(0)\epsilon}\right)^2; \tag{3.43}$$

$$\int_{-\infty}^{\infty} \frac{d\zeta}{\zeta - i\frac{\gamma}{kV_0'(0)\epsilon}} = \pm i\pi, \tag{3.44}$$

where we take upper sign when $\frac{\mathrm{Re}(\gamma)}{V_0'(0)} > 0$, otherwise lower sign is taken. Using the results of Eq. (38)

$$\int_{-\infty}^{\infty} \frac{\psi_0 - \lambda^{-3}\psi_1\zeta}{\zeta - i\frac{\gamma}{kV_0'(0)\epsilon}} d\zeta = \int_{\Gamma} \frac{\psi_0 - \lambda^{-3}\psi_1\zeta}{\zeta - i\frac{\gamma}{kV_0'(0)\epsilon}} d\zeta,$$

where Γ is a contour in complex ζ plane. If

$$\frac{B_0'(0)}{V_0'(0)}\left(1 - \frac{V_0'(0)^2}{B_0'(0)^2}\right) < 0,$$

Γ is closed in the lower half plane, while if

$$\frac{B_0'(0)}{V_0'(0)}\left(1 - \frac{V_0'(0)^2}{B_0'(0)^2}\right) > 0,$$

Γ is closed in the upper half plane. So if

$$\frac{B_0'(0)}{V_0'(0)}\left(1 - \frac{V_0'(0)^2}{B_0'(0)^2}\right)\frac{\mathrm{Re}(\gamma)}{V_0'(0)} < 0,$$

then

$$\int_{-\infty}^{\infty} \frac{\psi_0 - \lambda^{-3}\psi_1\zeta}{z - i\frac{\gamma}{kV_0'(0)\epsilon}} d\zeta = 0. \tag{3.45}$$

We obtain from Eq. (41) upon insertion of Eqs. (42), (43), (44), and (45)

$$\Delta' = \pm i\pi \frac{B_0''(0)B_0'(0) - V_0'(0)V_0''(0)}{B_0'(0)^2 - V_0'(0)^2}.$$

Since a pure imaginary Δ' cannot be made equal to the external real Δ', matching cannot be achieved in this case.

If

$$\frac{B_0'(0)}{V_0'(0)}\left(1 - \frac{V_0'(0)^2}{B_0'(0)^2}\right)\frac{\mathrm{Re}(\gamma)}{V_0'(0)} > 0, \tag{3.46}$$

$$\int_{-\infty}^{\infty} \frac{\psi_0 - \lambda^{-3}\psi_1\zeta}{z - i\frac{\gamma}{kV_0'(0)\epsilon}} d\zeta = \pm 2\pi i \psi_0 + O\left(\frac{\gamma}{kV_0'(0)\epsilon}\right), \tag{3.47}$$

where we take the upper sign when $B_0'(0)/V_0'(0)\,(1 - V_0'(0)^2/B_0'(0)^2) > 0$, otherwise the lower sign is taken. We obtain from Eq. (41) upon insertion of Eqs. (42), (43), (44), and (47)

$$\gamma = \pm(2\pi S_R)^{-1/2} \sqrt{\left|kV_0'(0)\left(1 - \frac{V_0'(0)^2}{B_0'(0)^2}\right)\right| \left(\Delta' \mp i\pi \frac{B_0''(0)B_0'(0) - V_0'(0)V_0''(0)}{B_0'(0)^2 - V_0'(0)^2}\right)}, \tag{3.48}$$

where the sign of the growth rate γ is determined by Eq. (46). Obviously, the above analysis is not valid when $1 - V_0'(0)^2/B_0'(0)^2 = 0$.

From Eq. (46) we see that only when

$$\left(1 - \frac{V_0'(0)^2}{B_0'(0)^2}\right) > 0$$

does there exist a growing tearing mode. When

$$\left(1 - \frac{V_0'(0)^2}{B_0'(0)^2}\right) < 0,$$

the kinetic energy overpowers the magnetic energy in the internal resistive region, the flow freezes the magnetic field and suppresses the tearing instability. This is not necessarily accompanied by an ideal mode. Numerically, Einaudi and Rubini (1986) solved the initial value problem for the following equilibrium profiles: $B_0 = \tanh y$, $V_0 = V_0 \tanh by$. They found the same scaling as Eq. (48) when $|V_0'(0)/B_0'(0)| \sim O(1)$. However, they also found that the tearing mode could be stabilized at some value $|V_0'(0)/B_0'(0)| < 1$, instead of $|V_0'(0)/B_0'(0)| = 1$. This can be explained by the influence of shear flow on the value of Δ'.

For the hyperbolic tangent profiles, $B_0''(0)B_0'(0) - V_0''(0)V_0'(0) = 0$, and the negative value of Δ' can stabilize the tearing mode. In the first example

of Appendix A, we evaluate Δ' for a piecewise linear approximation of tanh (cf. Eqs. (A1) and (A2)). Assume that V_0, the quantity that measures the magnitude of the flow, is less than unity. From Eqs. (A7), (A9) and Fig. 3.3, we conclude that when the flow shear length b is less than the magnetic shear length, but

$$\frac{V_0'(0)^2}{B_0'(0)^2} = \frac{V_0^2}{b^2} < 1,$$

then at some value of b, $\Delta' = 0$. This qualitatively explains the stabilization seen in the numerical works of Einaudi and Rubini (1975).

The result of Eq. (48) is different from that of Hofmann in that the second derivatives of the magnetic field and shear flow are included. This is far from trivial since it removes the $\Delta' > 0$ instability criterion if $B_0'(0)B_0''(0) - V_0'(0)V_0''(0) \neq 0$. Paris and Sy, Bondeson and Persson arrived at a similar conclusion by neglecting $V_0''(0)$, but in their growth rate expression, they omitted the very important factor of $1 - V_0'(0)^2/B_0'(0)^2$. Thus their growth rate does not stabilize when $V_0'(0)^2/B_0'(0)^2 > 1$. Einaudi and Rubini (1975) noticed the discrepancy between their numerical results and the growth rate expression of Ref. 4. Our result explains this discrepancy.

To end this section, let us check our assumptions. From Eqs. (32) and (48) we obtain

$$\left|\frac{\gamma}{kB_0'(0)\epsilon}\right| \sim \left|\sqrt{\epsilon\left(1 - \frac{V_0'(0)^2}{B_0'(0)^2}\right)\Delta'}\right| \ll 1. \tag{3.49}$$

The validity of our boundary layer approach requires $\epsilon \ll 1$; i.e.,

$$(kS_R)^{-1/3} \ll 1, \tag{3.50}$$

which requires the resistivity must be small. Equation (49) is similar to Eq. (28), it cannot be satisfied when $|\Delta'|$ is very large except in the case $1 - \frac{V_0'(0)^2}{B_0'(0)^2} \to 0$. We consider the case of very large $|\Delta'|$ in the next section.

3.4.2 Fast growth; $\left|\frac{\gamma}{kB_0'(0)\epsilon}\right| \sim 1$

In this limit, the anticipated time scale is comparable with the local Alfven time. In the case of no flow, this limit corresponds to the nonconstant-ψ tearing mode with a growth rate that scales as $S_R^{-1/3}$ (Coppi et al, 1976, Ara et al, 1978).

Equation (12) implies in this limit that $\psi \sim \phi$, assuming $|V_0'(0)/B_0'(0)| \lesssim O(1)$.

Neglecting the terms of order $O(\varepsilon)$, Eqs. (13) and (14) become

$$\left(\frac{\gamma}{kB_0'(0)\epsilon} + i\frac{V_0'(0)}{B_0'(0)}\zeta\right)\frac{\partial^2\phi}{\partial\zeta^2} = i\zeta\frac{\partial^2\psi}{\partial\zeta^2} \tag{3.51}$$

$$\left(\frac{\gamma}{kB_0'(0)\epsilon} + i\frac{V_0'(0)}{B_0'(0)}\zeta\right)\psi - i\zeta\phi = \frac{1}{kB_0'(0)\epsilon^3 S_R}\frac{\partial^2\psi}{\partial\zeta^2}. \tag{3.52}$$

Defining

$$A = \frac{\gamma}{kB_0'(0)\epsilon} + i\frac{V_0'(0)}{B_0'(0)}\zeta, \qquad \tilde{\phi} = \frac{i\phi}{A},$$

Eqs. (51), (52) become

$$\frac{\partial}{\partial\zeta}\left(A^2\frac{\partial\tilde{\phi}}{\partial\zeta}\right) = -\zeta\frac{\partial^2\psi}{\partial\zeta^2} \tag{3.53}$$

$$A(\psi - \zeta\tilde{\phi}) = \frac{1}{kB_0'(0)\epsilon^3 S_R}\frac{\partial^2\psi}{\partial\zeta^2}. \tag{3.54}$$

Integration of Eq. (53) yields

$$\zeta\frac{\partial\psi}{\partial\zeta} - \psi = -A^2\frac{\partial\tilde{\phi}}{\partial\zeta} + C_0 \equiv X, \tag{3.55}$$

where C_0 is a constant and we have defined a new dependent variable X.

Substituting Eq. (55) into Eq. (54), we obtain

$$\frac{1}{kB_0'(0)\epsilon^3 S_R}\left[\frac{\partial^2 X}{\partial\zeta^2}-\left(\frac{2}{\zeta}+\frac{\partial A/\partial\zeta}{A}\right)\frac{\partial X}{\partial\zeta}\right]=AX+\frac{\zeta^2}{A}(X-C_0)\,. \qquad (3.56)$$

In the case of very small flow shear, i.e., $|V_0'(0)/B_0'(0)| \ll 1$ we expand X and γ as

$$X=\sum_{n=0}^{\infty}X_n\left(i\frac{V_0'(0)}{B_0'(0)}\right)^n$$

$$\gamma=\sum_{n=0}^{\infty}\gamma_n\left(i\frac{V_0'(0)}{B_0'(0)}\right)^n. \qquad (3.57)$$

The leading order of Eq. (56) is

$$\frac{1}{kB_0'(0)\epsilon^3 S_R}\left(\frac{\partial^2 X_0}{\partial\zeta^2}-\frac{2}{\zeta}\frac{\partial X_0}{\partial\zeta}\right)=\frac{\gamma_0}{kB_0'(0)\epsilon}X_0+\frac{kB_0'(0)\epsilon}{\gamma_0}\zeta^2(X_0-C_0)\,. \qquad (3.58)$$

This equation has been solved by Coppi et al (1976) in the case where $\Delta' < 0$. In Appendix B we treat the case where $\left|\Delta'(kS_R)^{-1/3}\right| \gg 1$. In the case where $\Delta' \to \infty$, Eq. (58) has the solution

$$C_0=0, \qquad X_0=e^{-\zeta^2/2},$$

$$\frac{\gamma_0}{kB_0'(0)\epsilon}=\frac{1}{kB_0'(0)\epsilon^3 S_R}=1. \qquad (3.59)$$

To first order Eq. (56) yields

$$\frac{\partial^2 X_1}{\partial\zeta^2}-\frac{2}{\zeta}\frac{\partial X_1}{\partial\zeta}-\left(1+\zeta^2\right)X_1=\frac{\partial X_0}{\partial\zeta}+\zeta\left(1+\frac{\gamma_1}{\gamma_0}\right)X_0-\zeta^2\left(\zeta+\frac{\gamma_1}{\gamma_0}\right)X_0.$$

The appropriate solution to the above equation is

$$\gamma_1=0$$

$$X_1=\frac{1}{6}\zeta^3 e^{-\zeta^2/2}. \qquad (3.60)$$

To the second order, Eq. (56) yields

$$\frac{\partial^2 X_2}{\partial \zeta^2} - \frac{2}{\zeta}\frac{\partial X_2}{\partial \zeta} - \left(1+\zeta^2\right) X_2 = \frac{\partial X_1}{\partial \zeta} - \left(\zeta + \frac{\gamma_1}{\gamma_0}\right)\frac{\partial X_0}{\partial \zeta} + \left(\frac{\gamma_1}{\gamma_0}X_1 + \frac{\gamma_2}{\gamma_0}X_0 + \zeta X_1\right)$$

$$+ \zeta^2\left[-\left(\zeta + \frac{\gamma_1}{\gamma_0}\right)X_1 - \frac{\gamma_2}{\gamma_0}X_0 + \left(\zeta + \frac{\gamma_1}{\gamma_0}\right)^2 X_0\right]$$

$$= e^{-\zeta^2/2}\left[-\frac{1}{6}\zeta^6 + \zeta^4 + \left(\frac{3}{2} - \frac{\gamma_2}{\gamma_0}\right)\zeta^2 + \frac{\gamma_2}{\gamma_0}\right].$$

The appropriate solutions of the above equations are

$$X_2 = \frac{1}{72}\zeta^6 - \frac{3}{32}\zeta^4 - \frac{5}{16}\zeta^2$$

$$\frac{\gamma_2}{\gamma_0} = \frac{5}{8}. \tag{3.61}$$

Collecting the results of Eqs. (59), (60), and (61) yields

$$\gamma = \gamma_0 + i\frac{V_0'(0)}{B_0'(0)}\gamma_1 + \left(i\frac{V_0'(0)}{B_0'(0)}\right)^2 \gamma_2 + \cdots$$

$$= (kB_0'(0))^{2/3} S_R^{-1/3}\left(1 - \frac{5}{8}\frac{V_0'(0)^2}{B_0'(0)^2} + \cdots\right). \tag{3.62}$$

Thus we see that shear flow in this ordering tends to stabilize the $\Delta' = \infty$ tearing mode.

For the case where $\Delta' \neq \infty$, but $\left|(kS_R)^{-1/3}\Delta'\right| \gg 1$, there is a correction of $O\left(\frac{1}{(ks)^{-1/3}\Delta'}\right)$ to the case of no flow (see Appendix B). Including a small shear flow, the growth rate is

$$\frac{\gamma}{\gamma_0} = 1 - \frac{5}{8}\frac{V_0'(0)^2}{B_0'(0)^2} + O\left(\frac{1}{(kS_R)^{-1/3}\Delta'}\frac{V_0'(0)}{B_0'(0)}\right). \tag{3.63}$$

For sufficient large $|\Delta'|$, we can say that the small shear flow is stabilizing.

When $V_0'(0)/B_0'(0) \sim O(1)$, the quantity A in Eq. (56) is still $\sim O(1)$. The scaling should remain unchanged except in the case where $1 - V_0'(0)^2/B_0'(0)^2 \to 0$. When $1 - V_0'(0)^2/B_0'(0)^2 \to 0$, the scalings change to the constant-ψ tearing mode scaling as we discussed in the end of last section. Thus the tearing mode with $\left|(kS_R)^{-1/3}\Delta'\right| \gg 1$ is stabilized when $1-V_0'(0)^2/B_0'(0)^2 \to 0^-$, approaching zero from below. It is reasonable to ascribe this result to the idea that the flow freezes the magnetic field and suppresses the tearing mode with $\left|(kS_R)^{-1/3}\Delta'\right| \gg 1$ when $1 - V_0'(0)^2/B_0'(0)^2 < 0$. This conjecture agrees with the numerical results of Einaudi and Rubini (1986).

Our assumption $\left|\frac{\gamma}{kB_0'(0)\epsilon}\right| \sim 1$ is always satisfied if $|\epsilon\Delta'| \gg 1$ and $1 - V_0'(0)^2/B_0'(0)^2 \not\to 0$. This is seen by examination of Eqs. (59), (63), and (B15). The requirement of $\epsilon \ll 1$ leads to $(kS_R)^{-1/3} \gg 1$, which requires very small resistivity.

3.5 Transition to Ideal Instability

Since shear flow itself can drive Kelvin-Helmholtz instability, a potentially powerful instability, the results of the preceding sections could be overshadowed. However, the necessary condition for this to happen is that the flow velocity not be bounded by the magnetic field everywhere, in any reference frame (Kent, 1968). For all of the tearing modes treated here there exist velocity profiles that are Kelvin-Helmholtz stable.

An interesting case is where the Kelvin-Helmholtz instability is near marginality, since here its growth rate can be comparable to that of tearing. Also, the tearing analysis in the external ideal region corresponds to that of marginal ideal instability, so here is a natural place to begin tracking the tran-

sition from tearing to Kelvin-Helmholtz instability. In the papers by Einaudi and Rubini (1986), and Wang et al (1988), this transition was tracked numerically as the appropriate values of the flow parameters were varied. The profiles considered were $B_0 = \tanh y$ and either $V_0 = V_0 \mathrm{sech}(y/b)$ or $V_0 = V_0 \mathrm{sech}^2(y/b)$. In this section we track this transition analytically by expanding about the ideal instability at marginality.

For tractability we approximate the hyperbolic profiles by piecewise linear profiles, as discussed in example 2 of Appendix A, although we have changed frame so that $V_0(0) = 0$. These profiles are linear in three regions: $|y| < b$, $y > b$, and $y < -b$. Consider first the ideal problem with $b \leq 1$ and $|y| < b$. For convenience we define

$$H = \sqrt{u^2 + B_0^2} w; \tag{3.64}$$

hence, Eq. (6) can be rewritten as

$$\frac{d^2 H}{dy^2} - \left[k^2 - \frac{\omega^2/k^2}{(y^2 - \omega^2/k^2)^2} \right] H = 0, \tag{3.65}$$

where $\omega = -i\gamma$.

Marginal solution are given by solving the equation

$$\frac{d^2 H_N}{dy^2} - k^2 H_N = 0 \tag{3.66}$$

in the region $|y| < b$, and matching the solutions at $y = \pm b$ and $y = \pm 1$ to the appropriately decaying solution as $y \to \pm\infty$. Equation (66) has two solutions:

$$H_N^{\infty} = \sinh ky \tag{3.67}$$

with the matching condition $\bar{k} - \tanh \bar{k} + \bar{k}\beta \tanh \bar{k} = 0$; and

$$H_N^0 = \cosh ky \tag{3.68}$$

with the matching condition $1 - \bar{k}\tanh\bar{k} - \bar{k}\beta = 0$. In the above expressions, $\bar{k}$ and β are defined as in Eq. (A10). For the details of matching, we refer the reader to Appendix A. Hereafter, we denote the quantities corresponding to neutral solution by N, and fix the wavevector k.

From Eqs. (67), (68), (A3), and (A10), we see that H_N^∞ corresponds to the external tearing solution for the case where $\Delta' = \infty$; similarly, H_N^0 corresponds to $\Delta' = 0$.

Now upon multiplying Eq. (65) by H_N and Eq. (66) by H, and subtracting, we obtain

$$\frac{d}{dy}\left[H_N\frac{dH}{dy} - H\frac{dH_N}{dy}\right] = -\frac{\omega^2/k^2}{\left[y^2 - \omega^2/k^2\right]^2}HH_N. \tag{3.69}$$

Defining $Y = w'/w$, yields with Eq. (64)

$$\frac{1}{H}\frac{dH}{dy} = Y(y) + \frac{y}{y^2 - \omega^2/k^2}. \tag{3.70}$$

Shortly, we will need to use Eq. (70).

Consider now, instability that is near to the neutral mode; i.e., $H \to H_N$ and $\omega = \delta\omega$. Correspondingly, we assume the flow parameters

$$V_0 = V_{0N} + \delta V_0, \qquad b = b_N + \delta b.$$

In the discussion below we neglect terms of second order.

Integration of Eq. (69) yields

$$HH_N\left(\frac{1}{H}\frac{dH}{dy} - \frac{1}{H_N}\frac{dH_N}{dy}\right)\Big|_{-b_m^+}^{b_m^-} = -\int_{-b_m^+}^{b_m^-}\frac{\omega^2/k^2}{\left(y^2 - \omega^2/k^2\right)^2}HH_N dy, \tag{3.71}$$

where the limit b_m is the smaller of b and b_N. The upper and lower sign is used to avoid the discontinuity at $y = b_m$ as seen in Eq. (75). Using Eq. (70) and the symmetry of the problem, we obtain

$$\left(\frac{1}{H}\frac{dH}{dy} - \frac{1}{H_N}\frac{dH_N}{dy}\right)\Bigg|_{-b_m^+}^{b_m^-} \approx 2\left[Y\left(b_m^-\right) - Y_N\left(b_m^-\right)\right]. \tag{3.72}$$

Since the solution $Y(y)$ depends implicitly on ω, and the flow parameters V_0 and b, we have

$$Y\left(\omega, b, V_0; y\right) - Y_N\left(0, b_N, V_{0N}; y\right) \approx \frac{\partial Y(y)}{\partial \omega}\Bigg|_{\substack{\omega=0 \\ b=b_N \\ V_0=V_{0N}}} \delta\omega + \frac{\partial Y(y)}{\partial b}\Bigg|_{\substack{\omega=0 \\ b=b_N \\ V_0=V_{0N}}} \delta b$$

$$+ \frac{\partial Y(y)}{\partial V_0}\Bigg|_{\substack{\omega=0 \\ b=b_N \\ V_0=V_{0N}}} \delta V_0. \tag{3.73}$$

Using Eq. (6), $Y(y)$ satisfies the Riccatti equation

$$\frac{dY}{dy} = k^2 - Y^2 - \frac{\left(u^2 + B_0^2\right)'}{u^2 + B_0^2} Y,$$

$$Y(\pm 1) = \mp k. \tag{3.74}$$

$\left(u^2 + B_0^2\right) Y$ is continuous, as seen by the integration of Eq. (74), but $Y(y)$ must have a jump at $y = b$

$$Y\left(b^-\right) = \frac{y^2 - \left(\frac{\omega}{k} - V_0\right)^2}{y^2 - \omega^2/k^2} Y\left(b^+\right). \tag{3.75}$$

For $|y| < b$, we can write the solution of Eq. (74) as follows

$$Y\left(\omega, b, V_0; y\right) = f(\omega; y) - f\left(\omega; b^-\right) + \frac{y^2 - \left(\frac{\omega}{k} - V_0\right)^2}{y^2 - \omega^2/k^2} Y\left(b^+\right), \tag{3.76}$$

where $f(\omega, y)$ is a general solution of the equation

$$\frac{dY}{dy} = k^2 - Y^2 - \frac{2y}{y^2 - \omega^2/k^2} Y.$$

Assuming $y^2 - V_0^2 \neq 0$ for $b < |y| < 1$, $\left.\frac{\partial y(b_m^-)}{\partial \omega}\right|_{\substack{\omega=0 \\ b=b_N \\ V_0=V_{0N}}}$ is a real quantity up to first order. Let

$$g \equiv \left.\frac{\partial Y(b_m^-)}{\partial \omega}\right|_{\substack{\omega=0 \\ b=b_N \\ V_0=V_{0N}}} . \tag{3.77}$$

Using Eqs. (74) and (76), we have

$$\left.\frac{\partial Y(y)}{\partial b}\right|_{\substack{\omega=0 \\ b=b_N \\ V_0=V_{0N}}} = -\frac{V_{0N}^2}{b_N^2} k \left[k - \beta_N Y_N\left(b_N^+\right)\right]$$

$$\left.\frac{\partial Y(y)}{\partial V_0}\right|_{\substack{\omega=0 \\ b=b_N \\ V_0=V_{0N}}} = -\frac{2V_{0N}}{b_N^2} Y_N\left(b_N^+\right) + \left(1 - \frac{V_{0N}^2}{b_N^2}\right) \left.\frac{\partial Y_N(y)}{\partial V_{0N}}\right|_{y=b_N^+}, \tag{3.78}$$

where β_N is defined as in Eq. (A10), and $Y_N\left(b_N^+\right)$ satisfies Eq. (A11). Note, $Y(y)$ is independent of the parameter b_N for $b < y < 1$.

Combining Eqs. (72), (73), (77), (78), the right-hand side of Eq. (71) becomes

$$HH_N \left(\frac{1}{H}\frac{dH}{dy} - \frac{1}{H_N}\frac{dH_N}{dy}\right)\Bigg|_{-b_m^+}^{b_m^-} \approx 2H_N(b_N)^2 \left[g\delta\omega - \frac{V_{0N}^2}{b_N^2} k \left[k - \beta_N Y_N\left(b_N^+\right)\right] \delta b \right.$$

$$\left. + \left(2\frac{V_{0N}}{b_N^2} Y_N\left(b_N^+\right) - \left(1 - \frac{V_{0N}^2}{b_N^2}\right) \frac{\partial Y\left(b_N^+\right)}{\partial V_0}\right) \delta V_0 \right]. \tag{3.79}$$

For the right-hand side of Eq. (71), we evaluate the integral by considering the contour shown in Fig. 3.4. Assuming the imaginary part of ω is less than zero, we obtain

$$-\int_{-b_m}^{b_m} \frac{\omega^2/k^2}{\left(y^2 - \omega^2/k^2\right)^2} HH_N dy = -\frac{2\pi i \omega^2}{k^2} \frac{d}{dy}\left[\frac{H_N^2}{(y - \omega/k)^2}\right]\Bigg|_{y=-\omega/k}$$

$$= \begin{cases} \frac{1}{2} i\pi k\omega \text{ for } H_N = H_N^\infty = \sinh ky, \\ -\frac{1}{2} i\pi \frac{k}{\omega} \text{ for } H_N = H_N^0 = \cosh ky. \end{cases} \tag{3.80}$$

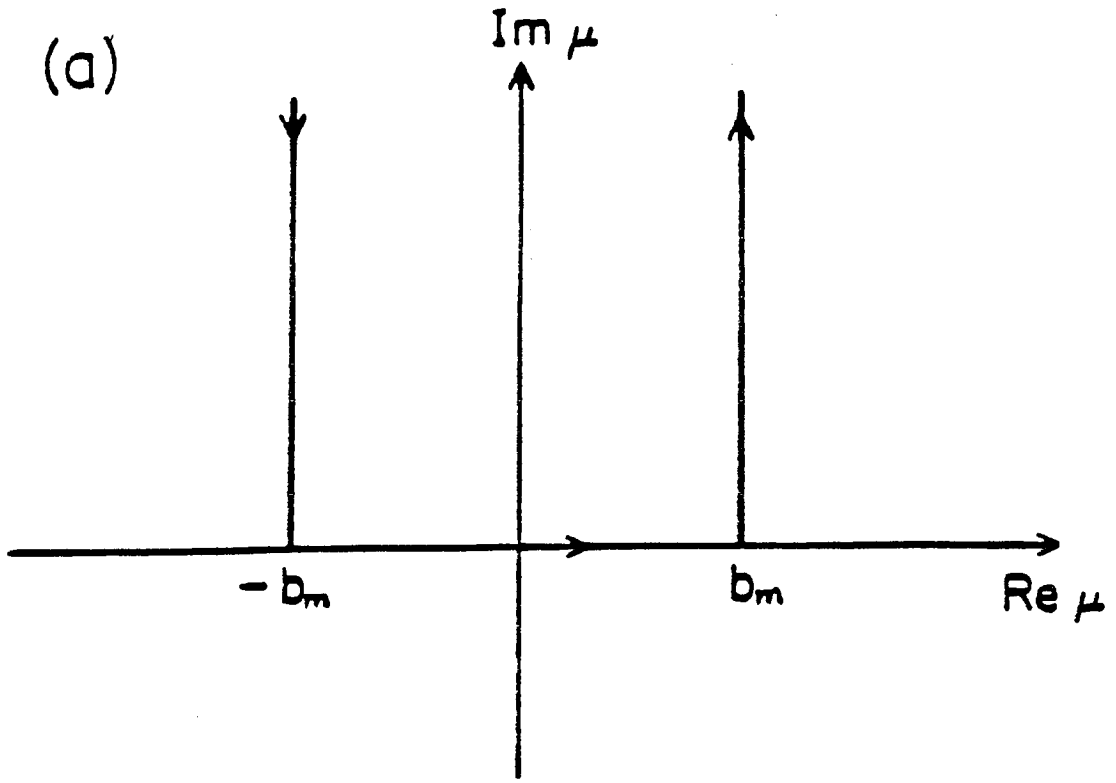

Figure 3.4: Integral contour

We insert Eq. (79) and (80) into Eq. (71). For the case $H_N = H_N^0$, there is no valid solution, since Eq. (80) diverges and Eq. (79) vanishes in the limit $\delta b = \delta\omega = \delta V_0 = 0$. This means the neutral mode corresponding to $\Delta' = 0$ is an isolated mode (at fixed k).

For the case $H_N = H_N^\infty$ the mode is not isolated and we obtain the following:

$$\delta\omega = \frac{2\sinh^2(kb)}{\frac{1}{2}ik\pi - 2\left(\sinh^2(kb_N)\right)g} \times [-\frac{V_{0N}^2}{b_N^2}k\left(k - \beta_\infty Y_N\left(b_N^+\right)\right)\delta b$$

$$- \left(\frac{2V_{0N}}{b_N^2}Y_N^\infty\left(b_N^+\right) - \left(1 - \frac{V_{0N}^2}{b_N^2}\right)\frac{\partial Y_N^\infty\left(b_N^+\right)}{\partial V_0}\right)\delta V_0] \qquad (3.81)$$

For the profile analogous to that studied by Wang et al, b is set to 1, $Y_N(y) = -k$ for $|y| > 1$, and $\beta = 1 - V_0^2$. Then Eq. (81) becomes

$$\delta\omega = \frac{4kV_{0N}\sinh^2 k}{\frac{1}{2}ik\pi - 2g\sinh^2 k}\delta V_0.$$

There exists instability when $\delta V_0 > 0$, meanwhile $\delta\beta < 0$. Now we evaluate V_{0N}, the flow parameter corresponding to the neutral mode for $k = 0.45$. This is done in order to compare with Wang et al's results. Using Eq. (A15) gives

$$1 - V_{0N}^2 = \beta_\infty = -\frac{k - \tanh k}{k\tanh k},$$

whence, $V_{0N} \approx 1.08$. Wang et al. (1988) observed strong ideal instability at $V_0 \approx 1.2$. This roughly agrees with our above analysis.

For the profile discussed by Einaudi and Rubini (1986) V_0 is fixed at unity. Thus Eq. (78) becomes

$$\delta\omega = \frac{-2\frac{V_{0N}^2}{b_N^2}k\left(k - \beta_\infty Y_N\left(b_N^+\right)\right)\sinh^2(kb_N)\,\delta b}{\frac{1}{2}ik\pi - 2g\sinh^2(kb)}.$$

We see from Eq. (A12) and Fig. 1a that $\left|Y_N^{\infty}\left(b_N^{+}\right)\right| < k$, and $|\beta_{\infty}| < 1$. Thus the instability appears when $\delta b < 0$, meanwhile $\delta\beta < 0$, as a result of Eq. (A13).

In both cases, when the flow parameter is varied so that β is decreased from β_{∞}, there exists instability. Using Fig. 3.3, we conclude that an ideal instability appears when Δ' becomes negative through ∞.

When a small resistivity is included in the above problem, there is no influence on the neutral mode corresponding to $\Delta' = 0$; while for the neutral mode corresponding to $\Delta' = \infty$, the growth rate is increased from zero to $(kB_0'(0))^{2/3} S_R^{-1/3}$. When the flow parameters are perturbed further, the Δ' value becomes negative and there exists a mixture of tearing and ideal instabilities. This connection of the tearing and ideal modes is similar to that discussed Ara et al. (1978).

3.6 Summary

In this Chapter, we have systematically studied the tearing mode in the presence of shear flow. It was found that shear flow has a significant influence on both the constant-ψ and the nonconstant-ψ tearing modes. In the external ideal region, the shear flow is as important as the magnetic field, some flow profiles can dramatically change the value of the matching quantity Δ'. It can change the scaling from constant to nonconstant ψ tearing. In the internal resistive region, the tearing mode is very sensitive to the flow shear at the magnetic null plane; i.e., $V'(0)$. When $V'(0)$ is very small, the scaling remains unchanged for both tearing modes, while it stabilizes the nonconstant-ψ tearing mode with sufficiently large Δ', but destabilizes the constant-ψ tearing mode. In the case where $V'(0)$ is comparable with the magnetic field shear, $B_0'(0)$,

the scaling of the constant-ψ tearing mode growth rate is changed from $S^{-3/5}$ to $S^{-1/2}$. The scale length of the singular layer is changed from $S^{-2/5}$ to $S^{-1/3}$, and the $\Delta' > 0$ instability criterion is removed provided $V'(0)V''(0) - B_0'(0)B_0''(0) \neq 0$. The scalings of the nonconstant-ψ tearing mode still remain unchanged. When the flow shear is larger than the magnetic field shear at the magnetic null plane, the flow freezes the magnetic field and stabilizes the tearing mode. Additionally, we have shown the parameter regions for the validity of the constant-ψ and nonconstant-ψ tearing modes. Finally, since the shear flow can drive ideal instability, we discussed the transition from the tearing mode to the ideal mode in two examples. It is found that this happens when the value of the matching quantity Δ' goes to negative through $\Delta' = \infty$, which is similar to the $m = 1$ tearing mode discussed by Ara et al. (1978).

The above results have further been tested numerically (Ofman et al, 1991). The figure below shows the growth rate scalings for two different flow profiles: the "sech" profile $V_0 = V_0(sech\,(by) - 1)$ with $V_0 = 1, b = 2.5$; the "tanh" profile $V_0 = V_0 tanh\, by$ with $V_0 = 1, b = 0.73$. The magnetic profile is fixed at $B_0 = tanh\, y$. For the "sech" profile the flow shear at the magnetic null plane is zero, however the flow in the idea region change the matching quatity Δ' from finite to infinite, and the tearing mode has nonconstant ψ scaling. For the "tanh" profile the flow shear at the magnetic null plane is comparable but smaller than the magnetic shear, and the constant ψ growth rate scaling is changed from $S_R^{-3/5}$ to $S_R^{-1/2}$.

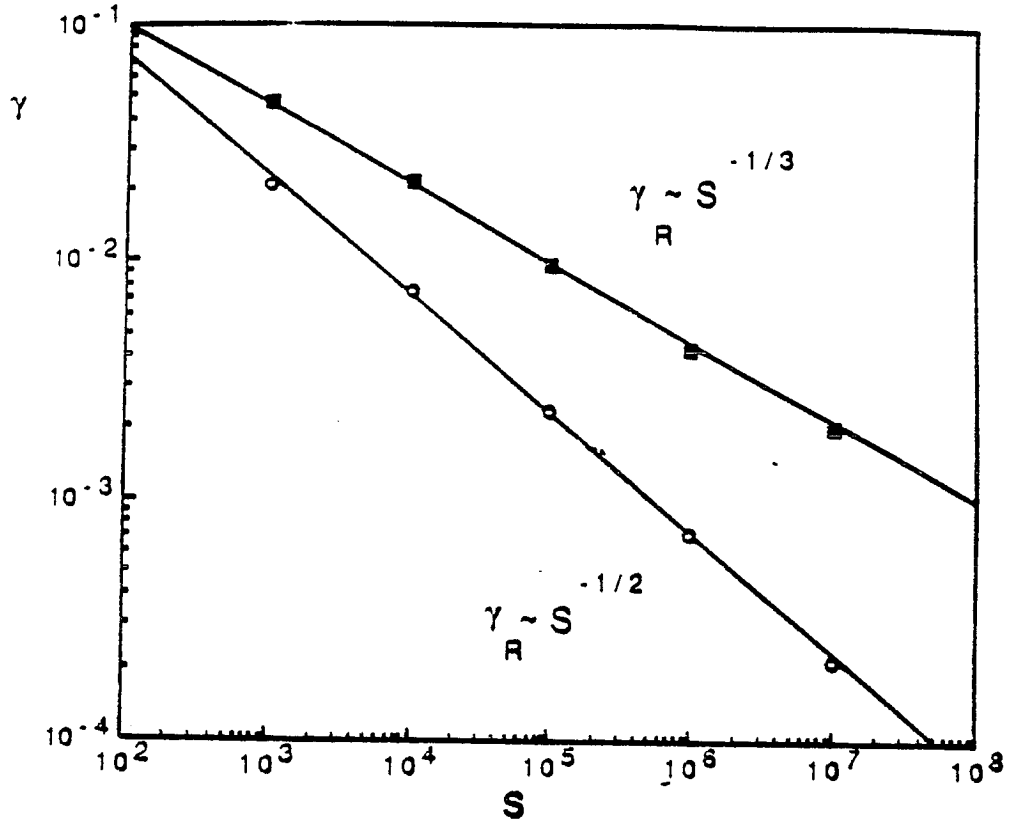

Figure 3.5: Growth rate scaling vs. magnetic Renolds number S_R for "sech" flow profile with $V_0 = 1, b = 2.5, k = 0.5$, the nonconstant ψ case (the squares are calculated points). The scaling for "tanh" flow profile with $V_0 = 1, b = 0.75, k = 0.5$, the constant ψcase (the circles are calculated points).

3.7 Appendix A - Δ' Value in the Presence of Equilibrium Flow

Here we evaluate the Δ' value in the presence of the equilibrium shear flow. We assume the equilibrium magnetic field has the form

$$B_0 = |y|, \quad |y| < 1; \qquad B_0 = 1, \quad y > 1; \qquad B_0 = -1, \quad y < -1. \tag{A1}$$

This piecewise linear profile can be viewed as a rough approximation of the profile $B_0 = \tanh y$.

In the *first example*, we assume the equilibrium shear flow to be

$$V = \frac{V_0}{b} y, \quad |y| < b; \qquad V = V_0, \quad y > b; \qquad V = -V_0, \quad y < -b. \tag{A2}$$

This piecewise linear profile can be viewed as an approximation of the profile $V = V_0 \tanh y/b$.

For convenience we define

$$Y \equiv \frac{w'}{w},$$

and

$$f(x_1, x_2) = \frac{1 - x_1 \tanh x_1 - x_1 x_2}{x_1 - \tanh x_1 + x_1 x_2 \tanh x_1}. \tag{A3}$$

The reason for these definitions will become clear below. Consider first the case where $b < 1$. In the region $|y| < b$, Eqs. (8) and (9) become

$$\psi = yw$$

$$w'' - \frac{2w'}{y} - k^2 w = 0,$$

which have the solution

$$\psi = A_{\pm} \frac{\sinh ky}{y} + B_{\pm} \frac{\cosh ky}{y}.$$

Here the A_+ and B_+ are as yet undetermined constants for the solution in the region $0 < y \leq b$, and A_- and B_- are constants for the solution in the region $-b \leq y < 0$. We have allowed for the discontinuity at $y = 0$ that arises because of the resistive layer. Thus Δ' is given by

$$\Delta' = \frac{\psi'}{\psi}\Big|_{0_-}^{0_+} = k\left(\frac{A_+}{B_+} - \frac{A_-}{B_-}\right).$$

The constants $A_\pm$ and $B_\pm$ are determined by the boundary conditions at $y = \pm\infty$. To find these constants we must trace the solution for $|y| > 1$ through the regions $b < y < 1$ and $-b < y < -1$. In these regions Eqs. (8) and (9) are

$$\psi = yw$$

$$w'' + \frac{2yw'}{y^2 - V_0^2} - k^2 w = 0. \tag{A4}$$

Equation (A4) has no simple solution, but it is transformed into a Riccatti equation by $Y \equiv w'/w$. We obtain

$$Y' = k^2 - Y^2 - \frac{2yY}{y^2 - V_0^2}. \tag{A5}$$

In the outer region, $|y| > 1$ the solutions are trivially given by

$$w \sim e^{-k|y|}.$$

From this we obtain two conditions $Y(1) = -k$ and $Y(-1) = k$. We can replace the two unknown quantities in Δ'; i.e., $A_\pm/B_\pm$ by $Y(\pm b) \equiv Y_\pm$. These quantities are in turn determined by solving the Riccatti equation (A5) subject to the boundary conditions $Y(1) = -k$ and $Y(-1) = k$. Matching at $y = \pm b$ yields

$$Y_\pm = \frac{\frac{A_\pm}{B_\pm} kb \pm kb \tanh kb - \frac{A_\pm}{B_\pm} \tanh kb \mp 1}{b \pm \frac{A_\pm}{B_\pm} b \tanh kb},$$

which implies

$$k\frac{A_\pm}{B_\pm} = \frac{\pm k^2 b \tanh kb \mp k - kby_\pm}{\pm Y_\pm b \tanh kb - kb + \tanh kb}.$$

Using the symmetry of the Riccatti equation: $Y \to -Y$; $y \to -y$, and the symmetry in the boundary conditions $Y(\pm 1) = \mp k$, we conclude that $Y_+ = -Y_-$. Finally we obtain the following expression for Δ':

$$\Delta' = 2kf\left(\bar{k}, \beta\right), \tag{A6}$$

where the function f was defined above in Eq. (A3), and $\beta = -\frac{1}{k}Y(b)$. The complete determination of Δ' has been reduced to finding β, which as noted requires solving Eq. (A5). However, the qualitative nature of the solution can be estimated. Assuming $V_0^2 < 1$ and $V_0^2/b^2 < 1$, it can be shown that $-\infty < Y(b) < -k$. This implies

$$1 < \beta < \infty. \tag{A7}$$

Moreover, as $V_0^2/b^2 \to 1$, $\beta \to \infty$.

Similarly in the case where $b > 1$ we obtain

$$\Delta' = 2kf(k, \beta),$$

where

$$\beta = -\frac{1}{k}Y(1),$$

and Y satisfies the Riccatti equation

$$\frac{dY}{dy} = k^2 - Y^2 - \frac{2y}{y^2 - b^2/V_0^2}Y,$$

$$Y(b) = -k. \tag{A8}$$

Assuming $V_0^2 < 1$, we obtain from the above $-k < Y(1) < 0$. This implies

$$0 < \beta < 1. \tag{A9}$$

Note, as $b^2/V_0^2 \to \infty$, $\beta \to 1$.

In the *second example*, we assume the equilibrium shear flow to be

$$V = 0, \quad |y| < b; \qquad V = -V_0, \quad |y| > b.$$

This profile is a linear approximation of the profile

$$V = V_0 \left(\operatorname{sech} \frac{y}{b} - 1 \right),$$

$$V = V_0 \left(\operatorname{sech}^2 \frac{y}{b} - 1 \right).$$

The linear profile has a discontinuity at $|y| = b$. Since $(B_0^2 - V_0^2)\, w'(y)$ is continuous, as seen by integration of Eq. (9), $w'(y)$ must have a jump at $y = b$, and therefore so does $Y(y)$.

Following the procedure used in the first example, but accounting for this jump, we obtain when $b < 1$

$$\Delta' = 2k f_{\cdot}\left(\bar{k}, \beta\right),$$

where $\bar{k} = kb$,

$$\begin{aligned} \beta &= -\frac{1}{k} Y\left(b^-\right) \\ &= -\frac{1}{k}\left(1 - \frac{V_0^2}{b^2}\right) Y\left(b^+\right), \end{aligned} \tag{A10}$$

and $Y(y)$ satisfies the Riccatti equation for $b^+ \leq y \leq 1$

$$\frac{dY}{dy} = k^2 - Y^2 - \frac{2y}{y^2 - V_0^2} Y,$$

$$Y(1) = -k. \tag{A11}$$

Assuming $V_0^2 \to 1$ from above, we obtain from Eqs. (A11), $-k < Y(b^+) < 0$, which implies

$$\beta < 0. \tag{A12}$$

Using Eqs. (A10) and (A11), we obtain

$$\frac{\partial \beta}{\partial b} = -2\frac{V_0^2}{kb^3} Y\left(b^+\right) - \frac{1}{k}\left(1 - \frac{V_0^2}{b^2}\right) \frac{dY}{dy}\Big|_{y=b^+}$$

$$= \frac{1}{k}\left(1 - \frac{V_0^2}{b^2}\right)\left[\frac{2}{b} Y\left(b^+\right) - \left(k^2 - Y\left(b^+\right)^2\right)\right] > 0. \tag{A13}$$

As $b \to 0$, $\beta \to -\infty$. When $b > 1$,

$$\Delta' = 2kf(k, \beta),$$

where

$$\beta = \frac{\left(2 - V_0^2\right) e^{-2k} - V_0^2 e^{-2kb}}{\left(2 - V_0^2\right) e^{-2k} + V_0^2 e^{-2kb}} < 1.$$

In all the above cases, Δ' has the form

$$\Delta' = 2kf\left(\bar{k}, \beta\right),$$

where $\bar{k} = kb$ if $b < 1$, otherwise $\bar{k} = k$. In the above expression, $\bar{k}$ and β measure the influence of the shear flow. In the case of no flow, $\bar{k} = k$ and $\beta = 1$.

At criticality $\Delta' = 0$, which implies $f\left(\bar{k}, \beta_0\right) = 0$. This defines a curve

$$\beta_0\left(\bar{k}\right) \equiv \frac{1 - \bar{k}\tanh\bar{k}}{\bar{k}}. \tag{A14}$$

Similarly, at $\Delta' = \infty$, $f\left(\bar{k}, \beta_\infty\right) = \infty$ implies

$$\beta_\infty\left(\bar{k}\right) \equiv -\frac{\bar{k} - \tanh\bar{k}}{\bar{k}\tanh\bar{k}}. \tag{A15}$$

Both $\beta_0\left(\bar{k}\right)$ and $\beta_\infty\left(\bar{k}\right)$ are monotonic decreasing functions of $\bar{k}$, which are shown in Fig. 3.6. Also the variation of Δ' with β at fixed $\bar{k}$ is shown in Fig. 3.7. Evidently shear flow can drastically change the value of Δ'.

3.8 Appendix B - Nonconstant-ψ Tearing Mode with $\left|kB_0' S_R^{-1/3}\Delta'\right| \gg 1$

The case of the no flow tearing mode with $\Delta' \sim O(1)$ and $\Delta' < 0$ was analyzed by FKR (1963) and Coppi et al (1976). Here we just discuss the case where $|\Delta'| \gg 1$.

Let

$$\frac{\left(kB_0'(0)\right)^2 \epsilon^4 S}{r_0} = 1, \qquad \hat{\lambda} = \frac{r_0}{\left(kB_0'(0)\right)^{2/3} S_R^{-1/3}}, \tag{B1}$$

and rewrite Eq. (58) as

$$\frac{\partial^2 X_0}{\partial\zeta^2} - \frac{2}{\zeta}\frac{\partial X_0}{\partial\zeta} = \hat{\lambda}^{3/2} X_0 + \zeta^2\left(X_0 - C_0\right), \tag{B2}$$

where

$$X_0 = \zeta\frac{\partial\psi}{\partial\zeta} - \psi = -\left(\frac{r}{kB_0'(0)\epsilon}\right)^2 \frac{\partial\tilde{\phi}}{\partial\zeta} + C_0.$$

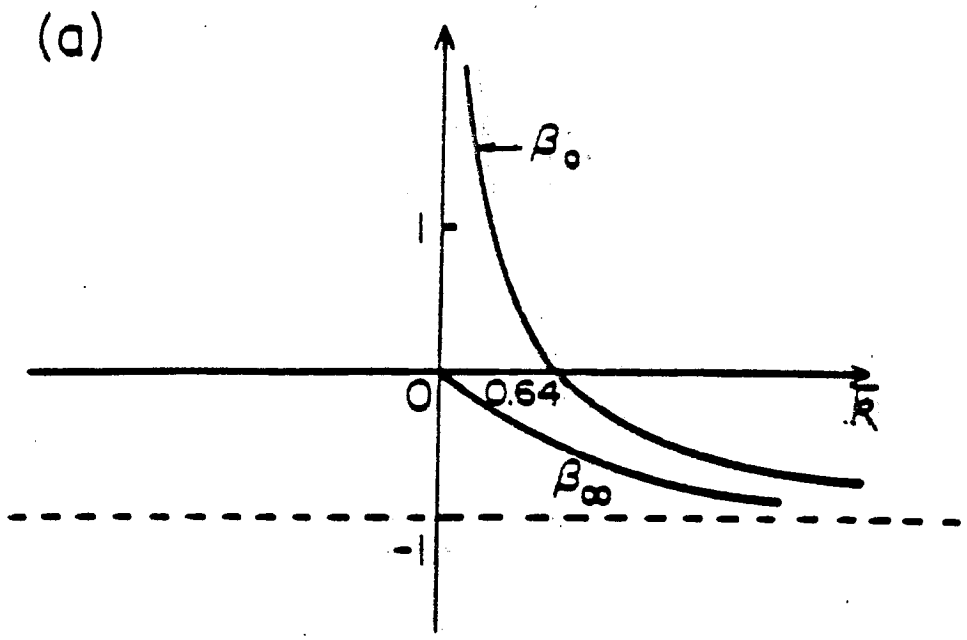

Figure 3.6: Sketch of functions $\beta_0(\bar{k})$ and $\beta_\infty(\bar{k})$; $\beta_0(\bar{k})$ and $\beta_\infty(\bar{k})$ are the parameters at which $\Delta'(\beta_0, \bar{k}) = 0$ and $\Delta'(\beta_\infty, \bar{k}) = \infty$, respectively.

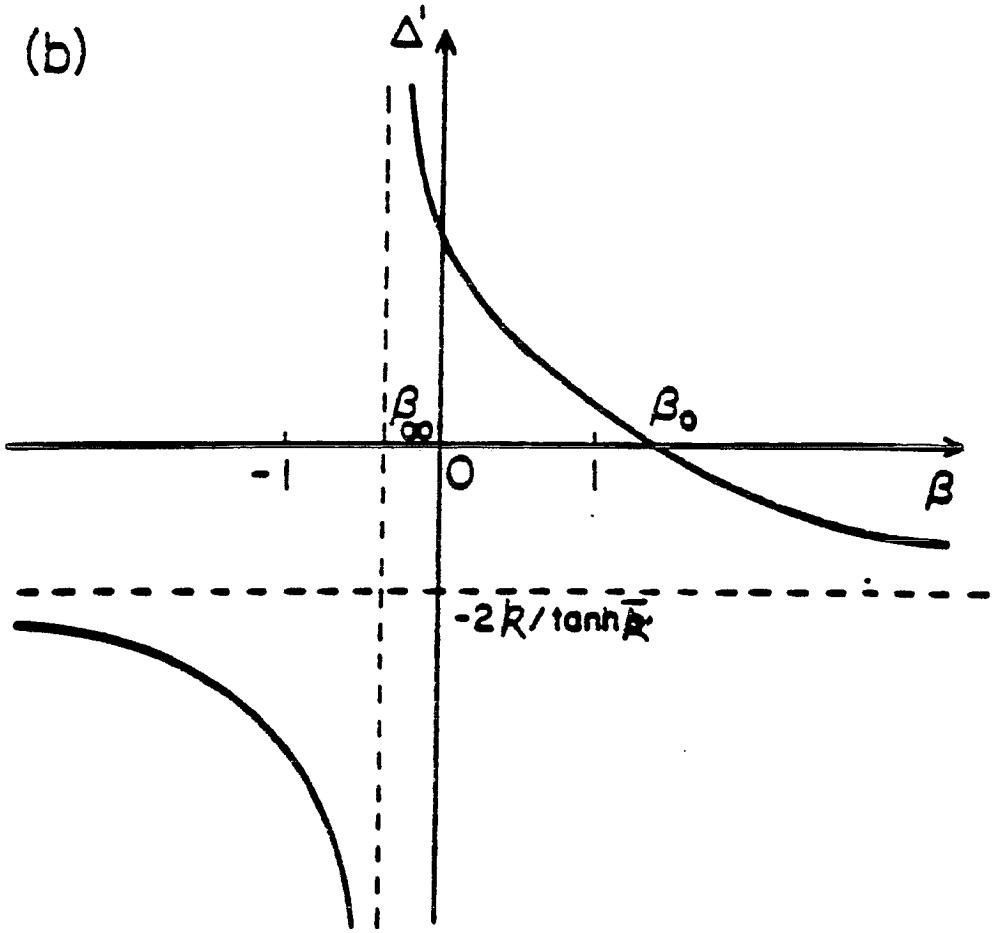

Figure 3.7: Sketch of variation of Δ' with parameter β.

The solution of the above that matches to the external solution should be asymptotic to C_0. We obtain from Eq. (B2)

$$X_0 \underset{|\zeta|\to\infty}{\longrightarrow} C_0 - \frac{\hat{\lambda}^{3/2}}{\zeta^2} C_0. \tag{B3}$$

We redefine

$$\Delta' = \frac{\int_{-\infty}^{\infty} \frac{1}{\zeta} \frac{\partial X_0}{\partial \zeta} d\zeta}{\epsilon C_0}. \tag{B4}$$

Let $\hat{X} = X_0 - C_0$, $\zeta^2 = t$, and rewrite Eq. (B2) as

$$t\frac{\partial^2 \hat{X}}{\partial t^2} - \frac{1}{2}\frac{\partial \hat{X}}{\partial t} - \frac{1}{4}\left(\hat{\lambda}^{3/2} + t\right)\hat{X} = \frac{1}{4}\hat{\lambda}^{3/2} C_0.$$

We find it convenient to convert this equation to a homogeneous equation by differentiation (Waelbroeck, 1989)

$$t\frac{\partial^3 \hat{X}}{\partial t^3} + \frac{1}{2}\frac{\partial \hat{X}}{\partial t} - \frac{1}{4}\left(\hat{\lambda}^{3/2} + t\right)\frac{\partial \hat{X}}{\partial t} - \frac{1}{4}\hat{X} = 0. \tag{B5}$$

Assume $\hat{X} = K \int_C e^{zt} v(z) dz$, where K is a constant. C is the path decided later. Substituting $\hat{x}$ into Eq. (B5) we obtain

$$\int_C \left[-z\left(z^2 - \frac{1}{4}\right)\frac{dv}{dz} + \left(-\frac{5}{2}z^2 - \frac{\hat{\lambda}^{3/2}}{4}z\right)v\right] e^{zt} dz + z e^{zt}\left(z^2 - \frac{1}{4}\right) v(z)\Big|_C = 0.$$

Let

$$\left[-z\left(z^2 - \frac{1}{4}\right)\frac{dv}{dz} + \left(-\frac{5}{2}z^2 - \frac{\hat{\lambda}^{3/2}}{4}z\right)v\right] = 0,$$

which yields

$$v = \left(z - \frac{1}{2}\right)^{-(5+\hat{\lambda}^{3/2})/4}\left(z + \frac{1}{2}\right)^{-(5-\hat{\lambda}^{3/2})/4}. \tag{B6}$$

Now we need to choose a path so that Eq. (B3) is satisfied and

$$z e^{zt}\left(z^2 - \frac{1}{4}\right) v(z)\Big|_C = z e^{zt}\left(z - \frac{1}{2}\right)^{-(1+\hat{\lambda}^{3/2})/4}\left(z + \frac{1}{2}\right)^{-(1-\hat{\lambda}^{3/2})/4}\Big|_C = 0.$$

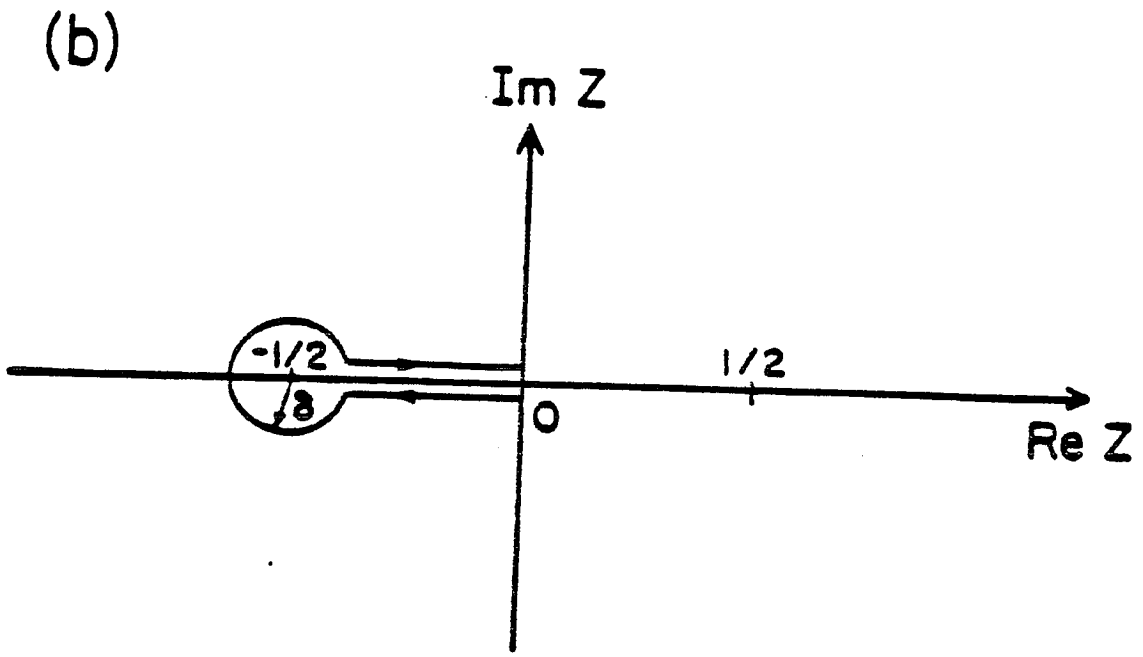

Figure 3.8: Integral contour

When $\hat{\lambda}^{3/2} > 1$, the path can be chosen from $z = -1/2$ to $z = 0$. By a substitution

$$z = -\frac{1-y}{2(1+y)},$$

we get the solution obtained by Coppi et al (1976). For the case $\hat{\lambda}^{3/2} < 1$, $z = -1/2$ becomes a singular point. In order to extend our solution to include $\hat{\lambda}^{3/2} < 1$, we modify our path as in Fig. 3.8. Thus

$$\hat{X} = K \int_C e^{zt} \left(z - \frac{1}{2}\right)^{-(5+\hat{\lambda}^{3/2})/4} \left(z + \frac{1}{2}\right)^{-(5-\hat{\lambda}^{3/2})/4} dz$$

$$= K \int_{C_\delta} e^{zt} \left(z - \frac{1}{2}\right)^{-(5+\hat{\lambda}^{3/2})/4} \left(z + \frac{1}{2}\right)^{-(5-\hat{\lambda}^{3/2})/4} dz$$

$$+ K \left(-1 + e^{-i\pi(5-\hat{\lambda}^{3/2})/2)}\right) \int_{-1/2+\delta}^{0} e^{zt} \left(z - \frac{1}{2}\right)^{-(5+\hat{\lambda}^{3/2})/4} \left(z + \frac{1}{2}\right)^{-(5-\hat{\lambda}^{3/2})/4} \quad \text{(B7)}$$

Now consider the case where $\left|1 - \hat{\lambda}^{3/2}\right| \ll 1$. Define $\left(1 - \hat{\lambda}^{3/2}\right)/4 = \sigma$, and rewrite Eq. (B7) as

$$\hat{X} \approx K \int_{C_\delta} e^{zt} \left(z - \frac{1}{2}\right)^{-3/2+\sigma} \left(z + \frac{1}{2}\right)^{-1-\sigma} dz$$

$$+ i2\pi\sigma K \int_{-1/2+\delta}^{0} e^{zt} \left(z - \frac{1}{2}\right)^{-3/2+\sigma} \left(z + \frac{1}{2}\right)^{-1-\sigma} dz. \quad \text{(B8)}$$

When $t \to \infty$,

$$\hat{X} \sim -iK \int_{-1/2+\delta}^{0} e^{zt} \left(\frac{1}{2}\right)^{-5/2} (2\pi i\sigma) dz = 2^{7/2}\pi\sigma \frac{K}{t}. \quad \text{(B9)}$$

Comparison with (B3) yields

$$K = -\frac{\hat{\lambda}^{3/2} C_0}{2^{7/2}\pi\sigma}. \quad \text{(B10)}$$

We choose the radius δ of C_δ so that $1 \gg \delta \gtrsim \sigma$. Let $z + 1/2 = \delta e^{i\theta}$ in C_δ, then

$$\int_{C_\delta} e^{zt} \left(z - \frac{1}{2}\right)^{-3/2+\sigma} \left(z + \frac{1}{2}\right)^{-1-\sigma} dz = \int_{C_\delta} e^{zt} \left(-i + \delta e^{i\theta}\right)^{-3/2+\sigma} \delta^{-\sigma} e^{-i\sigma\theta} d(i\theta)$$

$$= 2\pi e^{-\frac{1}{2}t} + O(\sigma). \quad \text{(B11)}$$

For the second term of Eq. (B8), we estimate the order of magnitude as

$$\left| \int_{-1/2+\delta}^{0} e^{zt} \left(z - \frac{1}{2}\right)^{-3/2+\sigma} \left(z + \frac{1}{2}\right)^{-1-\sigma} dz(2\pi i\sigma) \right| \lesssim 2\pi\sigma \int_{-1/2+\delta}^{0} \left(z + \frac{1}{2}\right)^{-1-\sigma} dz$$

$$\sim \sigma \ln \delta \sim O(\sigma). \quad \text{(B12)}$$

Substituting Eqs. (B11) and (B12) into Eq. (B8), yields

$$\hat{X} = -\frac{\hat{\lambda}^{3/2} C_0}{2^{5/2}\sigma}\left(e^{-\frac{1}{2}t} + O(\sigma)\right). \tag{B13}$$

For definiteness, we choose

$$-\frac{\hat{\lambda}^{3/2} C_0}{2^{5/2}\sigma} = 1. \tag{B14}$$

Substituting Eq. (B13) into Eq. (B4), we obtain

$$\Delta' = \frac{\hat{\lambda}^{3/2}}{4\sigma\epsilon}\sqrt{\pi} \gg 1,$$

or

$$\gamma \approx \left(1 - \frac{2\sqrt{\pi}}{3\left(kB_0'(0)S_R\right)^{-1/3}\Delta'}\right)\left(kB_0'(0)\right)^{2/3} S_R^{-1/3}. \tag{B15}$$

The above analysis requires $\left|\left(kB_0'(0)S_R\right)^{-1/3}\Delta'\right| \gg 1$.

Chapter 4

Effect of Viscosity on Resistive Tearing Mode with Equilibrium Shear Flow

4.1 Introduction

In this Chapter we generalize the work of the previous chapter by including, in addition to equilibrium shear flow, viscosity in the resistive tearing problem. Generally, viscosity is described by a complicated tensor (Braginskii, 1965). However, since plasma motion tends to exhibit transverse gradients near the magnetic null plane, the dominate viscosity comes from the transverse component (FKR, 1963, Dobrowonlny, 1983, Porcelli, 1983, Einaudi and Rubini, 1989). Thus the viscosity in our model equation should be understood to be transverse. Since this viscosity is often comparable with the resistivity in laboratory plasmas (FKR, 1963) and much larger than the resistivity in astrophysical plasmas, such as those that occur in the solar wind and active coronal regions (Dobrowonlny, 1983), one expects this to be an important effect. Moreover, as noted in the introduction, since the tearing instability produces vorticity, and equilibrium shear flow can enhance this production, the diffusive nature of viscosity should have a significant influence, one that depends upon the equilibrium shear flow.

Previously, the effect of viscosity on the resistive tearing mode without flow was treated (FKR, 1963, Porcelli, 1983). These authors found that the growth is suppressed while the width of the singular layer is increased. Also,

Dobrowolny *et al.* (1983) have given scalings in the case where it is assumed that the viscosity is comparable with the resistivity. Assuming that the viscous term dominates the inertial term in the singular layer, and that the shear flow is small, Bondeson and Persson (1986) solved the constant ψ tearing mode problem by making use of Fourier transforms. Recently, Einaudi and Rubini (1989) have investigated this problem numerically.

Here we generalized the work of Bondeson and Persson by allowing the equilibrium shear flow to be large (Chen and Morrison, 1990b). As in their work, we Fourier transform the internal singular layer equations in order to derive growth rate expressions. We find that for small viscosity there is a general tendency to diminish the growth rate. Also, when the viscosity becomes comparable with the resistivity and the flow shear is larger than the magnetic field shear at the magnetic null plane, and there is no constant ψ tearing mode. Matching in this case cannot be achieved. Another result of this paper is to justify the constant ψ approximation.

In Sec. (4.2) the basic equations are set up and we briefly discuss the role of viscosity in both the external region and the internal singular layer. In Sec. (4.3) the internal singular layer equations are discussed in two shear flow limits. Finally, in Sec. (4.4) we summarize.

4.2 Basic Equations

Including the viscosity term in Eqs. (3.1) and (3.2) results in the following linearized perturbation equations:

$$(\gamma + ikV_0)(\phi'' - k^2\phi) - ikV_0''\phi = ikB_0(\psi'' - k^2\psi) - ikB_0''\psi + \frac{1}{S_V}\frac{\partial^4\phi}{\partial y^4} \quad (4.1)$$

$$(\gamma + ikV_0)\psi - ikB_0\phi = \frac{1}{S_R}(\psi'' - k^2\psi) \ . \quad (4.2)$$

We assume that both the resistivity and viscosity are very small; i.e., $S_V \gg 1$, $S_R \gg 1$. For convenience, we choose a reference frame such that $V_0(0) = 0$, where as before $y = 0$ is the location of the magnetic null plane. Only the tearing mode is considered. Unlike the case without viscosity, the small resistivity and viscosity are not only important in the internal singular layer, but also important in a thin layer at the external physical boundary (Drazin and Reid, 1982; Currie, 1986). This boundary layer will affect the matching quantity Δ', which is defined by $\Delta' \equiv \frac{1}{\psi}\frac{d\psi}{dy}\Big|_{0-}^{0+}$. However, if the boundary is far away from the singular layer, this effect is negligible. In the internal singular layer, the viscosity influences magnetic diffusion by diffusing the vorticity produced during the tearing instability. We discuss this problem in the following section. Without loss of generality, we assume $B_0'(0) > 0$. Also, we assume $|V_0''(0)/B_0'(0)| \lesssim \mathcal{O}(1)$, $|B_0''(0)/B_0'(0)| \lesssim \mathcal{O}(1)$, and $k \lesssim \mathcal{O}(1)$.

4.3 Internal Singular Layer

Denoting that the scale length of the internal singular layer by ϵ, we consider Eqs. (1) and (2) near $y = 0$. Using the stretched variable $\zeta = y/\epsilon$, Eqs. (1) and (2) become

$$\left(\frac{\gamma}{kB_0'(0)\epsilon} + i\frac{V_0'(0)}{B_0'(0)}\zeta + \frac{1}{2}i\frac{V_0''(0)}{B_0'(0)}\epsilon\zeta^2\right)\frac{\partial^2\phi}{\partial\zeta^2} - i\epsilon\frac{V_0''(0)}{B_0'(0)}\phi$$

$$= \left(i\zeta + \frac{1}{2}i\frac{B_0''(0)}{B_0'(0)}\epsilon\zeta^2\right)\frac{\partial^2\psi}{\partial\zeta^2} - i\epsilon\frac{B_0''(0)}{B_0'(0)}\psi + D\frac{\partial^4\phi}{\partial\zeta^4} + \mathcal{O}(\epsilon^2) \quad (4.3)$$

$$\left(\frac{\gamma}{kB_0'(0)\epsilon} + i\frac{V_0'(0)}{B_0'(0)}\zeta + \frac{1}{2}i\frac{V_0''(0)}{B_0'(0)}\epsilon\zeta^2\right)\psi - \left(i\zeta + \frac{1}{2}i\frac{B_0''(0)}{B_0'(0)}\epsilon\zeta^2\right)\phi$$

$$= C \frac{\partial^2 \psi}{\partial \zeta^2} + \mathcal{O}(\epsilon^2) \ , \tag{4.4}$$

where D and C are defined by

$$D \equiv \frac{1}{kB_0'(0)\epsilon^3 S_V}$$

$$C \equiv \frac{1}{kB_0'(0)\epsilon^3 S_R} \ . \tag{4.5}$$

The quantities D and C measure respectively the diffusion of the vorticity and magnetic fields in the singular layer. When the viscosity is very small compared with resistivity; i.e., $\frac{D}{C} \ll 1$, magnetic diffusion dominates vorticity diffusion. In this case the viscosity only alters numerical coefficients of the tearing mode growth rate; the scaling is unchanged. Here we omit this case, but consider the more interesting case where viscosity is comparable or larger than the resistivity and the constant ψ approximation is assumed. As discussed by Chen and Morrison (1990a), the constant ψ approximation requires that $\left|\frac{\gamma}{kB_0'(0)\epsilon}\right| \ll 1$. This implies that the anticipated growth time is much longer than the local Alfvén time at the magnetic null plane. Also we consider the problem in two shear flow limits. One is the very small shear flow case, where flow shear is much less than the magnetic field shear at the null plane. In the other limit, the flow shear is comparable with the magnetic field shear.

4.3.1 Very small shear flow

Assuming $\left|\frac{V_0'(0)}{B_0'(0)}\right| \lesssim \left|\frac{\gamma}{kB_0'(0)\epsilon}\right|$, which implies the flow shear is so small that the convection terms are at most comparable with the inertia terms. From the constraint imposed by the external solution, we have the ordering $\phi \sim \frac{\gamma}{kB_0'(0)\epsilon}\psi$ in the internal singular layer (Chen and Morrison, 1990a) and

chap. 3. Thus even though the viscosity is much larger than the resistivity, the magnetic diffusion still dominates the vorticity diffusion. In order to facilitate comparison of the orders of various terms, we replace ϕ by a new variable φ defined by

$$\varphi = \phi \Big/ \left(-i\,\frac{\gamma}{kB_0'(0)\epsilon}\right) , \tag{4.6}$$

and rewrite Eqs. (3) and (4) as

$$-\left(\frac{\gamma}{kB_0'(0)\epsilon}\right)^2 \left(1 + i\,\frac{kV_0'(0)\epsilon}{\gamma}\right) \frac{\partial^2\varphi}{\partial\zeta^2} + D\,\left(\frac{\gamma}{kB_0'(0)\epsilon}\right) \frac{\partial^4\varphi}{\partial\zeta^4}$$

$$= \left(\zeta + \frac{1}{2}\,\frac{B_0''(0)}{B_0'(0)}\,\epsilon\zeta^2\right) \frac{\partial^2\psi}{\partial\zeta^2} - \epsilon\,\frac{B_0''(0)}{B_0'(0)}\,\psi + \mathcal{O}\left(\epsilon\,\frac{\gamma}{kB_0'(0)\epsilon}\right) , \tag{4.7}$$

$$\frac{\gamma}{kB_0'(0)\epsilon}\left[\left(1 + i\,\frac{kV_0'(0)\epsilon}{\gamma}\,\zeta\right)\psi - \zeta\varphi\right] + \frac{1}{2}\,i\,\frac{V_0''(0)}{B_0'(0)}\,\epsilon\zeta^2\psi$$

$$= C\,\frac{\partial^2\psi}{\partial\zeta^2} + \mathcal{O}\left(\epsilon\,\frac{\gamma}{kB_0'(0)\epsilon}\right) . \tag{4.8}$$

In order to find the solutions matching the external solutions, we must have the scaling

$$D\sqrt{\frac{S_V}{S_R}} \sim C\sqrt{\frac{S_R}{S_V}} \sim 1 ,$$

instead of $\dfrac{|\gamma|}{kB_0'(0)\epsilon}\,C \sim 1$ as required in the case of zero viscosity (FKR, 1963, Chen and Morrison, 1990a). This implies that the viscous term dominates the inertial term in Eq. (7), and the width of the internal singular layer scales as

$$\epsilon \sim \left(kB_0'(0)\sqrt{S_R\,S_V}\right)^{-1/3} . \tag{4.9}$$

The natural expansion parameter in Eqs. (7) and (8) is $\left(\dfrac{\gamma}{kB_0'(0)\epsilon}\sqrt{\dfrac{S_R}{S_V}}\right)$, instead of $\left(\dfrac{\gamma}{kB_0'(0)\epsilon}\right)^2$ in the case of no viscosity. This implies the following

expansions

$$\psi = \sum_n \left(\frac{\gamma}{kB_0'(0)\epsilon} \sqrt{\frac{S_R}{S_V}} \right)^n \psi_n$$

$$\varphi = \sum_n \left(\frac{\gamma}{kB_0'(0)\epsilon} \sqrt{\frac{S_R}{S_V}} \right)^n \varphi_n \ . \tag{4.10}$$

Inserting Eqs. (10) into Eqs. (7) and (8), the leading order of Eqs. (7) and (8) yield $\psi_0 =$ const., as expected. To the first order, Eqs. (7) and (8) yield

$$D\sqrt{\frac{S_V}{S_R}} \frac{\partial^4 \overline{\varphi}_0}{\partial \zeta^4} = \zeta \frac{\partial^2 \psi_1}{\partial \zeta^2} - \frac{\epsilon}{\left(\frac{\gamma}{kB_0'(0)\epsilon} \sqrt{\frac{S_R}{S_V}} \right)} \frac{B_0''(0)}{B_0'(0)} \psi_0 \tag{4.11}$$

$$\psi_0 - \zeta \overline{\varphi}_0 = C\sqrt{\frac{S_R}{S_V}} \frac{\partial^2 \psi_1}{\partial \zeta^2} \ , \tag{4.12}$$

where $\overline{\varphi}_0 = \varphi_0 - i \dfrac{kV_0'(0)\epsilon}{\gamma} \psi_0 - \dfrac{1}{2} i \dfrac{\epsilon}{\left(\frac{\gamma}{kB_0'(0)\epsilon} \sqrt{\frac{S_R}{S_V}} \right)} \zeta \psi_0$. We reduce the order of Eqs. (11) and (12) by Fourier transformation

$$\psi_1 = \int_{-\infty}^{\infty} e^{ik\zeta} \psi_1(k) dk$$

$$\overline{\varphi}_0 = \int_{-\infty}^{\infty} e^{ik\zeta} \overline{\varphi}_0(k) dk \ .$$

The transformed equations are

$$D\sqrt{\frac{S_V}{S_R}} k^4 \overline{\varphi}_0(k) \ = \ -i \frac{d}{dk} \left(k^2 \psi_1(k) \right) - \frac{\epsilon}{\left(\frac{\gamma}{kB_0'(0)\epsilon} \sqrt{\frac{S_R}{S_V}} \right)} \frac{B_0''(0)}{B_0'(0)} \psi_0 \delta(k) \tag{4.13}$$

$$\psi_0 \delta(k) - i \frac{d}{dk} \overline{\varphi}_0(k) \ = \ -C\sqrt{\frac{S_R}{S_V}} k^2 \psi_1(k) \ . \tag{4.14}$$

Integration of Eqs. (13) and (14) gives

$$\overline{\varphi}_0(0^+) - \overline{\varphi}_0(0^-) = -i\psi_0 \tag{4.15}$$

$$k^2\psi_1(k)\Big|_{0^-}^{0^+} = i\,\frac{\epsilon}{\left(\frac{\gamma}{kB_0'(0)\epsilon}\sqrt{\frac{S_R}{S_V}}\right)}\,\frac{B_0''(0)}{B_0'(0)}\,\psi_0. \tag{4.16}$$

Using Eq. (14), Eq. (16) yields

$$\frac{d}{dk}\overline{\varphi}_0(0^+) - \frac{d}{dk}\overline{\varphi}(0^-) = \frac{1}{\gamma S_R\epsilon}\,\frac{B_0''(0)}{B_0'(0)}\,\psi_0\ . \tag{4.17}$$

After Fourier transformation, the matching quantity Δ' becomes

$$\begin{aligned}\Delta' \;&=\; \frac{1}{\epsilon\psi}\,\frac{d\psi}{d\zeta}\Big|_{-\infty}^{\infty} \;=\; \frac{\gamma\sqrt{\frac{S_R}{S_V}}}{kB_0'(0)\epsilon^2\psi_0}\int_{-\infty}^{\infty}\frac{d^2\psi_1(\zeta)}{d\zeta^2}\,d\zeta \\ &=\; -i\pi\,\frac{\gamma\epsilon S_R}{\psi_0}\left(\frac{d\overline{\varphi}_0(0^+)}{dk} + \frac{d\overline{\varphi}_0(0^-)}{dk}\right)\ .\end{aligned} \tag{4.18}$$

Combining Eqs. (15), (17), and (18), we have

$$\left(\frac{\Delta'}{\pi} - i\,\frac{B_0''(0)}{B_0'(0)}\right)\frac{\varphi_0(0^+)}{\frac{d\varphi_0(0^+)}{dk}} - \left(\frac{\Delta'}{\pi} + i\,\frac{B_0''(0)}{B_0'(0)}\right)\frac{\varphi_0(0^-)}{\frac{d\varphi_0(0^-)}{dk}} = -2\gamma\,S_R\epsilon\ . \tag{4.19}$$

When $k \neq 0$, we obtain from Eqs. (13) and (14)

$$\frac{d^2\overline{\varphi}_0(k)}{dk^2} - DCk^4\overline{\varphi}_0(k) = 0\ , \tag{4.20}$$

with the boundary condition that $\overline{\varphi}_0(k)$ vanishes at infinity. Equation (20) is a special case of Eq. (A1) which is solved in the Appendix in terms of Kummer functions. Applying Eq. (A6) yields the quantities $\frac{\varphi_0(0^\pm)}{\frac{d\varphi_0(0^\pm)}{dk}}$, which are then substituted into Eq. (19), yielding

$$\gamma = \frac{1}{\pi}\left(\frac{1}{18}\,kB_0'(0)\right)^{1/3}\frac{\Gamma\left(\frac{1}{3}\right)^2}{\Gamma\left(\frac{2}{3}\right)^2}\,S_R^{-2/3}\left(\frac{S_V}{S_R}\right)^{1/6}\Delta'\ . \tag{4.21}$$

Neglecting the small shear flow in the corresponding result of Bondeson and Persson (1986) produces a growth rate equal to that given in Eq. (21).

Now we check the validity of our assumption $\left|\frac{\gamma}{kB_0'(0)\epsilon}\sqrt{\frac{S_R}{S_V}}\right| \ll 1$, the assumption that implies the constant ψ approximation. Equations (9) and (21) give

$$\left|\frac{\gamma}{kB_0'(0)\epsilon}\sqrt{\frac{S_R}{S_V}}\right| \sim |\epsilon\Delta'| \ll 1 \ ,$$

verifying the assumption. The form of the above is the same as the case without viscosity, however, viscosity increases the scale length of the internal singular layer. Obviously, our approximation is not valid when $\Delta' \to \infty$. This case is the regime of the no constant-ψ tearing mode. We do not consider this case here.

In the case without viscosity, the small flow shear $V_0'(0)$ contributes a destabilizing correction to the growth rate of $\mathcal{O}\left(\left(V_0'(0)/B_0'(0)\Big/\frac{\gamma}{kB_0'(0)\epsilon}\right)^2\right)$ (Paris and Sy, 1983, Chen and Morrison, 1990a). When viscosity is included and it is assumed that the viscous term dominates the inertial and convection terms, not only are the scalings changed, but also the correction to the growth rate due to $V_0'(0)$ is changed to $\mathcal{O}\left(V_0'(0)/B_0'(0)\right)$, and thus neglected. In the numerical work of Einaudi and Rubini (1989) and Ofman et al. (1991), the scaling of Eq. (21) is obtained in the limit $V_0'(0) = 0$, and so does Ofman et al (1991). We also want to emphasize that even though the flow shear at the magnetic null plane is small, the flow in the external ideal region could be large, which can significantly change the matching quantity Δ'. For the profile (5b) of Einaudi and Rubini (1989), where $V_0'(0) = 0$ and the flow scale length is small the $|\Delta'|$ value is too large for the validity of our constant ψ assumption. In this case a mixture of tearing and Kelvin-Helmholtz instabilities occurs, and it turns out (Einaudi and Rubini, 1989) that small viscosity has no significant influence. However, a very large viscosity will stabilize the instability.

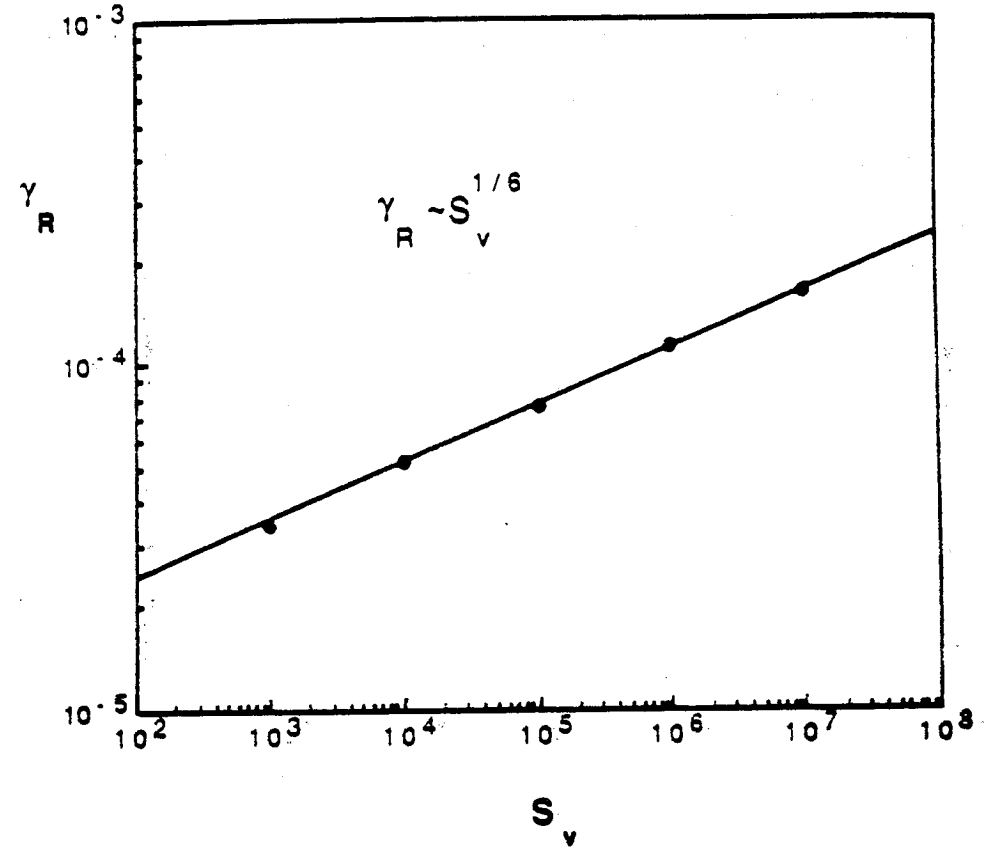

Figure 4.1: Growth rate scaling with viscosity parameter S_V. The other parameters are $S_R = 10^6, V_0 = 0, k = 0.5$.

4.3.2 Comparable shear flow

In this limit, we have the ordering $\frac{V_0'(0)}{B_0'(0)} \sim \mathcal{O}(1)$, and $\psi \sim \phi$ in the internal singular layer (Chen and Morrison, 1990a). Thus the convection term now dominates the inertial term, and the vorticity diffusion is greatly enhanced. The relative magnitude of resistivity and viscosity becomes important and decides which diffusive effect dominates in the singular layer. We consider the case where viscosity is comparable with the resistivity. Thus in Eqs. (3) and (4), we assume $D \sim C \sim 1$. This gives the scale length of the singular layer

$$\epsilon \sim (kB_0'(0)S_R)^{-1/3} \sim (kB_0'(0)S_V)^{-1/3} , \tag{4.22}$$

and the appropriate expansions become

$$\psi = \sum_n \left(\frac{\gamma}{kB_0'(0)\epsilon}\right)^n \psi_n$$

$$\phi = \sum_n \left(\frac{\gamma}{kB_0'(0)\epsilon}\right)^n \phi_n .$$

Inserting the above into Eqs. (3) and (4), the leading order leads to

$$\frac{V_0'(0)}{B_0'(0)}\psi_0 = \phi_0 = \text{ const } ,$$

which means in addition to the "constant ψ" approximation, we have a "constant ϕ" approximation in this limit.

To first order, Eqs. (3) and (4) yield

$$iD\frac{\partial^4\overline{\phi}_1}{\partial\zeta^4} + \frac{V_0'(0)}{B_0'(0)}\zeta\frac{\partial^2\overline{\phi}_1}{\partial\zeta^2} - \frac{\epsilon}{\left(\frac{\gamma}{kB_0'(0)\epsilon}\right)}\frac{V_0''(0)}{B_0'(0)}\phi_0$$

$$= \left(1 - \frac{V_0'(0)^2}{B_0'(0)^2}\right)\zeta\frac{\partial^2\psi_1}{\partial\zeta^2} - iD\frac{V_0'(0)}{B_0'(0)}\frac{\partial^4\psi_1}{\partial\zeta^4} - \frac{\epsilon}{\left(\frac{\gamma}{kB_0'(0)\epsilon}\right)}\frac{B_0''(0)}{B_0'(0)}\psi_0 \tag{4.23}$$

$$\psi_0 - i\zeta\overline{\phi}_1 = C\,\frac{\partial^2\psi_1}{\partial\zeta^2}\,, \tag{4.24}$$

where $\overline{\phi}_1 = \phi_1 - \dfrac{V_0'(0)}{B_0'(0)}\,\psi_1 + \dfrac{1}{2}\,\dfrac{\epsilon}{\left(\frac{\gamma}{kB_0'(0)\epsilon}\right)}\zeta\,\dfrac{V_0'(0)B_0''(0) - B_0'(0)V_0''(0)}{B_0'(0)^2}\,\psi_0.$

Equations (23) and (24) are similar to Eqs. (11) and (12). Again, Fourier transforming and following the same procedure as in the previous limit, yields the equations analogous to Eqs. (19) and (20),

$$\left(\frac{\Delta'}{\pi} + i\,\frac{B_0'(0)B_0''(0) - V_0'(0)V_0''(0)}{V_0'(0)^2 - B_0'(0)^2}\right)\frac{\overline{\phi}_1(0^+)}{\frac{d\overline{\phi}_1(0^+)}{dk}}$$

$$-\left(\frac{\Delta'}{\pi} - i\,\frac{B_0'(0)B_0''(0) - V_0'(0)V_0''(0)}{V_0'(0)^2 - B_0'(0)^2}\right)\frac{\overline{\phi}_1(0^-)}{\frac{d\overline{\phi}_1(0^-)}{dk}} = -2\gamma\epsilon S_R\,; \tag{4.25}$$

when $k \neq 0$,

$$\frac{\frac{V_0'(0)^2}{B_0'(0)^2} - 1}{C}\,\frac{d^2\overline{\phi}_1(k)}{dk^2} - \frac{V_0'(0)}{B_0'(0)}\,\frac{D+C}{C}\,k^2\,\frac{d\overline{\phi}_1(k)}{dk}$$

$$+\left(Dk^4 - 2k\,\frac{V_0'(0)}{B_0'(0)}\right)\overline{\phi}_1(k) = 0\,, \tag{4.26}$$

with the boundary condition that $\overline{\phi}_1(k)$ vanishes at infinity.

Equation (26) is exactly the same as Eq. (A1) in the appendix with $A = \dfrac{V_0'(0)}{B_0'(0)}$. When $\dfrac{V_0'(0)^2}{B_0'(0)^2} > 1$, there are no appropriate solutions to Eq. (26) that satisfy the boundary condition. Thus no constant ψ tearing mode exists. When $\dfrac{V_0'(0)^2}{B_0'(0)^2} < 1$, applying Eq. (A6) to Eq. (25) yields

$$\gamma = \frac{3^{-2/3}}{2\pi}\,\frac{\Gamma(\frac{1}{3})}{\Gamma(\frac{2}{3})}\left[kB_0'(0)\left(1 - \frac{V_0'(0)^2}{B_0'(0)^2}\right)\right]^{1/3}\left[4\,\frac{S_R}{S_V} + \frac{V_0'(0)^2}{B_0'(0)^2}\left(1 - \frac{S_R}{S_V}\right)^2\right]^{-1/6}$$

$$S_R^{-2/3} \times \left[\Delta'\left(\frac{\Gamma(\frac{1}{3} - \frac{1}{3}\delta)}{\Gamma(\frac{2}{3} - \frac{1}{3}\delta)} + \frac{\Gamma(\frac{1}{3} + \frac{1}{3}\delta)}{\Gamma(\frac{2}{3} + \frac{1}{3}\delta)}\right)\right.$$

$$\left. + i\pi\,\frac{B_0'(0)B_0''(0) - V_0'(0)V_0''(0)}{V_0'(0)^2 - B_0'(0)^2}\left(\frac{\Gamma(\frac{1}{3} - \frac{1}{3}\delta)}{\Gamma(\frac{2}{3} - \frac{1}{3}\delta)} - \frac{\Gamma(\frac{1}{3} + \frac{1}{3}\delta)}{\Gamma(\frac{2}{3} + \frac{1}{3}\delta)}\right)\right]\,, \tag{4.27}$$

where

$$\delta = \frac{V_0'(0)/B_0'(0)(S_R - S_V)}{\sqrt{V_0'(0)^2/B_0'(0)^2(S_R - S_V)^2 + 4S_R S_V}}$$

$$|\delta| < 1 \ .$$

The above result is very different from the case without viscosity, but if $\frac{V_0'(0)}{B_0'(0)} = 0$ the growth rate expression for small shear flow, Eq. (21), is obtained. The assumption $\left|\frac{\gamma}{kB_0'(0)\epsilon}\right| \ll 1$ requires $|\epsilon\Delta'| \ll 1$ as before. However, the special case $1 - \frac{V_0'(0)^2}{B_0'(0)^2} \to 0$ needs to be discussed.

If $B_0'(0)B_0''(0) - V_0'(0)V_0''(0) \neq 0$ and $S_R \neq S_V$, there is a singularity at $1 - \frac{V_0'(0)^2}{B_0'(0)^2} = 0$ for the growth rate; i.e. as $1 - \frac{V_0'(0)^2}{B_0'(0)^2} \to 0$ (from above), the imaginary part diverges, while the real part approaches zero as $\left(1 - \frac{V_0'(0)^2}{B_0'(0)^2}\right)^{1/3}$. The "constant ψ" approximation is not valid for any values of Δ', due to the large imaginary part of the growth rate.

If $B_0'(0)B_0''(0) - V_0'(0)V_0''(0) = 0$, or $S_R = S_V$, there is no imaginary part of the growth rate expression, and the "constant ψ" approximation is valid for all values of Δ' when $1 - \frac{V_0'(0)^2}{B_0'(0)^2} \to 0$.

Einaudi and Rubini(1989) have not explored this limit in detail. Qualitatively, their results agree with ours, in that the growth rate is suppressed when viscosity is comparable with resistivity and $\frac{V_0'(0)}{B_0'(0)} \sim \mathcal{O}(1)$. When the viscosity is much larger than the resistivity, vorticity diffusion dominates magnetic field diffusion. In this case there is streamline as well as magnetic field reconnection, and the viscosity enhances the growth rate. This has been shown in the numerical work of Einaudi and Rubini (1989).

4.4 Summary and Discussion

We have investigated the effect of viscosity on the constant-ψ" tearing mode, with the presence of equilibrium shear flow. This problem has been treated in two shear flow limits. When the flow shear is much smaller than the magnetic field shear at the magnetic null plane magnetic diffusion dominates vorticity diffusion and the scale length of the internal singular layer is changed from $S_R^{-2/5}$ to $(S_R S_V)^{-1/6}$, while the scaling of the growth rate is changed from $S_R^{-3/5}$ to $S_R^{-2/3}\left(\frac{S_V}{S_R}\right)^{1/6}$. The influence of $V_0'(0)$ is negligible, however, the flow in the external ideal region can be large and significantly change the matching quantity Δ'. When the flow shear is comparable with the magnetic shear, and the viscosity is comparable with the resistivity, vorticity diffusion is as important as magnetic diffusion in the singular layer. The scaling of the growth rate is changed from $S_R^{-1/2}$ to $S_R^{-2/3}$ and the scaling of the singular layer remains as $S_R^{-1/3}$. Moreover, the $\Delta' > 0$ instability criterion, which is removed in the case of no viscosity and $V_0'(0)V_0''(0) - B_0'(0)B_0''(0) \neq 0$, is restored. When $\frac{V_0'(0)^2}{B_0'(0)^2} > 1$, there is no constant-$\psi$ tearing mode.

We have also discussed the special case where $1 - \frac{V_0'(0)^2}{B_0'(0)^2} \to 0$. In this case, if $V_0'(0)V_0''(0) - B_0'(0)B_0''(0) = 0$, or $S_V = S_R$, the "constant ψ" approximation is valid for all values of Δ', and the growth rate goes to zero with a factor $\left(1 - \frac{V_0'(0)^2}{B_0'(0)^2}\right)^{1/3}$. While if $V_0'(0)V_0''(0) - B_0'(0)B_0''(0) \neq 0$ and $S_V \neq S_R$, there is a singularity at $1 - \frac{V_0'(0)^2}{B_0'(0)^2} = 0$ for the imaginary part of the growth rate, and the "constant ψ" approximation is not valid for any value of Δ'. Thus our calculation is not valid in this case. However, we can still conclude that the tearing instability is totally suppressed when $1 - \frac{V_0'(0)^2}{B_0'(0)^2} \to 0$, since

there is no tearing mode when $\frac{V_0'(0)^2}{B_0'(0)^2} > 1$, and the growth rate has a factor of $\left(1 - \frac{V_0'(0)^2}{B_0'(0)^2}\right)^{1/3}$ when $\frac{V_0'(0)^2}{B_0'(0)^2} < 1$.

Finally, in the case $V_0'(0)/B_0'(0) \sim \mathcal{O}(1)$ with viscosity much larger than resistivity, vorticity diffusion dominates magnetic field diffusion and viscosity enhances the growth rate (Einaudi and Rubini, 1989).

4.5 Appendix – Solution of General Second Order Singular Layer Equation

Here we consider the equation

$$\frac{A^2-1}{C}\frac{d^2f}{dk^2} - \frac{A(D+C)}{C}k^2\frac{df}{dk} + (Dk^4 - 2Ak)f = 0 \ , \qquad \text{(A1)}$$

where A, D, and C are real parameters and $D > 0$, $C > 0$. We seek solutions of Eq. (A1) subject to the boundary condition $\lim_{|k|\to\infty} f(k) = 0$, allowing discontinuity at $k = 0$.

Equation (A1) is similar to the equation discussed by Bondeson and Persson (1986). In terms of the variables

$$z = \frac{\sqrt{A^2(D-C)^2 + 4DC}}{A^2-1}k^3$$

$$d_\pm = \frac{1}{2}\left(\frac{A(D+C)}{\sqrt{A^2(D-C)^2+4DC}} \pm 1\right)$$

$$g = e^{-d_\pm z}f \ , \qquad \text{(A2)}$$

it becomes

$$z\frac{d^2g}{dz^2} + \left[\frac{2}{3} \pm z\right]\frac{dg}{dz} + \left[\pm\frac{1}{3} + \frac{1}{3}\delta\right]g = 0 \ , \qquad \text{(A3)}$$

where

$$\delta = \frac{A(D-C)}{\sqrt{A^2(D-C)^2+4DC}}$$

$$|\delta| < 1 \ .$$

It is easily seen that the signs of d_+ and d_- are opposite if $A^2 < 1$, and the same if $A^2 > 1$.

Equation (A3) is Kummer's equation (Abramowitz and Stegun, 1970). When $A^2 > 1$, there is no solution which satisfies the boundary condition. When $A^2 < 1$, the appropriate solution is

$$f = e^{d-z} U\left(\frac{1}{3} - \frac{1}{3}\delta, \frac{2}{3}, z\right) \ , \tag{A4}$$

if $k < 0$, and

$$f = e^{d+z} U\left(\frac{1}{3} + \frac{1}{3}\delta, \frac{2}{3}, -z\right) \ , \tag{A5}$$

if $k > 0$. In the above, U is the Kummer function.

Using the expansion of Kummer's function for small arguments

$$U(a,b,z) \approx \frac{\pi}{\sin(\pi b)} \left\{ \frac{1}{\Gamma(1+a-b)\Gamma(b)} - z^{1-b} \frac{1}{\Gamma(a)\Gamma(2-b)} \right\} \ ,$$

$$0 \leq b < 1 \ .$$

We obtain from Eqs. (A4) and (A5)

$$\frac{f(0^-)}{\frac{df(0-)}{dk}} = \frac{\Gamma(\frac{1}{3})\Gamma(\frac{1}{3}-\delta)}{\Gamma(\frac{2}{3})\Gamma(\frac{2}{3}-\frac{1}{3}\delta)} \left(\frac{1-A^2}{3^2\sqrt{A^2(D-C)^2+4DC}} \right)^{1/3}$$

$$\frac{f(0^+)}{\frac{df(0+)}{dk}} = -\frac{\Gamma(\frac{1}{3})\Gamma(\frac{1}{3}+\delta)}{\Gamma(\frac{2}{3})\Gamma(\frac{2}{3}+\frac{1}{3}\delta)} \left(\frac{1-A^2}{3^2\sqrt{A^2(D-C)^2+4DC}} \right)^{1/3} \ . \tag{A6}$$

The above results are used in Sec. (4.3).

Chapter 5

Nonlinear Interactions of Resistive Tearing Modes in the Presence of Equilibrium Shear Flow

5.1 Introduction

In the previous chapter we have assumed in Eq. (1.11) that the perturbations are very small that higher order nonlinear terms are discarded. In this chapter, we consider the case where nonlinear terms are important. For the nonlinear evolution of shear flow driven K-H instability, a lot of work has been done, e.g. Horton et al. (1987), Tajima et al. (1991). Here we are only interested in the nonlinear evolution of tearing modes in the presence of equilibrium shear flow. Center manifold reduction is employed.

For resistive tearing mode, the nonlinear evolution of a single mode has been treated before. Rutherford (1973), White et al (1977) found that when the width of the magnetic island exceeds the width of the singular layer, the growth of constant ψ tearing mode slows down from exponential to algebraic, finally saturating at a steady state. However the non-constant ψ tearing mode continues to grow exponentially even in the nonlinear phase (Waddell et al, 1976, Hazeltine et al, 1986). After a sufficiently long time, Thyagaraja and Haas (1990) shown that there exists a saturated m=1 tearing mode in a tokamak when the toroidal current density of the unperturbed equilibrium has a maximum within the m=1 resonant radius and parameter $\frac{d\log q(r)}{d\log \eta(r)}$ is sufficiently small. These authors used the nonlinear critical layer analysis (Benney and

Bergeron, 1969, Haberman, 1972, Thyagaraja, 1981). Numerically, Steinolfson and Van Hoven (1984) found that a secondary flow vortices, opposite in direction to the linear vortices, generate a new magnetic island centered at the initial x-piont. Saramito and Maschke (1985) applied bifurcation theory for compact operators to the general problem of the nonlinear solution of the 3D incompressible visco-resistive MHD equations; they proposed that there exists a saturated tearing mode state when S_R is larger than a critical value, where the original equilibrium loses stability. Recently, Grauer (1989) has studied the nonlinear interactions of two tearing modes near marginal stability. Applying center manifold reduction, the resistive MHD equations are reduced to four amplitude equations, which are significantly easier to analyze. Compared with the usual small amplitude expansion (Stuart, 1960, Waston, 1960) , the center manifold reduction has two advantages (Guckenheimer and Knobloch, 1983). Firstly, it has been rigorously shown to be locally attractive (Sijbrand, 1985, Crawford, 1990), i.e. any solution which stays sufficiently close to the original equilibrium must eventually converge to the center manifold. Thus for local time asymptotic states, such as steady state and periodic solutions, the center manifold reduced equations give a complete answer. Here "local" means that the solution is close to the original equilibrium. Secondly, unlike the usual small amplitude expansion in which the dependence upon small parameters must be specified, in center manifold reduction the order of magnitude of all variables is naturally expressed in terms of the (small) distance from the marginal equilibrium state. However, the calculation of the coefficients in the center manifold reduction is as tedious as the small amplitude reduction, and usually numerical evaluation is required.

If the model considered possesses certain symmetries, the reduced equations can be discussed in general terms without knowing the coefficients. Even though the presence of symmetry may complicate the problem by forcing the marginal modes to have a multiplicity larger than unity, it can greatly simplify the reduced equations by allowing only the terms satisfying symmetry constraints (Golubitsky et al, 1989, Crawford and Knobloch, 1991). Recent studies of mode interactions for systems possessing symmetries have been very successful in explaining complicated behaviors in some experiments; for example, Taylor-Couette flow (Golubitsky and Lanford, 1988), and the Faraday experiment (Crawford et al, 1990). The model used by Grauer possesses O(2) symmetry: the rotation, elements of SO(2) act by translation of X$\rightarrow$X+X_0, and the reflection, elements of Z(2) act by flipping X$\rightarrow -X$. This O(2) symmetry is common for systems with circular or periodic slab geometry. Features of O(2) symmetry-constrained amplitude equations have been well studied by Dengelmayer (1986) and Ambruster et al (1988). In those references it is shown that such systems can saturate at various types of symmetry-broken states depending on different parameters domains. The predicted states of a mixed mode, traveling and standing waves have been observed in Grauer's simulations (1989).

In many circumstances plasma equilibrium is not static, for example, in recent Tokamak experiments, shear flow plays an important role in the transition from Low to High confinement mode. When shear flow is present, the reflection [Z(2)] symmetry in Grauer's model will be broken, while the translation [SO(2)] symmetry remains. Consequently shear flow is expected to affect the nonlinear evolution of tearing modes. In recent numerical simulations,

based on straight cylinder reduced magnetohydrodynamic equations, Persson (1987), Persson and Bondeson (1990) have discussed nonlinear oscillating island states for the evolution of tearing modes, which are driven unstable by shear flow. They also found that these oscillating island states remain when the spectrum is limited to only the modes m/n = 2/1 and 4/2.

Here, we study the nonlinear evolution of tearing modes in the presence of shear flow. We consider an analytical slab geometry model , in which two modes with wave numbers k and 2k are near marginal, while all other modes are stable. Thus the nonlinear evolution of this model is dominated by the interaction of the modes k and 2k. The slab geometry is adopted for simplicity and to be consistent with our previous linear calculations. Since magnetic reconnection occurs only in a very thin layer, slab geometry provides a physical picture for understanding other more complicated geometries, such as cylindrical and toroidal. To find the asymptotic states of the nonlinear interaction, the dissipative MHD equations are reduced to four amplitude equations, using center manifold reduction. The model which we will use is similar to the one used by Grauer. However, the breaking reflection symmetry by the presence of shear flow allows the coefficients of the reduced equations to be complex. Thus the dynamics of the reduced amplitude equations are more complicated. Employing bifurcation analysis, various structures in addition to the oscillating island states have been discovered. Also the roles of the new parameters introduced by flow(imaginary part of the coefficients) are identified.

In Sec. (5.2), the model is described and results of linear calculations are briefly reviewed. Sec. (5.3) is devoted to the center manifold reduction, in light of the constraints of symmetry on the reduced equations. Solutions of

the reduced equations are discussed in Sec. (5.4). Finally Sec. (5.5) contains discussion and a summary.

5.2 Model and Linear Problem

Assuming periodic boundary conditions in the x-direction, the perturbed stream functions can be expanded as

$$\psi(x,y,t) = \sum_n \psi_n(y,t)e^{inkx} + c.c.$$
$$\phi(x,y,t) = \sum_n \phi_n(y,t)e^{inkx} + c.c. \qquad (5.1)$$

where $k = \frac{2\pi}{L}$, and L is the period in x direction.

The linear tearing mode problem with shear flow has been studied in previous chapters. In the region away from the magnetic null plane (the external ideal region), the magnetic field is frozen into flow, hence as noted several times now, global flow can dramatically change the matching quantity $\Delta'_n = \frac{1}{\psi_{1n}}(\frac{\partial\psi_{1n}(0^+)}{\partial y} - \frac{\partial\psi_{1n}(0^-)}{\partial y})$. In the region around the magnetic null plane(the singular layer), the tearing mode is very sensitive to the flow shear. If $\left|\gamma/kB_0'(0)\varepsilon\right| < \left|\frac{V_0'(0)}{B_0'(0)}\right|$, where γ is the growth rate , and ε is the width of the singular layer, i.e. convection dominates the inertia term, the scaling of the tearing mode will change. Hence near marginal stability, even small flow shear will cause significant change (Persson and Bondeson, 1989). It has also been shown that the stable tearing mode can be driven unstable by strong shear flow ($V_0'(0)/B_0'(0) \sim O(1)$) provided $V_0'(0)V_0''(0) - B_0'(0)B_0''(0) \neq 0$ and $S_V^{-1}/S_R^{-1} \ll 1$. In this case the condition of $\Delta' > 0$ for instability is removed. Such shear flow driven unstable tearing modes have been found numerically (Persson and Bondeson, 1989).

Suppose magnetic field and flow are characterized by parameters such as, their magnitudes, shear length etc. Here we want to find the critical parameters where two modes with wavenumbers k and 2k are marginally stable, while all other modes are stable. Then the nonlinear evolution near these critical parameters is studied. There are many situations where we can find such critical parameters. One example is a piecewise continuous magnetic field with a separated double jet flow

$$B_0(y) = \begin{cases} 1, & y > 1 \\ y, & |y| < 1 \\ -1, & y < -1 \end{cases},$$

$$V_0(y) = \begin{cases} 0, & |y| > b \\ V_0, & b > |y| > 1 \\ 0, & |y| < 1 \end{cases}.$$

In the above profiles, flow only exists in the external ideal region, and the tearing mode is unstable only if $\Delta' > 0$. With the assumed profiles, Δ' is equal to zero at wavenumber k_0 when

$$\frac{(1 - k_0 \tanh(k_0))}{k_0} = (1 - V_0^2)\frac{V_0^2 + (2 - V_0^2)e^{2k_0(b-1)}}{-V_0^2 + (2 - V_0^2)e^{2k_0(b-1)}}.$$

Assuming $1 < V_0^2 < 2$, then there exists two solutions for k_0. By choosing appropriate values of V_0 and b, we are able to get $\Delta_1 = 0$ and $\Delta_2 = 0$, while $\Delta_n < 0$ for $n \geq 3$. Thus the above profiles meets our requirements: there exits critical parameters V_0 and b where modes with wavenumber k and 2k are simultaneously marginal stable while other modes are stable. Another example can be constructed from a magnetic profile where the tearing modes are stable, i.e. $\Delta_n' < 0$ for all n, by including shear flow that drives the tearing modes unstable. This is the case treated in Persson and Bondeson's numerical simulations. Again by choosing parameters $V'(0)/B'(0), V''(0)/B''(0)$, and S_V^{-1}/S_R^{-1}

appropriately , the modes k and 2k can be driven simultaneously unstable while the other modes remain stable.

Below, we consider the nonlinear evolutions for parameters near to the critical values. To find the possible asymptotic states of the nonlinear evolution, the dissipative MHD equations are reduced to the four amplitude equations by center manifold reduction, to which we now turn.

5.3 Center Manifold Reduction

Center manifold reduction and related theorems can be found in many references (Marsden and McCracken, 1976, Guckenheimer and Holmes, 1983, Crawford, 1990). So here we just give a brief description. For simplicity and clarity, let us first look at an ordinary (finite) dynamical system

$$\dot{X} = AX + N(X,Y), \tag{5.2}$$

$$\dot{Y} = BY + M(X,Y), \tag{5.3}$$

have respective marginal and stable linear eigenvalues, M and N are nonlinear terms, and $M(0,0) = 0, N(0,0) = 0$. Thus $(X,Y) = (0,0)$ is an equilibrium state (fixed point). For the equations linearized about (X,Y)=(0,0), there exists an invariant center eigenspace spanned by the eigenvectors of A, i.e. Y=0. When the nonlinear terms are included, the main center manifold theorem states that there still exists an invariant subspace called the center manifold. The center manifold is tangent to the center eigenspace at (X,Y)=(0,0), as shown in Fig. 1, and has the same dimension as the center eigenspace. Thus center manifold can be expressed as a "graph of a function", i.e.

$$Y = h(X,Y), \tag{5.4}$$

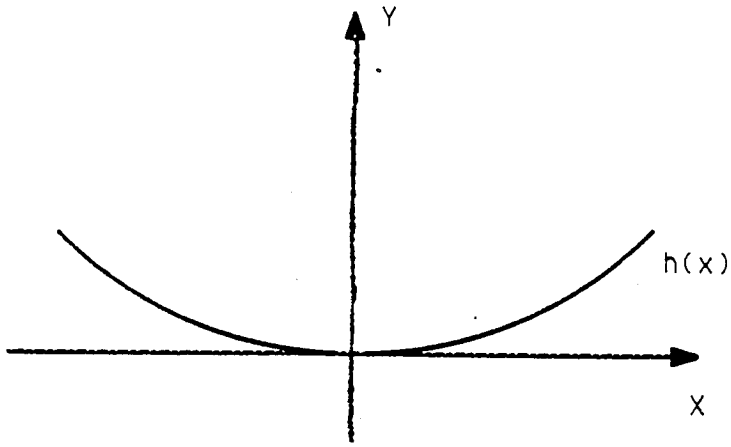

Figure 5.1: Center manifold depiction

with

$$h(0,0) = 0, \ D_X h(0,0) = 0. \tag{5.5}$$

Also, if M and N are differentiable to order r, then h is differentiable to order r-1. As mentioned earlier in the Introduction , center manifold is locally attractive. and so for the purpose of finding the local time asymptotic states, the system can be reduced to lower dimension, the dimension of the center manifold. The dynamics on the center manifold are expressed as

$$\dot{X} = AX + N(X, h(X)). \tag{5.6}$$

It now remains to calculate h(X), which is achieved by pluging Eq.(7) into Eq.(6). we have

$$h'(X)(AX + N(X, h(X)) = Bh(X) + M(X, h(X)). \tag{5.7}$$

In most cases Eq. (10) cannot be solved exactly for h(X)(otherwise an exact solution of the original equations would been found). However h(x) can be

approximated as a Taylor series near (X,Y)=(0,0), satisfying the conditions Eq. (8). Usually only a few terms are needed to unfold all of the local asymptotic states.

Center manifold reduction can also be extended to partial differential equations (Marsden and McCracken, 1976). However, the main center manifold theorem can not be applied directly to our present problem, since the modes k and 2k are not exactly on the imaginary axis, but this difference can be overcomed by shifting parameters. Let Z_0 denote the distance of the parameters from the critical values discussed in the last section, and expand the dynamical system by adding a new equation

$$\dot{Z}_0 = 0. \tag{5.8}$$

Since the modes k and 2k are near marginal, Z_0 is very small. Taking the equilibrium state of the enlarged system as $\begin{pmatrix} \phi_1 \\ \psi_1 \end{pmatrix} = 0$, $Z_0 = 0$, the spectrum of this new equilibrium with wavenumber k and 2k lies on the imaginary axis.

Analogous to Eq.(7), we have in the center manifold

$$\begin{pmatrix} \phi \\ \psi \end{pmatrix}(x,y,t) = \sum_{n=1,2} Z_n(t) \begin{pmatrix} \phi_{nc} \\ \psi_{nc} \end{pmatrix}(y) e^{inkx} + C.C. + h(x,y,Z_n,\bar{Z}_n,Z_0), \tag{5.9}$$

where $\begin{pmatrix} \phi_{nc} \\ \psi_{nc} \end{pmatrix}$ with n=1,2 corresponds respectively to the critical linear marginal eigenfunctions of modes k and 2k, Z_n are their amplitudes, $\bar{Z}_n$ is the complex conjugate of Z_n, and the function h is subject to the following constraints

$$h(x,y,0,0,0) = 0, \ \frac{\partial h}{\partial Z_n}(x,y,0,0,0) = 0,$$

$$\frac{\partial h}{\partial \bar{Z}_n}(x,y,0,0,0) = 0, \ \frac{\partial h}{\partial Z_0}(x,y,0,0,0) = 0.$$

Pluging Eq.(12) into Eq.(3) results in the following reduced amplitude equations (see the appendix for details)

$$\dot{Z}_1 = f_1(Z_1, \bar{Z}_1, Z_2, \bar{Z}_2, Z_0)$$

$$\dot{Z}_2 = f_2(Z_1, \bar{Z}_1, Z_2, \bar{Z}_2, Z_0) \tag{5.10}$$

with $f_1(0) = 0$, $f_2(0) = 0$, $\frac{\partial f_i}{\partial Z_0}(0) = 0$, $\frac{\partial f_i}{\partial Z_n}(0) = 0$, $\frac{\partial f_i}{\partial \bar{Z}_n}(0) = 0$ (n=1,2 and i=1,2). For the nonlinear evolution with $|Z|$ small, the functions in Eqs.(13) can be Taylor expanded. One needs only expand to some finite order to unfold the new branches of solutions. However, just third order the number of terms is very large, calculation of all of the coefficients is a tremendous amount of work. Fortunatly, in the present model many terms in the expansion will vanish due to the constraint imposed by the symmetry of the system. Thus the reduced amplitude equations are greatly simplified and can be discused as to their possible solutions even without knowing the coefficients . As noted in the case without flow, this model possesses O(2) symmetry, and Eqs(3) are "equivariant" under the following transformations.

$$T_{x_0}\begin{pmatrix}\phi_1\\ \psi_1\end{pmatrix}(x,y,t) = \begin{pmatrix}\phi_1\\ \psi_1\end{pmatrix}(x+x_0,y,t),$$

$$Z\begin{pmatrix}\phi_1\\ \psi_1\end{pmatrix}(x,y,t) = \begin{pmatrix}-\phi_1\\ \psi_1\end{pmatrix}(-x,y,t),$$

i.e. if $\begin{pmatrix}\phi_1\\ \psi_1\end{pmatrix}(x,y,t)$ is a solution of Eqs.(3), then so is $T_{x_0}\begin{pmatrix}\phi_1\\ \psi_1\end{pmatrix}(x,y,t)$ and $Z\begin{pmatrix}\phi_1\\ \psi_1\end{pmatrix}(x,y,t)$. Inclusion of shear flow breaks the reflection symmetry, however the translation symmetry is preserved. Thus the reduced amplitude equations are equivariant under the following operations:

$$T_{x_0}(z_1, z_2) = (e^{ikx_0}z_1, e^{2ikx_0}z_2).$$

The basic polynomial invariants for the above operations are $|Z_1|^2$, $|Z_2|^2$, $\bar{Z}_1{}^2 Z_2$, $Z_1^2 \bar{Z}_2$. Thus the expansion of Eq. (13) must have the form:

$$\dot{Z}_1 = (\lambda_1 + i\omega_{1c})Z_1 + a_1 \bar{Z}_1 Z_2 + b_1 Z_1 |Z_1|^2 + c_1 Z_1 |Z_2|^2 + 0(Z^4)$$

$$\dot{Z}_2 = (\lambda_2 + i\omega_{2c})Z_2 + a_2 Z_1^2 + b_2 Z_2 |Z_1|^2 + c_2 Z_2 |Z_2|^2 + 0(Z^4), \quad (5.11)$$

where $\lambda_i + i\omega_{ic}$ (i=1,2) are the linear eigenvalues of the near marginal modes, ω_i are the eigenfrequencies at the critical values $Z_0 = 0$, and $\lambda_i = \vartheta(Z_0)$. Formulas for the coefficients of Eqs.(14) are calculated in the appendix. Breaking reflection symmetry allows the coefficients a,b and c to be complex. Similar equations have been discussed by Knobloch and Proctor (1988) for studying interactions of two oscillators with 2:1 resonant frequencies. However, these authers mainly discussed the equations near a special degenerate parameter regime, where the pure mode (c.f. Sec. (3.4)) solutions has double zero eigenvalues. Here we are interested in more general parameter regimes.

Furthermore, the inessential nonlinear terms $Z_1|Z_1|^2$ can be removed by a near idendity SO(2) invariant coordinate transformation $Z_1 \to Z_1$, $Z_2 \to Z_2 - \frac{b_1}{a_1} Z_1^2$. Equations (14) become

$$\dot{Z}_1 = (\lambda_1 + i\omega_{1c})Z_1 + a_1 \bar{Z}_1 Z_2 + c_1 Z_1 |Z_2|^2 + 0(Z^4) \quad (5.12)$$

$$\dot{Z}_2 = (\lambda_2 + i\omega_{2c})Z_2 + a_2 Z_1^2 + bZ_2 |Z|^2 + c_2 Z_2 |Z_2|^2 + 0(Z^4), \quad (5.13)$$

where $b = b_2 + 2b_1$, and the small modification of coefficient a_2 is neglected. Now let $a_1 = \rho_3 e^{i\theta_3}$, $a_2 = \rho_4 e^{i\theta_4}$, $b = \rho_b e^{i\theta_b}$, $c_1 = \rho_1 e^{i\theta_1}$, $c_2 = \rho_2 e^{i\theta_2}$, and assume $|a_1 a_2 c_2| \neq 0$. We can reduce the number of parameters in Eqs(15) and(16) by the following rescaling

$$Z_1 \to \frac{\rho_3}{\rho_2}\sqrt{\frac{\rho_3}{\rho_4}} Z_1, \; Z_2 \to \frac{\rho_3}{\rho_2} e^{-i\theta_3} Z_2, \; t \to \frac{\rho_2}{\rho_3^2} t,$$

The rescaled equations are

$$\dot{Z}_1 = (\tilde{\lambda}_1 + \tilde{\omega}_{1c})Z_1 + \bar{Z}_1 Z_2 + \tilde{\rho}_1 e^{i\theta_1} Z_1 |Z_2|^2 + 0(Z^4) \quad (5.14)$$

$$\dot{Z}_2 = (\tilde{\lambda}_2 + \tilde{\omega}_{2c})Z_2 + e^{i\theta} Z_1^2 + \tilde{\rho}_b e^{i\theta_b} Z_2 |Z_1|^2 + e^{i\theta_2} Z_2 |Z_2|^2 + 0(Z^4), \quad (5.15)$$

where $\theta = \theta_3 + \theta_4$, $\tilde{\lambda}_1 = \frac{\rho_2}{\rho_3^2}\lambda_1$, $\tilde{\lambda}_2 = \frac{\rho_2}{\rho_3^2}\lambda_2$, $\tilde{\omega}_{1c} = \frac{\rho_2}{\rho_3^2}\omega_{1c}$, $\tilde{\omega}_{2c} = \frac{\rho_2}{\rho_3^2}\omega_{2c}$, $\tilde{\rho}_1 = \frac{\rho_1}{\rho_2}$,$\tilde{\rho}_b = \frac{\rho_3 \rho_b}{\rho_2 \rho_4}$. For convenience we drop "the tilde " in the following discussion. In the next section, bifurcation analysis is employed to find the possible time asymptotic states, i.e. branches of nonlinear solutions of the reduced amplitude equations that evolve from the linear dynamics.

5.4 Solutions of the Reduced Equations

Bifurcation analysis is the natural technique for finding the possible time asymptotic states when parameters Z_0 are away from but still near to, their critical values. There are two types of bifurcations (Guckenheimer and Holmes, 1983): "local" and "global" . Local bifurcation is recognized by a change in the stability of a solution. Depending on how the stability is changed, the local bifurcations are again divided into "Steady State" and "Hopf bifurcations". If stability is changed because an eigenvalue traverses zero, the bifurcation is of the steady state type; if the stability is changed because eigenvalues are pure imaginary at criticality, the bifurcation is of the Hopf type, and the new branch of solutions are periodic. As for the global bifurcation, it's existence is not revealed by local analyses and will not be of interest here. We are interested in the local bifurcation near the original equilibrium ($Z_1, Z_2, Z_0 = 0$). This problem has been reduced to the four dimensional amplitude equations (14) and their complex conjugate derived above.

In polar coordinate $Z_1 = r_1 e^{i\varphi_1}, Z_2 = r_2 e^{i\varphi_2}$, and Eqs.(17) and (18) become

$$\dot{r}_1 = (\mu_1 + r_2 cos\varphi + \rho_1 cos\theta_1 r_2^2) r_1 \tag{5.16}$$

$$\dot{r}_2 = \mu_2 r_2 + cos(\varphi - \theta) r_1^2 + \rho_b cos\theta_b r_1^2 r_2 + cos\theta_2 r_2^3 \tag{5.17}$$

$$\dot{\varphi} = \delta - (sin(\varphi - \theta)\frac{r_1^2}{r_2} + 2sin\varphi r_2) + \rho_b sin\theta_b r_1^2 + d r_2^2 \tag{5.18}$$

where $\mu_i = Re\lambda_i$, $\beta_i = Im\lambda_i$ $(i = 1, 2)$, $\delta = \omega_{2c} + \beta_2 - 2(\omega_{1c} + \beta_1)$, $\varphi = \varphi_2 - 2\varphi_1$, and $d = sin\theta_2 - 2\rho_1 sin\theta_1$. Since the frequencies ω_{ic} arises mostly from Dopler shifting, and such Dopler shifts are cancelled in the combination $\omega_{2c} - 2\omega_{1c}$, δ is a small parameter. In the case without flow, $\delta = sin\theta = d = sin\theta_b = 0$, and hence these are the parameters introduced by flow. Note that what matters in the nonlinear evolution is the phase difference, not the individual phase of each mode. Thus, the original four amplitude equations (17) and (18) and their complex conjugates are reduced to three independent eqs.(19)-(21). The variation of individual phases of each mode is governed by

$$\dot{\varphi_1} = \omega_{1c} + \beta_1 + sin\varphi r_2 + \rho_1 sin\theta_1 r_2^2,$$

$$\dot{\varphi_2} = \omega_{2c} + \beta_2 - sin(\varphi - \theta)\frac{r_1^2}{r_2} + \rho_b sin\theta_b r_1^2 + sin\theta_2 r_2^2.$$

Bifurcated solutions of Eqs.(19-21) have a magnetic flux function near to the magnetic null line (for constant ψ tearing mode) given by

$$\tilde{\psi} \approx -\frac{1}{2} B_0'(0) y^2 + r_1 cos(kx + \omega_1 t + \varphi_1) + r_2 cos(2(kx + \omega_1 t + \varphi_1) + \varphi), \tag{5.19}$$

where $\omega_1 = \omega_{1c} + \beta_1 + r_2 sin\varphi + r_2^2 \rho_1 sin\theta_1$. Note in the above expression we haven't take into account the rescalings of coefficients, but this does not

change the qualitative physical picture. If $\omega_1 = 0$, the solution is a steady state island, while if $\omega_1 \neq 0$, the solution is a traveling island state. It is interesting to note that a pure mode solution $r_1 = 0, r_2 \neq 0$ still solves the nonlinear interaction equations, even if higher order terms are included. This is due to the symmetry which has forced many nonlinear interaction terms to vanish. However, a pure mode $r_2 = 0, r_1 \neq 0$ is not a solution. A contour plots of Eq.(22) with $\omega_1 t + \varphi_1 = 0$ and $\varphi = 0$ is given in Fig.(2). If the stability of the bifurcated solution changes, a secondary bifurcation can happen. However, a secondary steady state bifurcation is not of much interest, since it does not change the magnetic field structure. What is interesting is a secondary Hopf bifurcation. When this happens, Eq.(22) become

$$\tilde{\psi} \approx -\frac{1}{2}B_0'(0)y^2 + (r_{10} + r_{11}cos(\omega_0 t))cos(kx + \omega_1 t + \varphi_1) +$$

$$(r_{20} + r_{21}cos(\omega_0 t))cos(2(kx + \omega_1 t + \varphi_1) + \varphi_0 + \varphi_{11}cos(\omega_0 t)), \qquad (5.20)$$

where ω_0 is the Hopf bifurcation frequency. In this new magnetic field structure, the amplitude and phase differences between two modes oscillates. If it is not far away from the secondary bifurcation, then $|\varphi_{11}| \ll 1$, and Eq.(20) is close to a modulated traveling wave state, or the oscillating island state observed in the simulations of (Persson, 1987, Persson and Bondeson, 1989). Below we will discuss the parameter domains for the pure mode, and the mixed mode solution with its secondary Hopf bifurcation. Since only the stable time asymptotic states are practically observable, we also discuss the stability of the solutions.

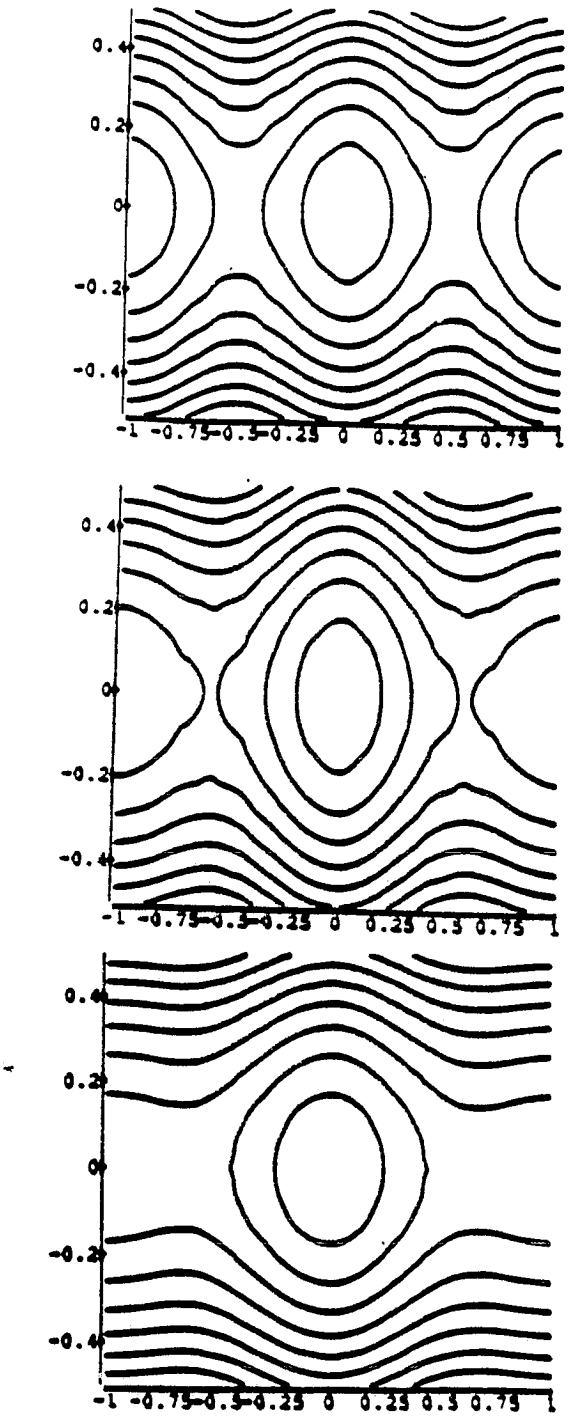

Figure 5.2: Contour plots of magnetic flux function with (a) $r_1 = 0, r_2 = 0.02$, (b) $r_1 = 0.02, r_2 = 0.02$, (c) $r_1 = 0.02, r_2 = 0.01$.

5.4.1 Pure mode solution ($r_1 = 0, r_2 \neq 0$)

In this case, the amplitude equations decouple from the phase equation. Eqs.(16-18) become

$$\begin{aligned} \dot{r_1} &= 0 \\ \dot{r_2} &= \mu_2 r_2 + cos\theta_2 r_2^3 \\ \dot{\varphi_2} &= \omega_{2c} + \beta_2 + sin\theta_2 r_2^2, \end{aligned} \tag{5.21}$$

which have the solution

$$r_2^2 = -\frac{\mu_2}{cos\theta_2}, \quad \text{if} \quad \frac{\mu_2}{cos\theta_2} < 0. \tag{5.22}$$

Generally this solution is a traveling wave state with phase velocity $(\omega_{2c} + \beta_2 + sin\theta_2 r_2^2)/2k = (\omega_{2c} + \beta_2 - \frac{sin\theta_2}{cos\theta_2}\mu_2)/2k$, which differs from the steady state when there is no flow. The contour plot of magnetic flux corresponding to the pure mode is shown in Fig. 5.2a. Observe, there are two magnetic islands in one period length. From Eqs.(16) and (17), stability of this solution is determined by the eigenvalues $-2\mu_2$ and $\mu_1 + \sqrt{-\frac{\mu_2}{cos\theta_2}}cos\varphi - \frac{\rho_1 cos\theta_1}{cos\theta_2}\mu_2$. Since phase difference φ is arbitrary, pure mode is stable when $\mu_2 > 0, \mu_1 < 0$, and $\mu_1 + \sqrt{-\frac{\mu_2}{cos\theta_2}} < 0$. A secondary bifurcation occurs when the stability changes. The first stability eigenvalue changes at $\mu_2 = 0$, which already gives the bifurcated pure mode solution. The second eigenvalue comes from the perturbations of the mode k, thus its secondary bifurcated solutions will be a mixed mode solution, which will be discussed next.

5.4.2 Mixed mode solution ($r_1 r_2 \neq 0$)

Equations (16)-(18) yield

$$cos\varphi r_2 + \rho_1 cos\theta_1 r_2^2 = -\mu_1 \tag{5.23}$$

$$\sigma cos(\varphi - \theta) r_2 + (\rho_b cos\theta_b \sigma + cos\theta_2) r_2^2 = -\mu_2 \tag{5.24}$$

$$-(\sigma sin(\varphi - \theta) + 2sin\varphi) r_2 + (\rho_b sin\theta_b \sigma + d) r_2^2 = -\delta, \tag{5.25}$$

where $\sigma = r_1^2/r_2^2$ denotes the ratio of the amplitudes of the two modes. Let us first look at the stability of the solutions. Stability is determined by the solutions of a third order polynomial

$$\lambda^3 - d_1\lambda^2 + d_2\lambda - d_3 = 0, \tag{5.26}$$

where $d_1 = -2(\sigma cos(\varphi - \theta) + cos\varphi) r_2 + \vartheta(r_2^2)$, $d_2 = [(\sigma - 4sin\varphi sin(\varphi - \theta)) - \frac{4r_2}{\sigma} cos\varphi cos\theta_2] r_1^2 + \vartheta(r_1^2 r_2)$, $d_3 = 2(\sigma cos\varphi + 2cos(\varphi - \theta)) r_1^2 r_2 + \vartheta(r_1^2 r_2^2) + \vartheta(\sigma r_1^2 r_2^2)$. A stable solution requires that $d_1 < 0$, $d_2 > 0$, $d_3 < 0$. If three eigenvalues are real, the above conditions are also sufficient. If two eigenvalues are complex, then $d_1 d_2 - d_3 < 0$ guarantees stability. For $d_2 > 0$, and $d_1 d_2 - d_3 = 0$, there exists pure imaginary eigenvalues $\lambda = \pm i\sqrt{d_2}$. Thus a secondary Hopf bifurcation could occur along $d_1 d_2 - d_3 = 0$. Due to the exchange stability principle (Iooss and Joseph, 1980), the Hopf bifurcated solution is stable on the side $d_1 d_2 - d_3 > 0$, while unstable on the side $d_1 d_2 - d_3 < 0$. The side on which the Hopf bifurcated solution appears depends on the sign of the coefficients of higher order terms.

Eqs.(23)-(25) are still very difficult to solve directly, so we consider several special cases: $\theta = 0$, $\theta = \pi$ and $\theta = \pi/2$. For the cases $\theta = 0$ and

$\theta = \pi$, we discuss the difference made by the flow induced parameter δ; while $\theta = \pi/2$ is the case only possible with flow.

(i) $\theta = 0$ In this case, Eqs.(23)-(25) imply

$$r_2 = \frac{\sqrt{(2\mu_1 + \mu_2)^2 + \delta^2}}{\sigma + 2}(1 + \vartheta(r_2))$$

$$cos\varphi = -\frac{2\mu_1 + \mu_2}{\sqrt{(2\mu_1 + \mu_2)^2 + \delta^2}} + \vartheta(r_2) \tag{5.27}$$

$$sin\varphi = \frac{\delta}{\sqrt{(2\mu_1 + \mu_2)^2 + \delta^2}} + \vartheta(r_2).$$

In the case without flow, the solution requires that phases differences of the two modes φ must be either 0 or π. Here φ can be any value depending on the ratio $(2\mu_1 + \mu_2)/\delta$.

The coefficients in the stability eigenvalue equations (26) become

$$d_1 = -2(\sigma + 1)cos\varphi r_2 + \vartheta(r_2^2),$$

$$d_2 = (\sigma - 4sin^2\varphi - \frac{4r_2}{\sigma}cos\varphi cos\theta_2)r_1^2 + \vartheta(r_1^2 r_2),$$

$$d_3 = 2(\sigma + 2)cos\varphi r_1^2 r_2 + \vartheta(r_1^2 r_2^2) + \vartheta(\sigma r_1^2 r_2^2).$$

Thus a stable solution is possible only if $cos\varphi \sim \vartheta(r_2)$, either $\sigma > 4$ or $\sigma \ll 1$ with $-4 - \frac{r_2}{\sigma}cos\varphi cos\theta_2 > 0$. The secondary Hopf bifurcation is possible also only if the above conditions are satisfied. From Eq. (27), $cos\varphi \sim \vartheta(r_2)$ requires $\left|\frac{2\mu_1+\mu_2}{\delta}\right| \sim \vartheta(r_2) \ll 1$. Since δ is the parameter introduced by flow, there exists no stable solution and secondary Hopf bifurcation in the case $\theta = 0$ without flow.

(ii) $\theta = \pi$. In this case, there exists a special amplitude ratio $\sigma = 2$, at which the phase difference φ can be any value even in the case without flow. We first consider the special case where $\sigma = 2$. Equations (23)-(25) yield

$$r_2^2 = -\frac{2\mu_1 + \mu_2}{2\rho_1 cos\theta_1 + 2\rho_b cos\theta_b + cos\theta_2}$$

$$= -\frac{\delta}{2\rho_b sin\theta_b + d} > 0$$

$$cos\varphi = -\frac{\mu_1}{r_2} + \vartheta(r_2) = -\frac{\mu_2}{2r_2} + \vartheta(r_2).$$

The coefficients of the stability equations (26) for $\theta = \pi$ become

$$d_1 = 2(\sigma - 1)cos\varphi r_2 + \vartheta(r_2^2),$$

$$d_2 = (\sigma + 4sin^2\varphi - \frac{4r_2}{\sigma}cos\varphi cos\theta_2)r_1^2 + \vartheta(r_1^2 r_2),$$

$$d_3 = 2(\sigma - 2)cos\varphi r_1^2 r_2 + \vartheta(r_1^2 r_2^2) + \vartheta(\sigma r_1^2 r_2^2).$$

Thus a stable solution with $\sigma = 2$ requires $cos\varphi < 0$. A secondary Hopf bifurcation can occur when $cos\varphi \sim \vartheta(r_2)$, which requires

$$\frac{2\mu_1}{2\mu_1 + \mu_2} \sim \frac{\mu_2}{2\mu_1 + \mu_2} \sim \vartheta(1).$$

Now for the case $\sigma \neq 2$, Eqs. (23)-(25) yield

$$r_2^2 = \frac{\sqrt{(2\mu_1 + \mu_2)^2 + \delta^2}}{(\sigma - 2)^2}(1 + \vartheta(r_2))$$

$$cos\varphi = \pm\frac{2\mu_1 + \mu_2}{\sqrt{(2\mu_1 + \mu_2)^2 + \delta^2}} + \vartheta(r_2) \tag{5.28}$$

$$sin\varphi = \frac{\delta}{\sqrt{(2\mu_1 + \mu_2)^2 + \delta^2}} + \vartheta(r_2).$$

If $|\frac{r_2}{cos\varphi}| \ll 1$, the solution is stable only if either $\sigma > 2$, $cos\varphi < 0$ or $\sigma < 1$, $cos\varphi > 0$. Equations (23)-(25) yield in this limit

$$r_2 = -\frac{\mu_1}{cos\varphi}(1 + \vartheta(\frac{r_2}{cos\varphi})),\ \sigma = -\frac{\mu_2}{\mu_1}(1 + \vartheta(\frac{r_2}{cos\varphi})) + \vartheta(\frac{r_2}{cos\varphi}). \qquad (5.29)$$

The assumption $|\frac{r_2}{cos\varphi}| \ll 1$ requires that $|\frac{\mu_1\delta^2}{(2\mu_1+\mu_2)^2}| \ll 1$. A secondary Hopf bifurcation can only occur for $\sigma < 1$, which implies from Eq. (29)

$$-\frac{\mu_2}{\mu_1} < 1.$$

Obviously flow induced parameters are not important in this limit.

If $cos\varphi \sim \vartheta(r_2)$, similar to the case discussed in $\theta = 0$, it is required that $\frac{2\mu_1+\mu_2}{\delta} \sim \vartheta(r_2)$. A secondary Hopf bifurcation is possible when $4 - (4r_2/\sigma)cos\ \varphi cos\ \theta_2$.

(iii) $\theta = \pi/2$. This case is only possible with flow. The coefficients of the stability eigenvalue equations become

$$d_1 = -2(\sigma sin\varphi + cos\varphi)r_2 + \vartheta(r_2^2),$$

$$d_2 = (\sigma + 2sin2\varphi - \frac{4r_2}{\sigma}cos\varphi cos\theta_2)r_1^2 + \vartheta(r_1^2 r_2),$$

$$d_3 = 2(\sigma cos\ \varphi + 2sin\varphi)r_1^2 r_2 + \vartheta(r_1^2 r_2^2) + \vartheta(\sigma r_1^2 r_2^2).$$

When $\sigma > \sqrt{2}$, the solution is stable only if $sin\varphi > 0$, $cos\varphi < 0, -\sigma/2 < tan\varphi < -1/\sigma$, and $\sigma + 2sin2\varphi > 0$. When $\sigma < \sqrt{2}$, the solution is stable only if $sin\varphi < 0$, $cos\varphi > 0, -\sigma/2 > tan\varphi > -1/\sigma$, and $\sigma + 2sin2\varphi - \frac{4r_2}{\sigma}cos\varphi cos\theta_2 > 0$.

Assuming $\sigma \gg 1$, Eqs.(23)-(25) give

$$r_2^2 \approx \frac{\sqrt{(2\mu_1 + \mu_2)^2 + \delta^2}}{\sigma}$$

$$cos\varphi \approx -\frac{\delta}{\sqrt{(2\mu_1+\mu_2)^2+\delta^2}} \tag{5.30}$$

$$sin\varphi \approx -\frac{\mu_2}{\sqrt{(2\mu_1+\mu_2)^2+\delta^2}}.$$

Eqs. (30) implies that $|\frac{\mu_1}{\mu_2}| \ll 1$, or $|\frac{\mu_1}{\delta}| \ll 1$. A secondary Hopf bifurcation can occur when $|tan\varphi| \sim 1/\sigma \ll 1$, which implys that $|\frac{\mu_2}{\delta}| \ll 1$.

From the above calculations, we see that in the case without flow, a secondary Hopf bifurcation can only occur with $\theta = \pi$, $\sigma < 1$ or $\sigma = 2$. Thus shear flow plays an important role in driving the oscillating islands with ($\sigma \gg 1$) as in Persson and Bondeson's simulations.

5.5 Discussion and Summary

The nonlinear evolution of plasmas can saturate in time asymptotic states, or a transition to turbulence may occur. Generally the governing partial differential equations are analytically intractable and so we are unable to predict these asymptotic states. Even though there are some methods for simplifying nonlinear partial differential equations and make them solvable, such as inverse scattering method (Drazin and Johson, 1989), which reduces nonlinear equations to linear ones, and similarity methods (Ames, 1967), which reduces partial differential equation to ordinary differential equations, these methods are only applicable to a limited set of equations. However, in recent years studies of nonlinear finite dimensional systems have been successful. Very complicated behavior, even chaotic states, have been found in finite dimensional systems. Since finite dimensional systems appear to possesses solutions as complicated as those expected for plasma evolution, it is natural to attempt

to model the dynamics of plasmas by some finite system. This is also reasonable physically, since in many situations only a finite number of degrees-of-freedom is excited. For example, magnetic island coalescence (Finn and Kaw, 1977) can be modeled by the interaction of two modes with the wave numbers k and 2k. In this case the model equations are the same as Eqs.(14) with the restriction that the coefficients be real. Given the pure mode state, i.e. that there are two magnetic islands in one period length, the analysis in part A of Sec. (5.3) tells us that we have stability only if $\mu_2 > 0, \mu_1 < 0$ and $\mu_1 + \sqrt{-\frac{\mu_2}{cos\theta_2}} < 0$. For the magnetic profiles chosen by Finn and Kaw, $\mu_1 > 0$ if $\mu_2 > 0$. Thus the given pure mode is unstable and will evolve to a mixed mode state, i.e. two islands in one period length will coalesce, as shown in Fig. 5.2. In another example, Parker et al. (1990) studied the nonlinear evolution of tearing modes without flow, using the period length as the bifurcation parameter. When the period length is short, only one tearing mode is excited, then the finite time asymptotic state is the usual saturated state of e.g. White et al, 1977. When the period length becomes longer, more modes will be excited (from the linear calculation of Parker et al), and we can model the situation with the interactions of two, three or more modes. The symmetry (O(2)) will limit the nonlinear terms in the model amplitude equations, and enable us to discuss the solution in general terms. The two mode interaction with O(2) symmetry has been well studied by Dangelmayer (1986), Ambruster et al (1988) and Grauer (1989). Even though the above suggested reduced models are not rigorously justified, they give some qualitative insights into the problem. The interaction of near marginal modes, the model can be justified by using either small amplitude or center manifold reduction. Strictly speaking these reductions are valid only close to the original marginal equilibrium, however, very often results are valid

well away from marginality.

In the present chapter we have studied the interactions of two near marginal tearing modes with wavenumbers k and 2k in the presence of equilibrium shear flow. Employing the center manifold reduction method, the resistive MHD equations are reduced to amplitude equations. In this reduction method, a good knowledge of the linear problem is required. The model which we used is similar to the one used by Grauer (1989). However the presence of shear flow in our problem breaks the reflection symmetry, and allows the coefficients of the reduced equations to be complex. The most important parameter introduced by shear flow are δ and $sin\theta \neq 0$. Bifurcation analysis was used to find possible time asymptotic states in different parameter regimes. Various states such as traveling and oscillating magnetic islands were found, and their observable parameter domains were discussed. It was shown that shear flow plays an important role in driving the oscillating island state with $\sigma \gg 1$, i.e. the mode k dominates the mode 2k.

5.6 Appendix - Calculation of Coefficients

Let $L = L_c + \Delta L$ where L_c corresponds to the linear operator at criticality, and $\Delta L = \frac{\partial L}{\partial Z_0}|_{Z_0=0} Z_0$. Here for convenience we denote $\bar{Z}_1$ and $\bar{Z}_2$ by Z_3 and Z_4, respectively. The function h(x,y) in Eq.(9) is expanded in powers of the amplitudes

$$h(x,y) = \sum_{m,n=0,4}^{4} Z_m(t) Z_n(t) \begin{pmatrix} \phi_{mn} \\ \psi_{mn} \end{pmatrix} + \sum_{m,n,p=0,4}^{4} Z_m(t) Z_n(t) Z_p(t) \begin{pmatrix} \phi_{mnp} \\ \psi_{mnp} \end{pmatrix} + \cdots$$

Inserting Eqs(9) into Eqs.(1.11), and equating terms of order $\vartheta(|Z|)$ yields the linear problem

$$L_c \begin{pmatrix} \phi_{nc} \\ \psi_{nc} \end{pmatrix} - i\omega_{nc} \begin{pmatrix} \nabla_\perp^2 \phi_{nc} \\ \psi_{nc} \end{pmatrix} = 0. \tag{A1}$$

The corresponding adjoint problem is

$$L_c^\perp \begin{pmatrix} \bar{\phi}_{nc}^\perp \\ \bar{\psi}_{nc}^\perp \end{pmatrix} - i\omega_{nc} \begin{pmatrix} \nabla_\perp^2 \bar{\phi}_{nc}^\perp \\ \bar{\psi}_{nc}^\perp \end{pmatrix} = 0, \tag{A2}$$

with

$$L_c^\perp = \begin{pmatrix} S_V^{-1}\nabla_\perp^4 - \phi_0'\nabla_\perp^2 \frac{\partial}{\partial x} - 2\phi_0'' \frac{\partial}{\partial y}\frac{\partial}{\partial x} & \psi_0' \frac{\partial}{\partial x} \\ \psi_0' \nabla_\perp^2 \frac{\partial}{\partial x} + 2\psi_0'' \frac{\partial}{\partial y}\frac{\partial}{\partial x} & S_R^{-1}\nabla_\perp^2 - \phi_0' \frac{\partial}{\partial x} \end{pmatrix}.$$

The normalization is defined as

$$(\phi_{mc}^\perp, \nabla_\perp^2 \phi_{nc}) + (\psi_{mc}^\perp, \psi_{nc}) = \int\int (\bar{\phi}_{mc}^\perp \nabla_\perp^2 \phi_{nc} + \bar{\psi}_{mc}^\perp \psi_{nc})\, dx\, dy = \delta_{mn}.$$

To order $\vartheta(|Z|^2)$ we obtain

$$\sum_{0\le m\le n\le 4} Z_m Z_n [L_c \begin{pmatrix} \phi_{mn} \\ \psi_{mn} \end{pmatrix} - i(\omega_m + \omega_n) \begin{pmatrix} \nabla_\perp^2 \phi_{mn} \\ \psi_{mn} \end{pmatrix}] = \begin{pmatrix} \phi_{inh} \\ \psi_{inh} \end{pmatrix} \tag{A3}$$

with

$$\phi_{inh} = [(\frac{\lambda_1}{Z_0} Z_0 Z_1 + a_1 \bar{Z}_1 Z_2)\nabla_\perp^2 \phi_{1c} + (\frac{\lambda_2}{Z_0} Z_0 Z_2 + a_2 Z_1^2)\nabla_\perp^2 \phi_{2c} + c.c.]$$

$$+ \sum_{1\le m\le n\le 4} Z_m Z_n \frac{1}{1+\delta_{mn}} [\frac{\partial \phi_{mc}}{\partial x}\frac{\partial \Omega_{nc}}{\partial y} - \frac{\partial \phi_{mc}}{\partial y}\frac{\partial \Omega_{nc}}{\partial x} - \frac{\partial \psi_{mc}}{\partial x}\frac{\partial j_{nc}}{\partial y}$$

$$+ \frac{\partial \psi_{mc}}{\partial y}\frac{\partial j_{nc}}{\partial x} + \text{terms interchanging m and n}] - \sum_{m=1}^{4} \frac{\partial L}{\partial Z_0} Z_m Z_0 \phi_{mc}$$

$$\psi_{inh} = [(\frac{\lambda_1}{Z_0} Z_0 Z_1 + a_1 \bar{Z}_1 Z_2)\psi_{1c} + (\frac{\lambda_2}{Z_0} Z_0 Z_2 + a_2 Z_1^2)\psi_{2c} + c.c]$$

$$+ \sum_{1\le m\le n\le 4} Z_m Z_n \frac{1}{1+\delta_{mn}} [\frac{\partial \phi_{mc}}{\partial x}\frac{\partial \psi_{nc}}{\partial y} - \frac{\partial \phi_{mc}}{\partial y}\frac{\partial \psi_{nc}}{\partial x}$$

$$+ \text{terms interchanging m and n}] - \sum_{m=1}^{4} \frac{\partial L}{\partial Z_0} Z_0 \psi_{mc}.$$

Considering, respectively, terms with Z_0Z_1 and Z_0Z_2, one can obtain the following through the Fredholm solvability condition:

$$\frac{\lambda_1}{Z_0} = \iint (\bar{\phi}_{1c}^{\perp}\frac{\partial L}{\partial Z_0}\phi_{1c} + \bar{\psi}_{1c}^{\perp}\frac{\partial L}{\partial Z_0}\psi_{1c})\,dx\,dy$$

$$\frac{\lambda_2}{Z_0} = \iint (\bar{\phi}_{2c}^{\perp}\frac{\partial L}{\partial Z_0}\phi_{2c} + \bar{\psi}_{2c}^{\perp}\frac{\partial L}{\partial Z_0}\psi_{2c})\,dx\,dy.$$

Actually if we had already solved the linear problem, λ_1 and λ_2 could be written down immediatelly. For terms with $\bar{Z}_1Z_2$, rewrite Eqs.(A3) as

$$\bar{Z}_1Z_2[L_c\begin{pmatrix}\phi_{32}\\ \psi_{32}\end{pmatrix} - i\omega_1\begin{pmatrix}\nabla_\perp^2\phi_{32}\\ \psi_{32}\end{pmatrix}] = [i(\omega_2-2\omega_1)\begin{pmatrix}\nabla_\perp^2\phi_{32}\\ \psi_{32}\end{pmatrix} + a_1\begin{pmatrix}\nabla_\perp^2\phi_{1c}\\ \psi_{1c}\end{pmatrix} + \cdots]\bar{Z}_1Z_2.$$

Since $\begin{pmatrix}\phi_{32}\\ \psi_{32}\end{pmatrix} + \begin{pmatrix}\phi_{1c}\\ \psi_{1c}\end{pmatrix}$ is also a solution of the above equations, the gauge is defined by $(\phi_{1c}^{\perp}, \nabla_\perp^2\phi_{32}) + (\psi_{1c}^{\perp}, \psi_{32}) = 0$. In the linear problem, the eigenfrequencies arises mostly from Dopler shifting, so $\omega = \omega_2 - 2\omega_1$ is a small quantity. Applying the Fredholm solvability condition to the above equation yields

$$a_1 = \iint [\bar{\phi}_{1c}^{\perp}(-\frac{\partial\phi_{1c}}{\partial x}\frac{\partial\nabla_\perp^2\phi_{2c}}{\partial y} - \frac{\partial\phi_{2c}}{\partial x}\frac{\partial\nabla_\perp^2\phi_{1c}}{\partial y} + \frac{\partial\phi_{1c}}{\partial y}\frac{\partial\nabla_\perp^2\phi_{2c}}{\partial x} + \frac{\partial\phi_{2c}}{\partial y}\frac{\partial\nabla_\perp^2\phi_{1c}}{\partial x}$$
$$+ \frac{\partial\psi_{1c}}{\partial x}\frac{\partial\nabla_\perp^2\psi_{2c}}{\partial y} + \frac{\partial\psi_{2c}}{\partial x}\frac{\partial\nabla_\perp^2\psi_{1c}}{\partial y} + \frac{\partial\psi_{1c}}{\partial y}\frac{\partial\nabla_\perp^2\psi_{2c}}{\partial x} + \frac{\partial\psi_{2c}}{\partial y}\frac{\partial\nabla_\perp^2\psi_{1c}}{\partial x}) + \bar{\psi}_{1c}^{\perp}$$
$$(\ -\frac{\partial\phi_{1c}}{\partial x}\frac{\partial\psi_{2c}}{\partial y} + \frac{\partial\phi_{1c}}{\partial y}\frac{\partial\psi_{2c}}{\partial x} - \frac{\partial\phi_{2c}}{\partial x}\frac{\partial\psi_{1c}}{\partial y} + \frac{\partial\phi_{2c}}{\partial y}\frac{\partial\psi_{1c}}{\partial x})]\,dx\,dy + 0(\omega) \qquad \text{(A4)}$$

Similarly, we obtain

$$a_2 = \iint [\bar{\phi}_{2c}^{\perp}(\frac{\partial\phi_{1c}}{\partial x}\frac{\partial\nabla_\perp^2\phi_{1c}}{\partial y} - \frac{\partial\phi_{1c}}{\partial y}\frac{\partial\nabla_\perp^2\phi_{1c}}{\partial x} - \frac{\partial\psi_{1c}}{\partial x}\frac{\partial\nabla_\perp^2\psi_{1c}}{\partial y} +$$
$$\frac{\partial\psi_{1c}}{\partial y}\frac{\partial\nabla_\perp^2\psi_{1c}}{\partial x}) + \bar{\psi}_{2c}^{\perp}(\frac{\partial\phi_{1c}}{\partial x}\frac{\partial\psi_{1c}}{\partial y} - \frac{\partial\phi_{1c}}{\partial y}\frac{\partial\psi_{1c}}{\partial x})]\,dx\,dy + 0(\omega) \qquad \text{(A5)}$$

So a_1 and a_2 are determined by linear marginal eigenfunctions to order $0(\omega)$.

Continuing the procedure, coefficients of order $\vartheta(|Z|^3)$ are calculated:

$$b_1 = \int\int [\bar{\phi}_{1c}^{\perp}(\frac{\partial\phi_{11}}{\partial x}\frac{\partial\Omega_{3c}}{\partial y} - \frac{\partial\phi_{11}}{\partial y}\frac{\partial\Omega_{3c}}{\partial x} - \frac{\partial\psi_{11}}{\partial x}\frac{\partial j_{3c}}{\partial y} + \frac{\partial\psi_{11}}{\partial y}\frac{\partial j_{3c}}{\partial x}$$
$$+\frac{\partial\phi_{13}}{\partial x}\frac{\partial\Omega_{1c}}{\partial y} - \frac{\partial\phi_{13}}{\partial y}\frac{\partial\Omega_{1c}}{\partial x} - \frac{\partial\psi_{13}}{\partial x}\frac{\partial j_{1c}}{\partial y} + \frac{\partial\psi_{13}}{\partial y}\frac{\partial j_{1c}}{\partial x})$$
$$+\bar{\psi}_{1c}^{\perp}(\frac{\partial\phi_{11}}{\partial x}\frac{\partial\psi_{3c}}{\partial y} - \frac{\partial\phi_{11}}{\partial y}\frac{\partial\psi_{3c}}{\partial x} + \frac{\partial\phi_{13}}{\partial x}\frac{\partial\psi_{1c}}{\partial y} - \frac{\partial\phi_{13}}{\partial y}\frac{\partial\psi_{1c}}{\partial x})]\,dx\,dy \qquad \text{(A6)}$$

$$b_2 = \int\int [\bar{\phi}_{2c}^{\perp}(\frac{\partial\phi_{12}}{\partial x}\frac{\partial\Omega_{3c}}{\partial y} - \frac{\partial\phi_{12}}{\partial y}\frac{\partial\Omega_{3c}}{\partial x} - \frac{\partial\psi_{12}}{\partial x}\frac{\partial j_{3c}}{\partial y} + \frac{\partial\psi_{12}}{\partial y}\frac{\partial j_{3c}}{\partial x}$$
$$+\frac{\partial\phi_{23}}{\partial x}\frac{\partial\Omega_{1c}}{\partial y} - \frac{\partial\phi_{23}}{\partial y}\frac{\partial\Omega_{1c}}{\partial x} - \frac{\partial\psi_{23}}{\partial x}\frac{\partial j_{1c}}{\partial y} + \frac{\partial\psi_{23}}{\partial y}\frac{\partial j_{1c}}{\partial x}$$
$$+\frac{\partial\phi_{13}}{\partial x}\frac{\partial\Omega_{2c}}{\partial y} - \frac{\partial\phi_{13}}{\partial y}\frac{\partial\Omega_{2c}}{\partial x} - \frac{\partial\psi_{13}}{\partial x}\frac{\partial j_{2c}}{\partial y} + \frac{\partial\psi_{13}}{\partial y}\frac{\partial j_{2c}}{\partial x})$$
$$+\bar{\psi}_{2c}^{\perp}(\frac{\partial\phi_{12}}{\partial x}\frac{\partial\psi_{3c}}{\partial y} - \frac{\partial\phi_{12}}{\partial y}\frac{\partial\psi_{3c}}{\partial x} + \frac{\partial\phi_{23}}{\partial x}\frac{\partial\psi_{1c}}{\partial y} - \frac{\partial\phi_{23}}{\partial y}\frac{\partial\psi_{1c}}{\partial x}$$
$$+\frac{\partial\phi_{13}}{\partial x}\frac{\partial\psi_{2c}}{\partial y} - \frac{\partial\phi_{13}}{\partial y}\frac{\partial\psi_{2c}}{\partial x})]\,dx\,dy \qquad \text{(A7)}$$

$$c_1 = \int\int [\bar{\phi}_{1c}^{\perp}(\frac{\partial\phi_{12}}{\partial x}\frac{\partial\Omega_{4c}}{\partial y} - \frac{\partial\phi_{12}}{\partial y}\frac{\partial\Omega_{4c}}{\partial x} - \frac{\partial\psi_{12}}{\partial x}\frac{\partial j_{4c}}{\partial y} + \frac{\partial\psi_{12}}{\partial y}\frac{\partial j_{4c}}{\partial x}$$
$$+\frac{\partial\phi_{24}}{\partial x}\frac{\partial\Omega_{1c}}{\partial y} - \frac{\partial\phi_{24}}{\partial y}\frac{\partial\Omega_{1c}}{\partial x} - \frac{\partial\psi_{24}}{\partial x}\frac{\partial j_{1c}}{\partial y} + \frac{\partial\psi_{24}}{\partial y}\frac{\partial j_{1c}}{\partial x}$$
$$+\frac{\partial\phi_{14}}{\partial x}\frac{\partial\Omega_{2c}}{\partial y} - \frac{\partial\phi_{14}}{\partial y}\frac{\partial\Omega_{2c}}{\partial x} - \frac{\partial\psi_{14}}{\partial x}\frac{\partial j_{2c}}{\partial y} + \frac{\partial\psi_{14}}{\partial y}\frac{\partial j_{2c}}{\partial x})$$
$$+\bar{\psi}_{1c}^{\perp}(\frac{\partial\phi_{12}}{\partial x}\frac{\partial\psi_{4c}}{\partial y} - \frac{\partial\phi_{12}}{\partial y}\frac{\partial\psi_{4c}}{\partial x} + \frac{\partial\phi_{24}}{\partial x}\frac{\partial\psi_{1c}}{\partial y} - \frac{\partial\phi_{24}}{\partial y}\frac{\partial\psi_{1c}}{\partial x}$$
$$+\frac{\partial\phi_{14}}{\partial x}\frac{\partial\psi_{2c}}{\partial y} - \frac{\partial\phi_{14}}{\partial y}\frac{\partial\psi_{2c}}{\partial x})]\,dx\,dy \qquad \text{(A8)}$$

$$c_2 = \int\int [\bar{\phi}^{\perp}_{2c}(\frac{\partial \phi_{22}}{\partial x}\frac{\partial \Omega_{4c}}{\partial y} - \frac{\partial \phi_{22}}{\partial y}\frac{\partial \Omega_{4c}}{\partial x} - \frac{\partial \psi_{22}}{\partial x}\frac{\partial j_{4c}}{\partial y} + \frac{\partial \psi_{22}}{\partial y}\frac{\partial j_{4c}}{\partial x}$$

$$+\frac{\partial \phi_{24}}{\partial x}\frac{\partial \Omega_{2c}}{\partial y} - \frac{\partial \phi_{24}}{\partial y}\frac{\partial \Omega_{2c}}{\partial x} - \frac{\partial \psi_{24}}{\partial x}\frac{\partial j_{2c}}{\partial y} + \frac{\partial \psi_{24}}{\partial y}\frac{\partial j_{2c}}{\partial x})$$

$$+\bar{\psi}^{\perp}_{1c}(\frac{\partial \phi_{22}}{\partial x}\frac{\partial \psi_{4c}}{\partial y} - \frac{\partial \phi_{22}}{\partial y}\frac{\partial \psi_{4c}}{\partial x} + \frac{\partial \phi_{24}}{\partial x}\frac{\partial \psi_{2c}}{\partial y} - \frac{\partial \phi_{24}}{\partial y}\frac{\partial \psi_{2c}}{\partial x})]\, dx\, dy. \qquad \text{(A9)}$$

BIBLIOGRAPHY

[1] Abramowitz, M. and Stegun, I.A. *Handbook of Mathematical Functions,* (Dover Publications, Inc., New York, 1970).

[2] Adler, E.A. , Kulsrud, R.M. and White, R.B. Phys. Fluids **23**, 1375 (1980)

[3] Ambruster, D. , Guckenheimer, J. and Holms, P. Phsica D **29** ,257(1988).

[4] Ames, W.F. Nonlinear partial differential equations, (Academic press, New York, 1967).

[5] Ara, G., Basu, B., Coppi, B., Laval, G., Rosenbluth, M. N. and Waddell, B.V. Annals of Phys. **112**, 443–476 (1978).

[6] Barston, E. M. Ann. Phys. , **29**, 292(1964).

[7] Barston, E. M. Phys. Fluids, **12**, 2162(1969).

[8] Bateman, G. MHD instabilities, (Cambridge, 1978)

[9] Begelman, M.C. , Blandford, R.D. and Rees, M.J. Rev. Mod. Phys., **56**, 255(1984).

[10] Benney, D. J. and Bergeron, R. F. Stud. Apll. Math. **48**, 181 (1969).

[11] Bondeson, A. and Sobel, J. R. Phys. Fluids, **27**, 2028 (1984)

[12] Bondeson, A. and Persson, M. ,Phys. Fluids **29(9)**, 2997 (1986).

[13] Braginskii, S.I. , Reviewsof Plasma Physics, pp.205 (ed. A.M.A. Leontovich, Consultants Bureau, New York, 1965).

[14] Burch, J. L. Rev. Geophys. Space Phys. **21**, 463(1983).

[15] Case, K.M. Phys. Fluids **3**,143(1960)

[16] Chandra, K. J. Physical Society of Japan **34**, 539(1973)

[17] Chandraseker, S. Hydrodynamic and Hydromagnetic Stability (Clarendon, Oxford,1961).

[18] Chen, F. F. Introduction to plasma physics and controlled fusion (Plenum Press, NewYork, 1984).

[19] Chen, X.L. and Morrison, P.J. Phys. Fluids **B2** 495 (1990a).

[20] Chen, X.L. and Morrison, P.J. Phys. Fluids **B2** 2575(1990b).

[21] Chen, X.L. and Morrison, P.J. Phys. Fluds **B3** 863 (1991).

[22] Chiueh, T. , Terry, P. W. , Diamond, P. H. and Sedlak, J. E. Physics of Fluids **29**, 231(1986).

[23] Chiueh, T. and Zweibel, G. The astrophysical Journal, **317**, 900 (1987).

[24] Coppi, B. , Greene, J. M. , Johnson, J. L. Nucl. Fusion, **6**, 101 (1966).

[25] Coppi, B. , Galvao, R. , Pellat, R. , Rosenbluth, M.N.and Rutherford, P. Sov. J. Plasma Phys., Vol. 2, No. 6, 533 (1976).

[26] Crawford, J.D. Introduction to bifurcation theory (to appear in Rev. Mod. Phys 1991)

[27] Crawford, J.D. Knobloch, E. Annu. Rev. Fluid Mech. 23, 341 (1991)

[28] Crawford, J.D. Knobloch, E. and Riecke, H. Physica D **44**, 340 (1990).

[29] Currie, I.G. Fundamental mechnics of Fluids, (McCraw-Hill, New York,1974).

[30] Dangelmayer, G. , Dynamics and stability of systems Vol.1 **159**(1986)

[31] Diamond, P. , Hazeltine, R. D. , An, Z. G. , Carreras, B.A. and Hicks, H. R. Phys. Fluids, **27**, 1449 (1984).

[32] Dobrott, D. , Prager, S. C. and Taylor, J. B. Phys. Fluids, **20**, 1850 (1977).

[33] Dobrowolny, M. Veltri, P. and Mangeney, A. J. Plasma Phys., Vol. 29, Part 3, 303 (1983).

[34] Drake, J. F. , and Lee, Y. C. , Phys. Fluids, 1341 (1977).

[35] Drake, J. F. , Phys.Fluids, 1777(1978).

[36] Drazin, P. G. and Howard, L. N. In advances in applied mechnics, Vol. **7**, ed. Keurti, G. , pp. 1-89 (Academic Press, New york, 1966)

[37] Drazin, P. G. and Johson, R. S. Solitons: An introduction, (Cambridge University press, 1989).

[38] Drazin, P.G. and Reid, W.H. ,Hydrodynamic stability, (Cambridge University Press, New York, 1982).

[39] Dungey, J. S.. Cosmic Electrodynamics, pp. 98-102 (Cambridge U. P. , New York,.1958).

[40] Einaudi, G. and Rubini, F. Phys. Fluids **29**, 2563 (1986).

[41] Einaudi, G. and Rubini, F. Phys. Fluids **B1**, 2224 (1989).

[42] Finn, J.M. and Kaw, P.K. Phys. Fluids, **20**, 72(1977).

[43] Fjortoft, R. Geophy. Publ. , **17**, 1 (1950).

[44] Freidberg, J. R. Reviews of Modern Physics, **54**, 801 (1982).

[45] Friedricks, K. O. Fluid Dynamics, Chapter IV , mimeographed lecture notes, Brown University, Providence, Rhode Island (1982).

[46] Furth, H. P. , Killeen, J. and Rosenbluth, M. N. Phys. Fluids **6**, 459 (1963).

[47] Furth, H. P. , Rutherford, P. H. and Selberg, H. Phys. Fluids, **16**, 1054 (1973)

[48] Galeev, A. A. , and Sudan, R. N. Basic Plasma Physics, (Elsevier Science Inc. , 1989).

[49] Glasser, A. H. , Greene, J. M. and Johnson, J. L. Phys. Fluids, **18**, 875 (1975).

[50] Glasser, A. H. , Furth, M. P. and Rutherford, P. M. Phys. Rev. Lett. , **38**, 234 (1977).

[51] Golubitsky, M. and Lanford, W.F. ,Physica D **32**, 362(1988).

[52] Golubitsky, M. , Stewart, I. and Schaeffer, D.G. Singularities and groups in bifurcation theory, Vol.II, (springer-verlag, Newyork, 1989).

[53] Grauer, R. Physica D **35**, 107(1989).

[54] Groebner, R.J. , Gohil, P. , Burrell, K. H. , Osborne, T. H. , Seraydarian, R. P. and John, H. St. in Proceeding of the 16th European Conference on Controlled Fusion and Plasma Physics, Budapest, Hungary, (European Physical Soc. 1989) Vol.I, p. 245.

[55] Grossmann, W. and Tataronis, J. Z. Physik, **261**, 217 (1973).

[56] Gu, D., Phys. Fluids, **A2**, 2068 (1990).

[57] Guckenheimer, J. and Knobloch, E. Geophys. astrophys. Fluid dynamics, **23**,247(1983)

[58] Guckenheimer J. and Holmes, P. Nonlinear oscilators, Dynamical systems, and Bifurcation of vector fields, (springer-verlag, Berlin, 1983)

[59] Hahm, T. S. and Kulsrud, R. M. Phys. Fluids, 2412 (1985).

[60] Haberman, R. Stud. Appl. Math. **51**, 139 (1972).

[61] Hazeltine, R. D., F. R. C. Report, University of Texas at Austin (1977).

[62] Hazeltine, R. D. and Meiss, J. D. , Phys. Reports, **121**, 1(1985).

[63] Hazeltine, R. D. , Meiss, J. D. and Morrison, P. J. Phys. Fluids **29**, 1633 (1986).

[64] Hofman, I., Plasma Phys. **17**, 143 (1975).

[65] Hones, M. (ed.) Magnetic Reconnection in Space and Laboratory Plasmas. A. G. U. , Washington, D. C. (1984).

[66] Horton, W. , Tajima, T. and Kamimura, T. , Phys. Fluids, **30**, 3485(1987).

[67] Howard, L. N. J. Fluid Mech. , **10**, 509 (1961).

[68] Howard, L. N. Journal de Mecanique, **3**, 434 91964).

[69] Hu, Pung Ning, Phys. Fluids, **26**, 2234 (1983).

[70] Ionson, J. A. Astrophys. J. , **226**, 650 (1978).

[71] Iooss, G. and Joseph, D. D. Elementary stability and Bifurcation theory, (Springer-verlag, New York, 1980).

[72] Jardin, M. and Priest, E. R. J. Plasma Phys. , **40**, 143 (1988a).

[73] Jardin, M. and Priest, E. R. Geophys. Astrophys. Fluid Dyn. , **42**, 163 (1988b).

[74] Jardin, M. and Priest, E. R. J. Plasma Phys. , **40**, 505 (1988c).

[75] Jardin, M. and Priest, E. R. J. Plasma Phys. , **42**, 111 (1989).

[76] Kent, A. Phys. Fluids **9**, 1286(1966)

[77] Kent, A. J. Plasma Phys. Vol. 2, Part 4, 543–556 (1968).

[78] Knobloch, E. and Proctor, M.R.E. Proc. R. Soc. Lond. **A 415** , 61(1988)

[79] Killeen, J. , In Physics of Hot Plasmas, edited by B. J. Rye and J. C. Taylor, pp. 212 (Plennum, New York, 1970).

[80] Krall, N. A. and Trivelpiece, A. W. Principles of Plasma Physics, (McGraw-Hill, NewYork, 1973), 464-474.

[81] Liewer, P. C. and Payne, D. G. , The Astrophysical Journal, **353**, 658 (1990).

[82] Liewer, P. C. and Payne, D. G. , Geophysical Research Letters, **17**, 2047 (1990).

[83] Lin, C. C. Quart. Appl. Math. , **3**, 218 (1945).

[84] Lin, C.C. The Theory of Hydrodynamic Stability (Cambridge University Press, London, 1955)

[85] Marsden, J. and McCrancken, M. The Hopf bifurcation and it's application, Springer-verlag (1976).

[86] Morrison, P.J. Ph.D Thesis, University of California at SanDiego (1979).

[87] Ofman, L. , Chen, X.L. , Morrison, P.J. and Steinolfson, R.S. Phys. Fluids, (1991, to appear).

[88] Paris, R. B. and W. N-C Sy, Phys. Fluids **26(10)**, 2966 (1983).

[89] Parker, R.D. , Dewar, R.L. and Johnson, J.L. Phys. Fluids, **B2**, 508 (1990).

[90] Penrose, O. Phys. Fluids **3**, 259(1960).

[91] Persson, M. Ph.D. thesis "Resistive MHD stability for rotating plasmas", Chalmers University of Technology technical report NO.177 (1987), Goteborg,Sweden;

[92] Persson, M. and Bondeson, A. Phys. Fluids, **B2**, October(1990).

[93] Pollard, R. K. and Taylor, J. B. Phys. Fluids, **22**, 126 (1978).

[94] Porcelli, F. Phys. Fluids **30**, 1734 (1987).

[95] Porcelli, F. Phys. Rev. **66**, 425(1991).

[96] Priest, E. R. , Rep. Prog. Phys. **48**, 955 (1985)

[97] Priest, E. R. and Forbes, T.G. J. Geophy. Res. , **91**, 5579 (1986).

[98] Priest, E. R. and Lee, L. C. J. Plasma Phys. , **91**, 5579 (1986).

[99] Rosenbluth, M.N. and Simon, A. Phys. Fluids **7**, 557(1963)

[100] Rutherford, P.H. Phys. Fluids **14**,1903(1973).

[101] Rosenbluth, M. N. and Rutherford, P. H. , Tokamak Plasmas Stability, Fusion, **1**, 31(ed. Teller, 1981).

[102] Saramito, B. , Maschke, E. in: Magnetic Reconnection and turbulence, M.A. Dubois, D.Gresillon and M.N. Bussac, eds(les Editions de physique, courtaboenf,orsay,1985).

[103] Shiramoggi, B. K. , Phys. Fluids, **30**, 1228 (1987).

[104] Sijbrand, J. Am. Math. Soc. 289, 431(1985).

[105] Sonnerup, B. U. O. , Solar System Plasma Physics (ed. L. T. Lanzerotti, C. F. Kennel and E. N. Parker), pp. 45, (North-Holland, 1979).

[106] Steinolfson, R. S. and Van Hoven, G. Phys. Fluids **26**, 117 (1983).

[107] Steinolfson, R. S. and Van Hoven, G. Phys. Fluids **27**, 1207 (1984).

[108] Stern, M.E. Phys. Fluids **6**, 636(1963).

[109] Strauss, H. R. , Phys. Fluids, **29**, 3668 (1986).

[110] Strauss, H. R. , The Astrophysical Journal, **326**, 472 (1988).

[111] Stuart, J. J. Fluid Mech. **9**, 353 (1960).

[112] Tajima, T. , Horton, W. , Morrison, P.J. , Schutkeker, J. , Kamimura, T. , Mima, K. and Abe, Y. Institute for Fusion Studies report #IFSR 418(1990), Austin, Texas. (to appear in Phys. Fluids **B3**, 1991).

[113] Tataronis, J. and Grossmann, W. , Z. Physik, **261**, 203 (1973).

[114] Thyagaraja, A. Phys. Fluids **24**, 1716 (1981).

[115] Thyagaraja, A. and Haas, F. A. Phys. Fluids **B3**, 580 (1990).

[116] Udell, Y. and Luke, L. Integrals of Bessel Functions (McGraw-Hill, 1962).

[117] Van Kampen, N. G. and Felderhof, B. U. Theoretical Methods in Plasma Physics (John Wiley and Sons, Inc. New York, 1967).

[118] Vasyliunas, V. M. Review of Geophysical and Space Physics, **13**, 303 (1975).

[119] Wang, S. Lee, L.C. and Wei, C. Q. Phys. Fluids **31**, 1544(1988).

[120] Waelbroeck, F. private communication (1989).

[121] Waddell, B. V. , Rosenbluth, M. N. , Monticello, D. A. and White, R. B. Nuclear Fusion **163**, 528 (1976).

[122] Wasow, W. Ann. Math. , **49**, 852(1948).

[123] Wasow, W. Ann. Math. , **58**, 222(1953).

[124] Watson, J. J. Fluid Mech. **9**, 371 (1960).

[125] Wesson, J. A. Nuclear Fusion, **18**, 87 (1978).

[126] White, R.B. , Monticello, D.A. , Rosenbluth, M.N. and Waddell, V. Phys. Fluids, **20**,800(1977).

[127] White, R. B. Reviews of Modern Physics, **58**, 183 (1986).

VITA

Xiao Liang Chen was born in Hubei, P.R. China, on March 4, 1965, the son of Bao Cin Chen and Yue er Wang. After completing his work at Huandiqiao high school, Daye, Hubei in 1980, he entered Wuhan University. He received the degree of Bachelor of science in physics from Wuhan University in July 1984. During the time from October 1984 to May 1985, he attended Beijing Language Institute for special training in English. In September 1985, he entered the graduate school of the University of Texas at Austin. Since then he was employed as a Teaching Assistant in Physics Department and Research Assistant in the Institute for Fusion Studies.

Permanent address: c/o Bao-Chin Chen
Huangshi teacher's
vocational studies College
Hubei, P.R. China

This dissertation was typeset with LaTeX by the author.